WATER FLOODING PERFORMANCE PREDICTION USING STREAMLINE SIMULTION

BY

Hesham Mohammed

A Thesis Presented to the

DEANSHIP OF GRADUATE STUDIES

KING FAHD UNIVERSITY OF PETROLEUM & MINERALS

DHAHRAN, SAUDI ARABIA

In Partial Fulfillment of the
Requirements for the Degree of

MASTER OF SCIENCE

In

PETROLEUM ENGINEERING

JUNE 2010

KING FAHD UNIVERSITY OF PETROLEUM & MINERALS
DHAHRAN 31261, SUADI ARABIA

DEANSHIP OF GRADUATE STUDIES

This thesis, written by **HESHAM MOHAMMED** under the direction of his thesis advisor and approved by his thesis committee, has been presented to and accepted by the Dean of Graduate Studies, in partial fulfillment of the requirements for the degree of **MASTER OF SCIENCE IN PETROLEUM ENGINEERING**.

Thesis Committee

Dr. Abdul-Aziz Al-Majed (Thesis Advisor)

Dr. Hasan Al-Yousef (Member)

Dr. Mahmoud Doklah (Member)

Dr. Abdul-Aziz Al-Majed
(Department Chairman)

Dr. Salam A. Zummo
(Dean of Graduate Studies)

23/1/11
Date

Dedicated

to

My loving Family and my greatest Wife

Acknowledgment

All praises and adorations are due to Allah, the lord of incomparable majesty. May Allah bestow peace on his Prophet Mohammed (Peace and Blessings of Allah be upon him), his family.

Acknowledgement is due to the King Fahd University of Petroleum & Minerals for supporting this research.

I acknowledge, with deep gratitude and appreciation, the inspiration, encouragement, supervision and support rendered to me by my thesis advisor, Dr. Abdul-Aziz Al-Majed. I also wish to thank the other members of my thesis committee Dr. Hasan Al-Yousef and Dr. Mahmoud Doklah for their constructive guidance, technical support and patronage.

Numerous gratitude and thanks goes to the Petroleum Engineering Department and the KFUPM Research Institute for making the necessary facilities and resources available to accomplish this research.

I would also like to express my huge gratitude to the Department of Petroleum Engineering for their tutelage throughout my Master's Degree to which I owe my success and rapid skill in acquiring the necessary concepts in the field of Petroleum Engineering.

Further, I would like to thank Dr. Ahmed Al-Hutheli for his great support and my dear friends Abdul-Rahman Shaheen, Faisal Ba-Naema, Fattahi and Mohammed Naik for their constructive advice, support and companionship in the long hours that lead to fulfillment of my research work.

Table of Contents

List of Tables

List of Figures

Thesis Abstract

Full Name : Hesham Mohammed

Thesis Title : Improving Water Flooding Performance Prediction Using Streamline Simulation
Major Field : Petroleum Engineering
Date of Degree : June, 2010.

Recent advances in technology have led to the development of streamline simulation techniques aimed at the estimation of the best injection profile to acquire excellent efficiency improvement in the water flooding process.

The present study evaluates three recent automated optimization methodologies on the responses of increasing efficiency of enhanced oil recovery using water flooding. The programming procedures for the three presented methods are highlighted. Two artificial models and two real models are simulated to find out the advantages and disadvantages of each optimization process. In addition, helpful software was utilized that was developed at KFUPM-RI and capable of dealing with streamline simulation output and generating efficiency plots.

The results obtained from this study highlighted the differences in the presented methods of productivity arising and water flooding efficiency. Furthermore, it was noticed that Huthali method had the greatest influence in increasing flooding efficiency performance. However, less oil amount is produced compared to the other two methods for the same time scale.

خلاصة الرسالة

الإســـــم : **هشام محمد**
عنوان الرسالة : **تطوير كفاءة ضخ المياه للحقول باستخدام محاكاة انسياب خطوط التدفق**
التخصص : **هندسة بترول**
تاريخ التخرج : **جمادى الآخر 1430**

قد أدت التطورات الحديثة في التكنولوجيا لتبسيط تطوير تقنيات المحاكاة بهدف القدرة للحصول على أفضل حقن ممتاز لتحسين كفاءة استخدام المياه في عملية الدفع المائي للنفط.

هذه الدراسة تقيم آخر ثلاث آليات للتحسين الآلي لكفاءة الاستخلاص المعزز للنفط باستخدام ضخ المياه في الحقول .كما يسلط الضوء على إجراءات البرمجة للأساليب الثلاثة المذكورة .تمت محاكاة نموذجين اصطناعية واثنين من النماذج الحقيقية لاكتشاف مزايا وعيوب كل نظرية من نظريات التحسين .وبالإضافة إلى ذلك، تم استخدام برامج مفيدة تم تطويرها في معهد أبحاث جامعة الملك فهد وقادرة على تبسيط مخرجات المحاكاة وتكوين رسومات بيانية بالنتائج

أبرز النتائج التي تم الحصول عليها من هذه الدراسة الاختلافات في الأساليب المعروضة من الإنتاجية وكفاءة استخدام المياه لدعم تدفق النفط .وعلاوة على ذلك، فقد لوحظ أن أسلوب الهذلي كان له أكبر تأثير على زيادة الكفاءة للحصول على أداء فيضانات المياه، ومع ذلك، أنتج كمية أقل من النفط بالمقارنة مع الطريقتين ضمن إطار زمني واحد.

CHAPTER 1

INTRODUCTION

Water flooding has been widely applied in hydrocarbon fields either to support the reservoir pressure during depletion and/or to increase hydrocarbon production as a secondary recovery process. The technique consists of injecting water with the purpose of maintaining pressure and/or displacing and producing hydrocarbons. Reservoir simulation is an essential tool for controlling and predicting water flooding efficiency. The most popular reservoir simulation technique which has been used for several decades is the finite difference approach (FD).

FD simulation based on detailed and accurate reservoir description is an essential tool for controlling and predicting the outcome of a water flooding project. Unfortunately it (FD) is not able to provide details about the way the flow occurs or move inside the reservoir. For these reasons, current flood managements are heavily dependent on standard surveillance methods or workflows centered on the conventional finite different simulation.

Streamline simulation has emerged as a powerful and complementary tool in the past 10 years. One powerful aspect of streamline simulation is the ability to visualize reservoir flows that result because of well positions, well rates, geological description and reservoir continuity.

In general, the main reasons for using streamline simulation are that (a) it is computationally efficient and fast, (b) a full field simulation can be performed within a reasonable time frame, (c) it can quantify flow distribution in injectors and producers, (d) it can provide efficiency of injectors and producers, (e) it provides flow visualization, (f) it can identify areas of low sweep in a water flood, and (g) it can provide possible locations for new injectors/producers to improve sweep efficiency.

Many approaches were introduced to the industry recently to improve water flooding efficiency using streamline simulation, wells allocation factors and streams efficiency. These methods are using different methodologies and concepts to optimize injection rates which improve the water flooding efficiency.

CHAPTER 2

LITERATURE REVIEW

The need for production optimization of reservoir fields has arisen as a result of the global increase in demand for oil and gas. Several applications of optimization process have been developed using streamline simulation. These optimization techniques have proved to be beneficial in increasing the hydrocarbon recovery in large fields.

Streamline simulation (Milliken et al, 2000; Thierry et al., 1996)[1] is an alternative approach to the conventional finite difference technique (Mattax and Dalton, 1990) [1] of modeling fluid flow in hydrocarbon reservoirs. It is an IMPES (Implicit Pressure Explicit Saturation) method of simulation in which initially, as with finite difference models, the pressure field is solved implicitly over the whole grid. The next step is where the difference arises, in that the pressure field is then used to trace the path that a single fluid would follow as it flows across the reservoir producing streamlines. The saturations are then mapped from the grid onto the streamlines, flow along the streamlines is calculated, and then the updated saturations are mapped back to the model grid. FrontSim [9] performs this calculation using front tracking. This means that the fluid flow is modeled as a series of saturation fronts moving along the streamlines. Thus, streamline simulation provides good flow visualization where the remaining reserves

can be located spatially. Conventional simulation doesn't show the detailed water movement directions inside the reservoir. Unfortunately, streamline simulation has minimal predictive capabilities.

Therefore, many papers were published about using streamline simulation in water flooding optimization process. In this section, some papers and previous work done on that field will be reviewed.

2.1 Thiele and Batycky [4] (2003)

This paper describes an approach to optimize injection and production well rates in a water flood using streamline-based (SL) flow simulation. The method is automated and therefore applicable to very large fields with many wells. They verify that streamline based flow simulation is unique in that it allows quantifying the amount of injected and produced fluids between well pairs via well allocation factors (WAF's) where:

$$q_j^{p-i} = WAF^{p-i} q_j^p$$

WAFs' allow calculating the efficiency of injection wells as the ratio of injected water to the oil produced at offset wells. With injection efficiencies known across the field for each injector, water can be reallocated from low-efficiency to high efficiency wells, thereby optimizing production for each barrel of water injected.

2.2 Ghori et. al [5] (2006)

The authors had studied improving water flooding in a real reservoir using both finite difference and streamline simulation as complementary tools. During the course of the study a few limitations of the streamline simulator have been encountered, highlighted, and discussed. The results showed that streamline simulation is still in the development stage in highly compressible systems.

It is tricky to follow field/group rate targets and limits along with the individual well rate targets in prediction mode. Prior to the optimization phase of the study, the streamline simulator was successfully applied to reproduce the historical performance of the reservoir during primary depletion in the absence of any water injection. Valuable information was obtained from streamline simulation; a) distribution of injected water to associated producers, b) water loss to the aquifer, c) percentage of oil produced due to each supporting injector, and d) amount of water cut attributable to each supporting injector.

2.3 Pamila A.Marescalco [6] (2008)

This paper explores a different complementary approach, represented by streamline-based simulation, coupled with a tool to optimize waterflooding campaigns and to help quick decision making. In that study, waterflooding simulation is performed using two commercial softwares. A finite different and a streamline-based simulator (3DSL) were used, to highlight advantages and disadvantages of both simulation techniques in

describing a water injection campaign and to exploit the two approaches' uniqueness in parallel. The final goal of iteratively converging to the optimal waterflooding scheme is achieved through a customized Matlab script. The injection rate is optimized using the average reservoir injection efficiency. The generated automatic procedure shows its effectiveness in improving oil recovery, expediting decision making and saving time and FD simulation runs. The main concept in this study is to calculate the new injection rate using the weighting average of the streams efficiency ω_i as shown below :

$$q_i^{new} = (1+\omega_i).q_i^{old}$$

$$e_i \geq \bar{e} \Rightarrow \omega_i = MIN(\omega_{\max}, \omega_{\max}.(\frac{e_i - \bar{e}}{e_{\max} - \bar{e}})^{\alpha})$$

$$e_i \leq \bar{e} \Rightarrow \omega_i = MAX(\omega_{\min}, \omega_{\min}.(\frac{\bar{e} - e_i}{\bar{e} - e_{\min}})^{\alpha})$$

$\bar{e}$: reservoir average efficiency

α : is equal to 0.5 or 1 or 2

Then, correction factor is calculated through Matlab and used for iteration to get the optimized injection rates.

2.4 Huthali, Gupta, Yuen and Fontanilla [17] (2009)

In this paper an approach was proposed that is computationally efficient and suitable for large field cases. It is based on equalizing arrival time of the waterfront at all producers for maximizing the sweep efficiency. Streamlines were used to efficiently and analytically compute the sensitivity of the arrival times with respect to well rates. Also,

geologic uncertainty was accounted for a stochastic optimization framework using multiple realizations. Analytical forms for gradients and Hessian of the objective functions are derived, making optimization computationally efficient for large-scale applications. Finally, optimization is performed under operational and facility constraints using a sequential quadratic programming approach. The major steps in this approach are outlined below:

I. **Tracing Streamlines and Arrival-Time Computation.** The first step is to generate streamlines and compute the time of flight. Tracing streamlines has been discussed by several authors (King and Datta-Gupta 1998; Datta-Gupta and King 1995; Pollock 1988) [(1)]. The time of flight, which is defined as the time required by a neutral-tracer particle to travel along a streamline, will form the basis for computing the arrival time of the waterflood front at all producers. If a streamline simulator is being used, all these quantities are already available and this step can be bypassed.

II. **Residuals and Sensitivity Computation.** In this step, the residuals that quantify the difference between the desired arrival time and the computed arrival time at each of the producing wells are computed. Also, the sensitivity of the arrival time at the producer to well rates is calculated analytically, using simple integrals along streamlines. The sensitivities are partial derivatives that relate changes in arrival time to small perturbations in production and injection rates. They are an integral part of rate optimization process.

III. **Minimization and Optimal Rate Allocations.** Sequential quadratic

programming (SQP) procedures are used to minimize the arrival time residuals (Nocedal and Wright 2006) [(1)]. This step generates the required changes in rates to equalize waterflood front arrival time at the producing wells subject to appropriate field constraints.

IV. **Mobility Effects and Changing Field Conditions.** The previous steps are repeated until the norm of the residuals meets a predefined stopping criterion. Once this criterion is met, we move to a new time interval, update streamlines, and perform the optimization again to account for mobility effects and changing field conditions.

CHAPTER 3

PROBLEM STATEMENT AND OBJECTIVE OF STUDY

3.1 Problem Statement

Water flooding is the most efficient and widely used method to increase oil recovery from hydrocarbon reservoirs. With the realization of water flooding importance many research projects have been done, for large oil fields, using finite different simulation to increase water flooding efficiency and to achieve maximum recovery from hydrocarbon reservoirs. Finite difference simulation doesn't show the detailed water movement inside the reservoir.

In recent years, streamline simulation was introduced and practiced with the ability to visualize reservoir fluid flows. This option helped in surveillance and improvement of water flooding efficiency. The disadvantage of a streamline surveillance model is that it has minimal predictive capabilities. However, it provides good flow visualization where the remaining reserves can be located spatially.

Many approaches were introduced to increase the water flooding efficiency in the simulated model. These studies were done using different techniques and aspects. Up

to the moment, no one has compared these methods in one field to figure out the strengths and weaknesses for each one.

3.2 Objectives of Study

The main objective of the proposed study is to compare the different approaches of enhanced oil recovery by increasing water flooding efficiency using streamline simulation. These methods are: Huthali et al [17], Pamila [6] and Thiele et al [4]. Huthali approach used the arrival times with respect to well rates to improve water flooding efficiency. Pamila [6] and Thiele [4] approaches depend on injection efficiency and wells allocation factors' to optimize the injection rate for each well.

The outcome of the study will be used to select the best method that improves injection, enhances sweep efficiency and hydrocarbon recovery.

CHAPTER 4

DATA PREPARATION

In order to elucidate dissimilarity between the three methods of optimization, different models were simulated. For that purpose, four models were generated and simulated to clarify that purpose. These models are organized from a simple homogeneous one layer model to a real very complex heterogeneous model. In this chapter, we will cover the models description, characterization and Frontsim input file for each model.

4.1 FrontSim Input Data

FrontSim [9] is a reservoir simulator based on an IMPES (Implicit Pressure Explicit Saturation) formulation and a streamline/front-tracking concept. The governing equations are split into two equations, the pressure equation and the saturation equation. More details about the mathematical formulations are presented in Appendix A.

The pressure equation is solved implicitly by a control volume finite difference method. If the grid is regular, a standard finite difference method is used.

After the pressure solution is obtained FrontSim computes a set of streamlines to represent the flow in the reservoir. The streamlines are computed based on the pressure gradients and represent the total Darcy velocities (the sum of phase velocities). Each

streamline represents a constant volumetric rate and acts as a one-dimensional space for the saturation solver.

The saturation solver in FrontSim is quite different from other simulators. Unlike standard finite difference solvers, the saturation solver in FrontSim is designed to capture the fronts (discontinuities in saturation) that are present on a macro-scale in the reservoir.

The saturation equation is solved by a front-tracking method, which is applied along streamlines. The saturation on each streamline is then mapped onto the grid to form a global saturation for output. One can choose the size of the time step, and there is basically little limit on the step length.

The FrontSim input data file consists of eight main sections as described below:

RUNSPEC: Title, problem dimensions, switches, phases present, etc.

GRID: Specification of geometry of computational grid (location of grid block corners), and of rock properties (porosity, absolute permeability etc.) in each grid block.

EDIT: Modifications to calculated pore volumes, grid block center depths and transmissibilities.

PROPS: Tables of properties of reservoir rock and fluids as functions of fluid pressures, and saturations (density, viscosity, relative permeability, etc.).

REGIONS: Splits computational grid into regions for calculation of (a) PVT properties, (b) Saturation properties, (c) Initial conditions, and (d) Fluids in place

SOLUTION: Specification of initial conditions in reservoir may be calculated using (a) using specified fluid contact depths to give potential equilibrium, or (b) reading from a restart file

RESTART: File set up by an earlier run

SUMMARY: Specification of data to be written to the SUMMARY file after each time step. FrontSim presently reads this section for compatibility with ECLIPSE, but does not use it. All supported vectors are always written to the SUMMARY file after each time step.

SCHEDULE: Specifies the operations to be simulated (production and injection controls and constraints), and the times at which output reports are required. Simulator tuning parameters may also be specified in the SCHEDULE section.

4.2 Simulation Models

In order to pick a great understanding of the optimization methods mechanism, several models should be simulated. It's important to know each model description and organize them in a certain way to highlight the differences between optimization methods and get the best result from this research. These models are named M1, M2, M3 and M4.

4.2.1 Models Illustration

The first model in this study (M1) is a very simple homogeneous one layer model. The full field model dimension of M1 is 50 X 50 X 1 with 2500 active cells. Figure 4.1 illustrate M1 model.

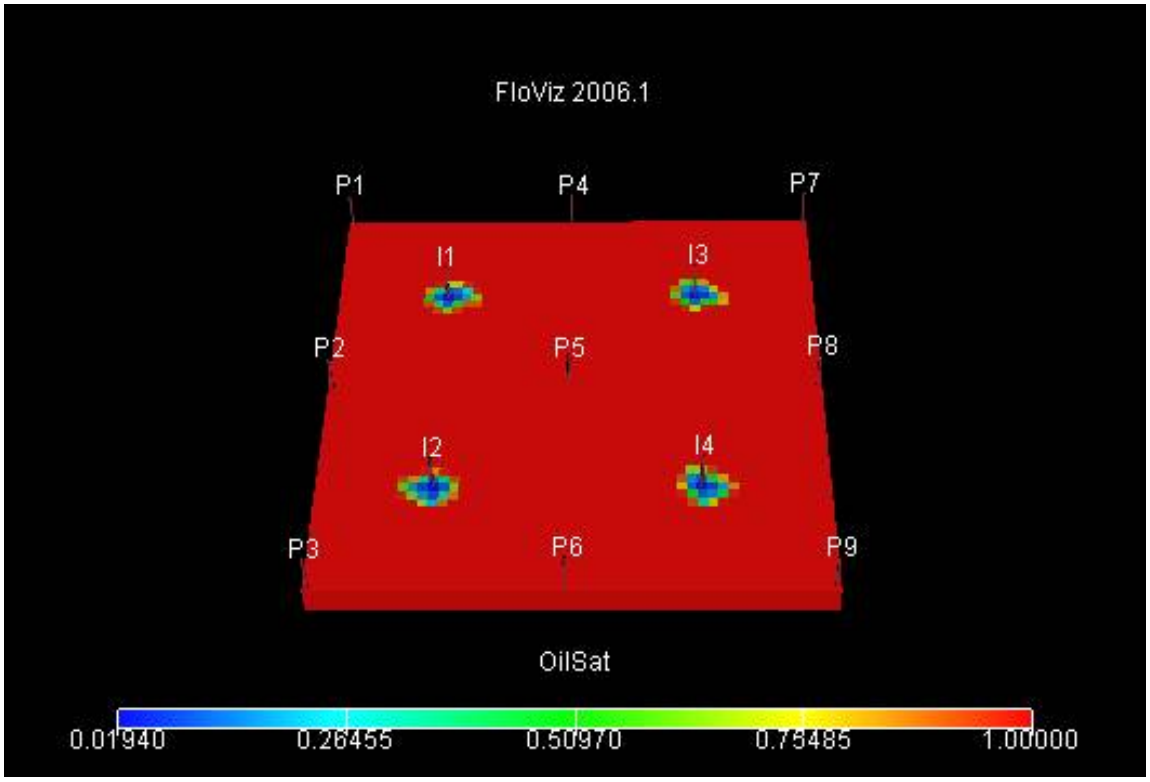

Figure 4.1: M1 model description

The second model (M2) is a 6 layers heterogeneous reservoir with anticline dome shape. The full field model dimension of M2 is 100 X 80 X 6 with 6561 active cells. Figure 4.2 illustrate the model.

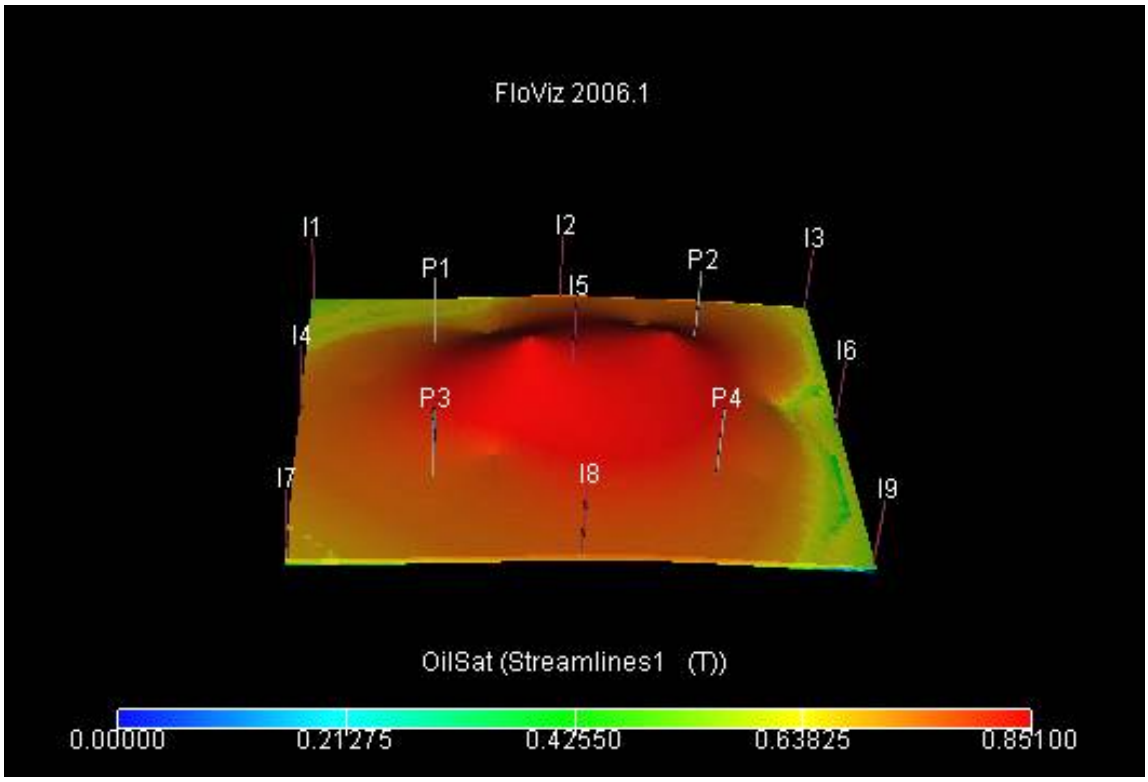

Figure 4.2: M2 model description

The last two models are real models in the Middle East. The full field model dimension of M3 is 100 x 190 x 24, with 411,237 active cells while M4 has the dimension 48 x 118 x 36, with 154,699 active cells. Figures 4.3 and 4.4 illustrate the respective models.

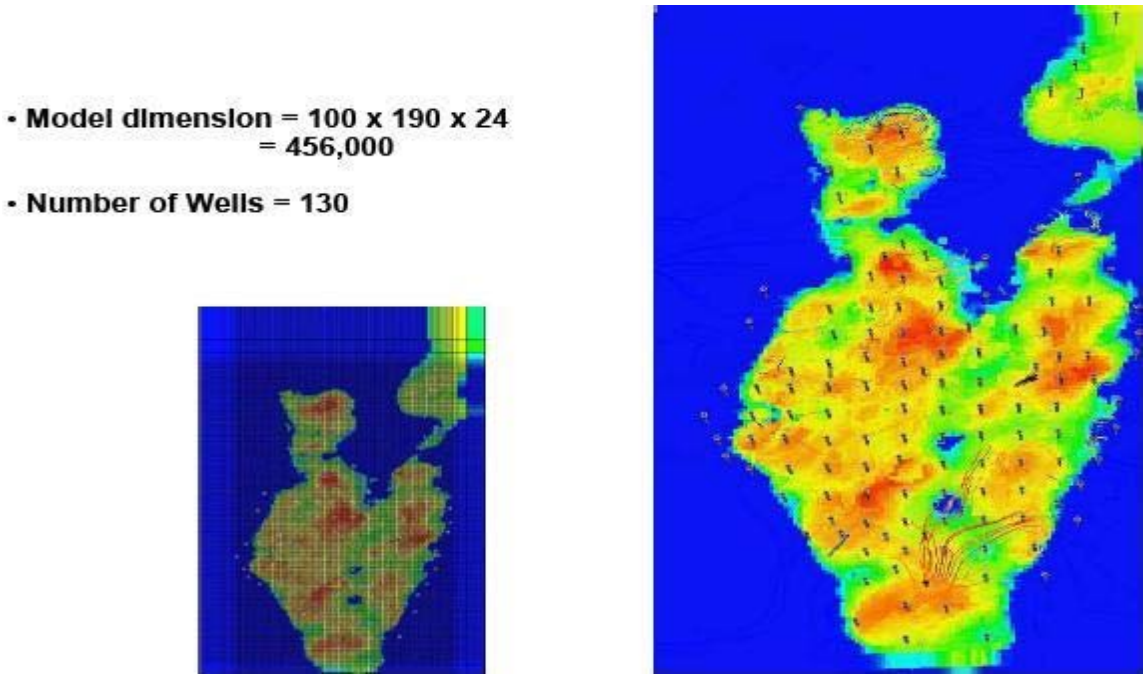

Figure 4.3: M3 model description

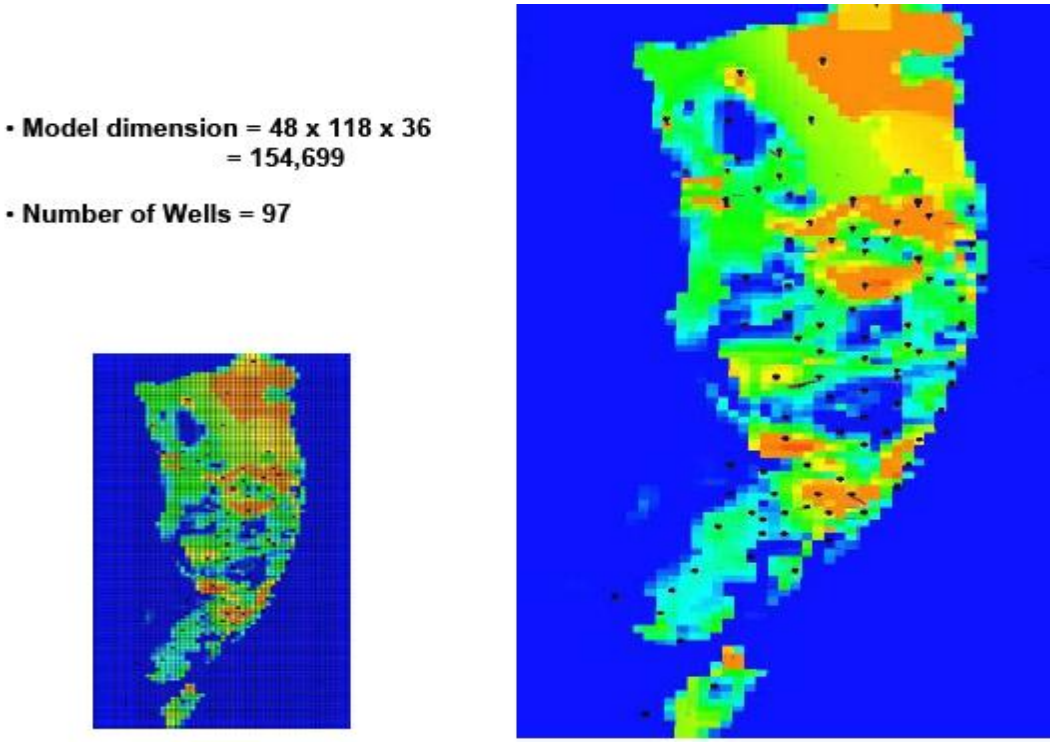

Figure 4.4: M4 model description

4.2.2 Reservoir Rock and Fluid Data

The four reservoir models are not having the same rock and fluid properties in order to make the comparisons in this study more realistic. The models characterizations and fluid properties are explained as follows:

4.2.2.1 (M1) Field Properties

Initial oil saturation data for the top layer of the field is shown in **Figure** 4.5.

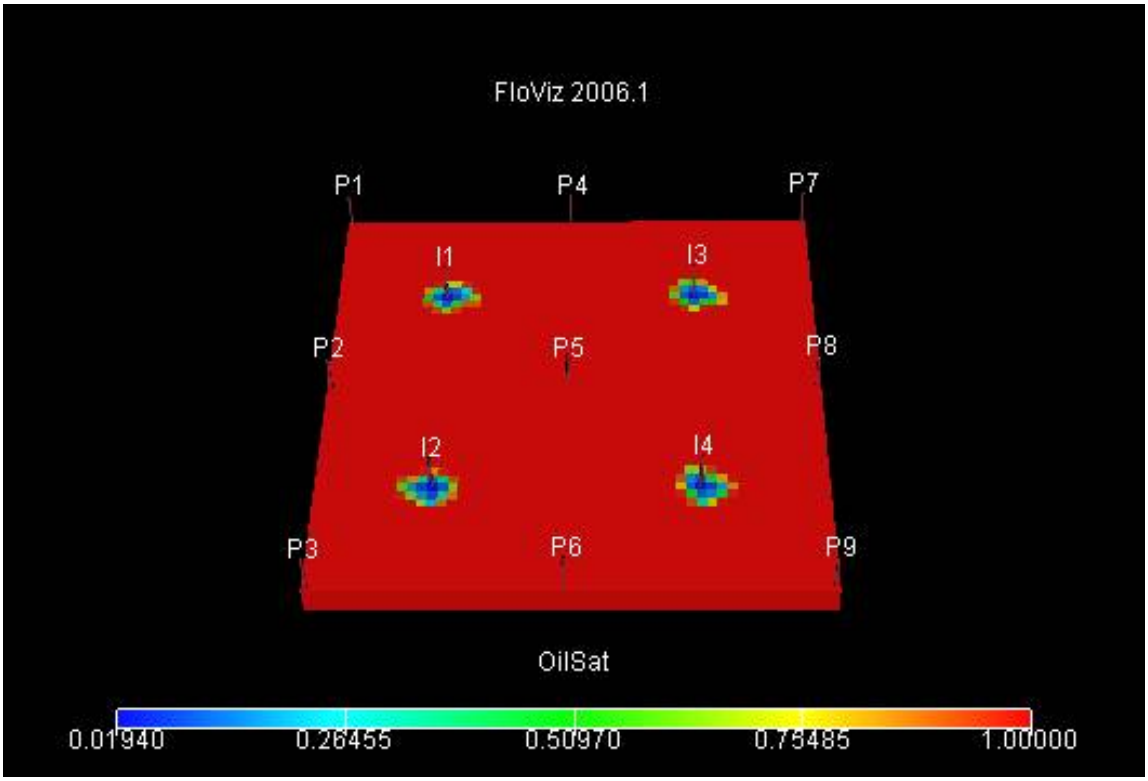

Figure 4.5: M1 Initial oil distribution

Water/oil and Gas/oil relative permeability data and capillary pressure data are shown in **Figures** 4.6 through 4.8.These curves were used to match the relatively fast moving water-front.

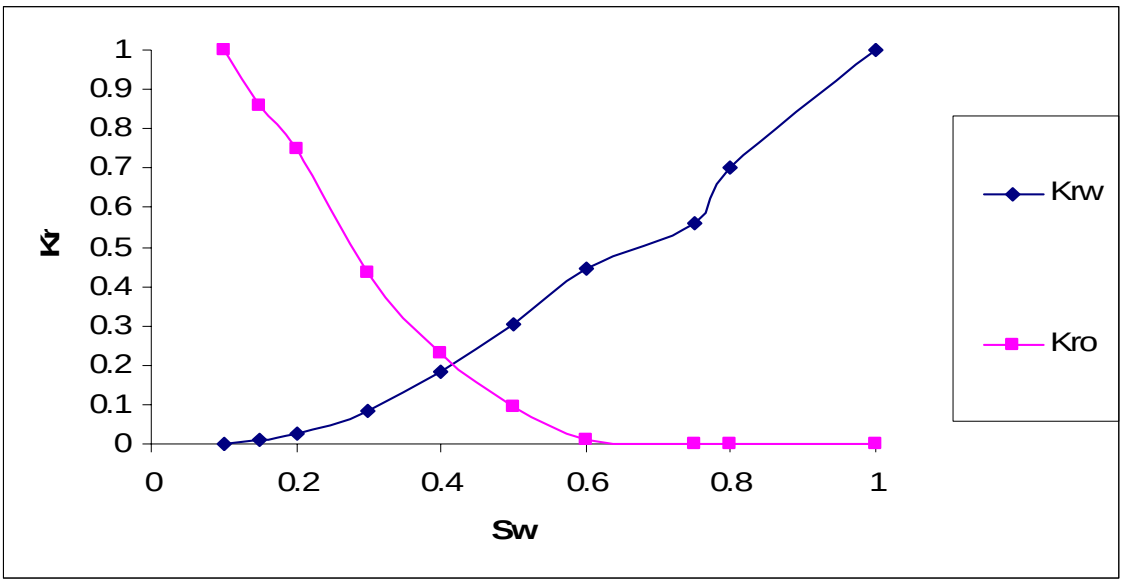

Figure 4.6: Water/oil relative permeability for M1

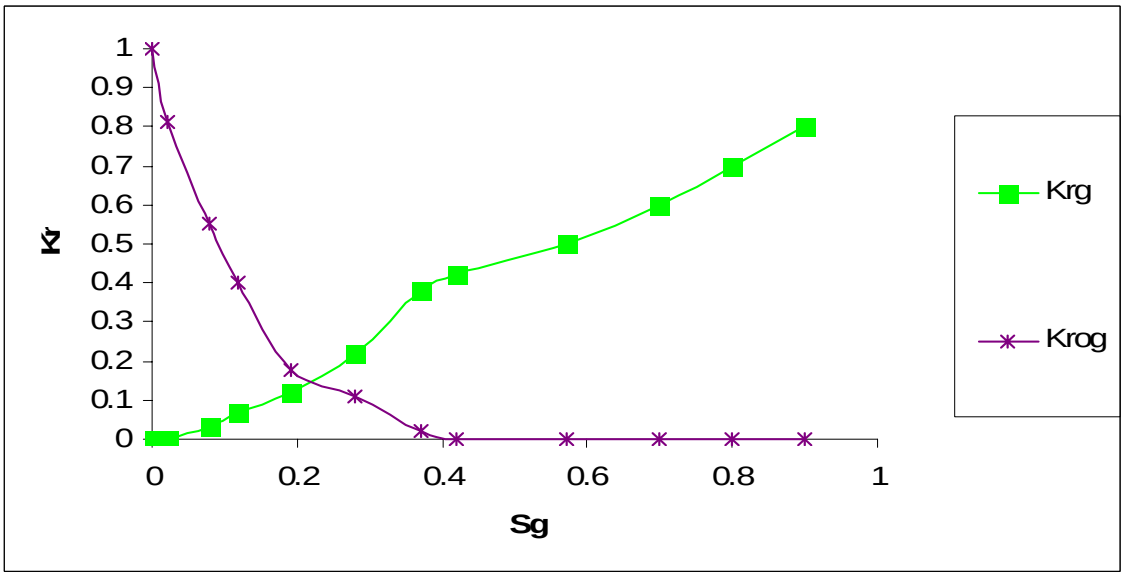

Figure 4.7: Oil/gas relative permeability for M1

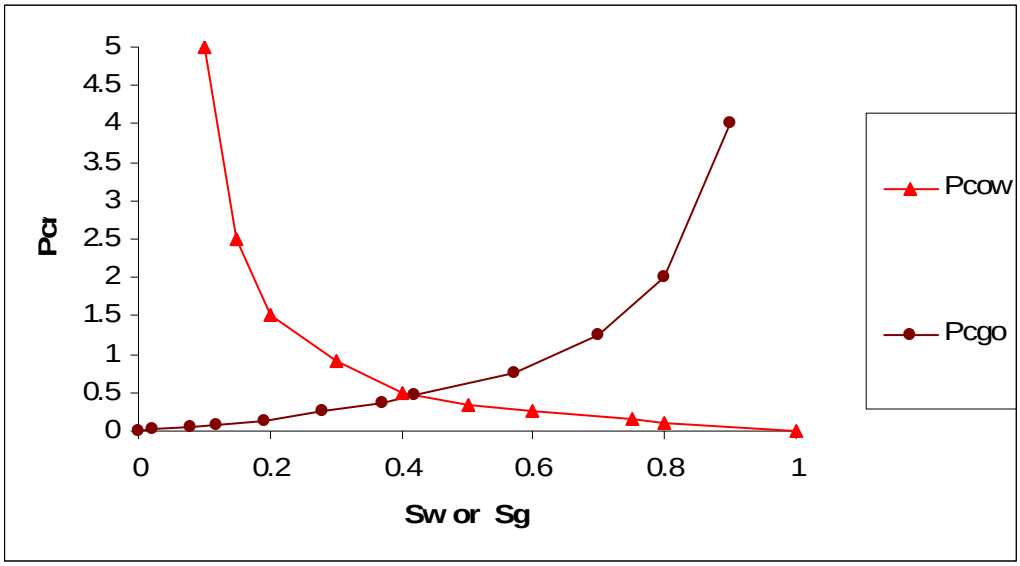

Figure 4.8: Capillary pressure curves for M1

It's important to mention that FrontSim does not incorporate capillary pressure. However, it has the option to use capillary pressure data for the generation of initial saturations distribution.

The gas gravity with respect to air at standard condition is 0.701. The water gravity with reference to pure water was specified as 1.004 at standard conditions. Water viscosity is 0.47 cp, the water formation volume factor Bw is 1.02 rb/stb. The permeability in Y and X directions is equal while in Z-direction it is multiplied by 0.1.

4.2.2.2 (M2) Field Properties

Initial oil saturation data for the top layer are shown in **Figure** 4.9. Permeability distributions of the first and second layers are shown in **Figure** 4.10 and **Figure** 4.11. The fluid and gas properties are explained in **Figure** 4.12 through **Figure** 4.18. These curves were used to match the relatively fast moving water-front.

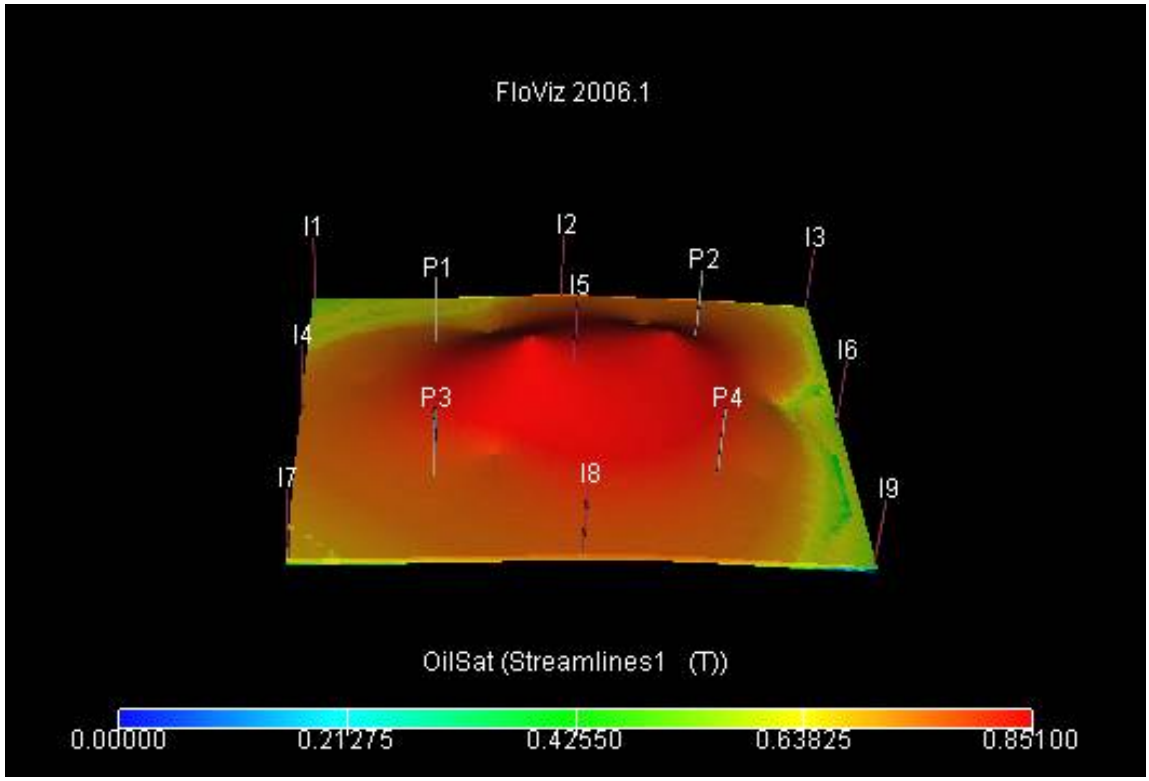

Figure 4.9: Initial oil saturation for top layer for M2

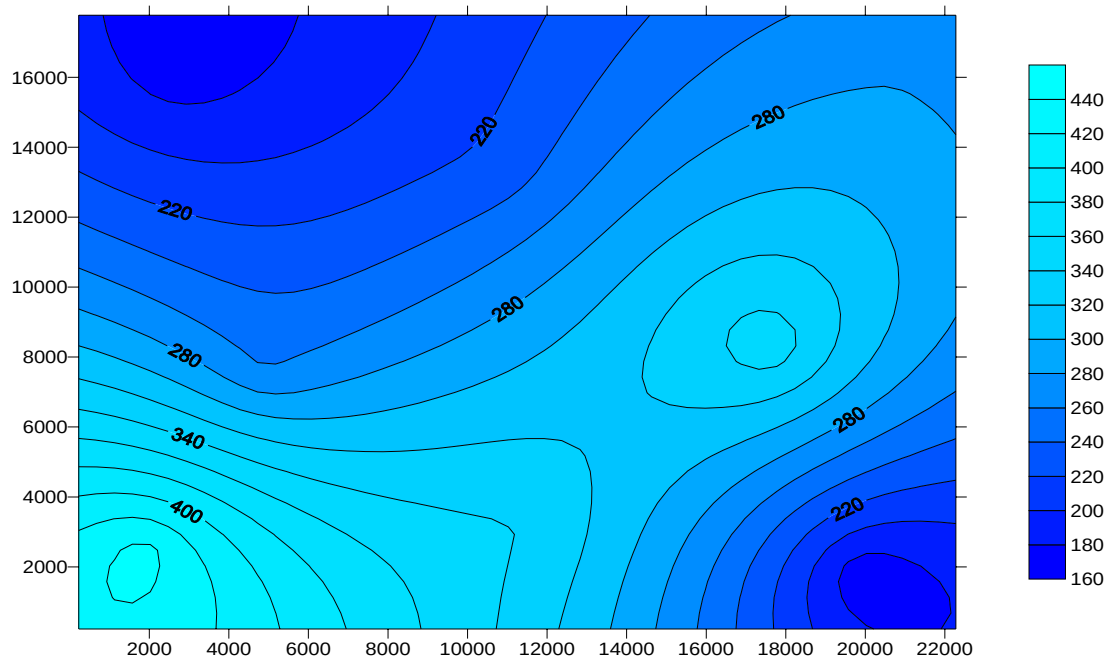

Figure 4.10: Permeability distribution of top layer in M2

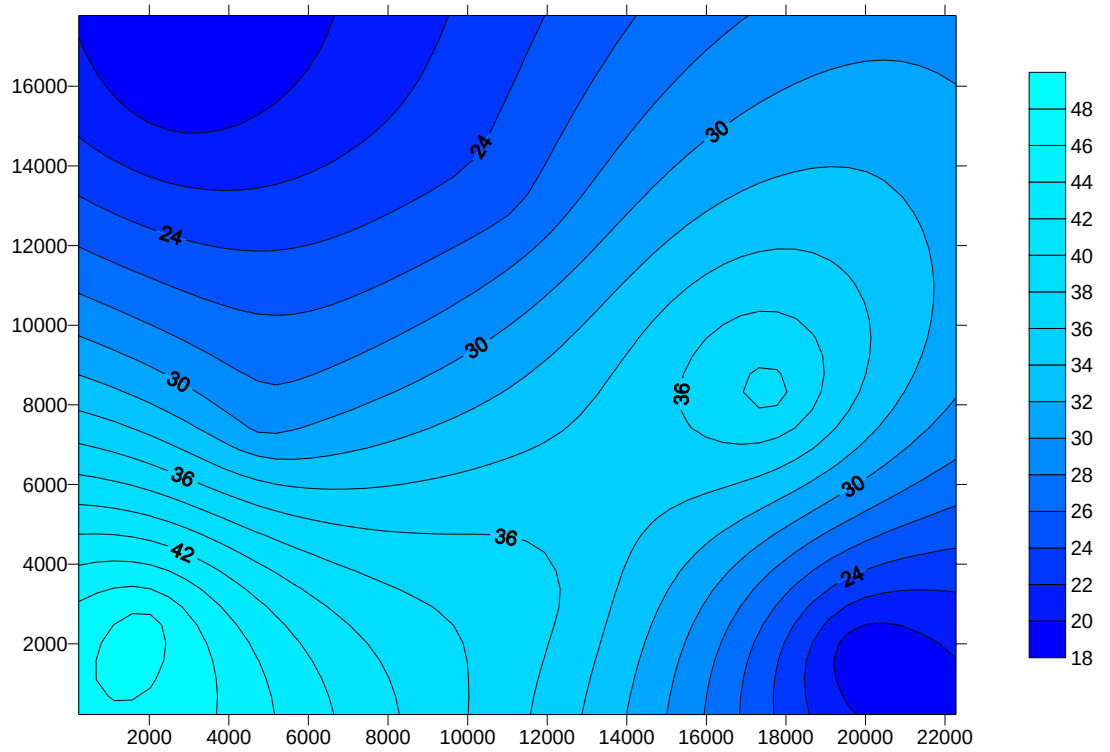

Figure 4.11: Permeability distribution of 2nd layer in M2

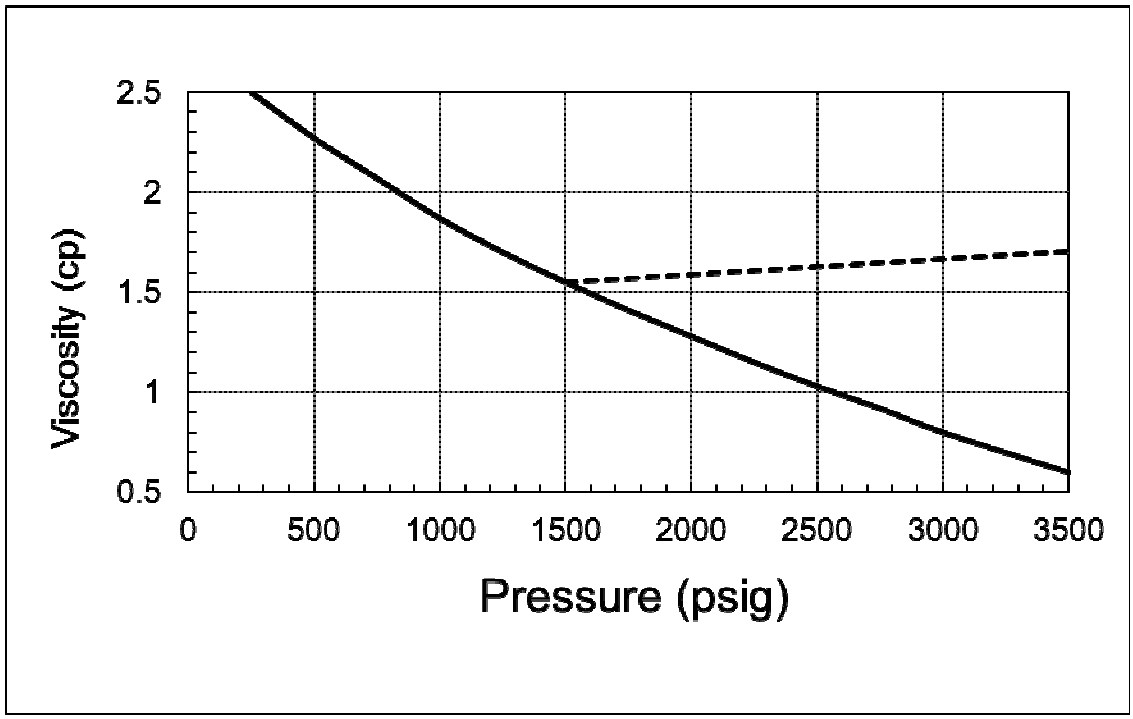

Figure 4.12: Oil viscosity profile in M2

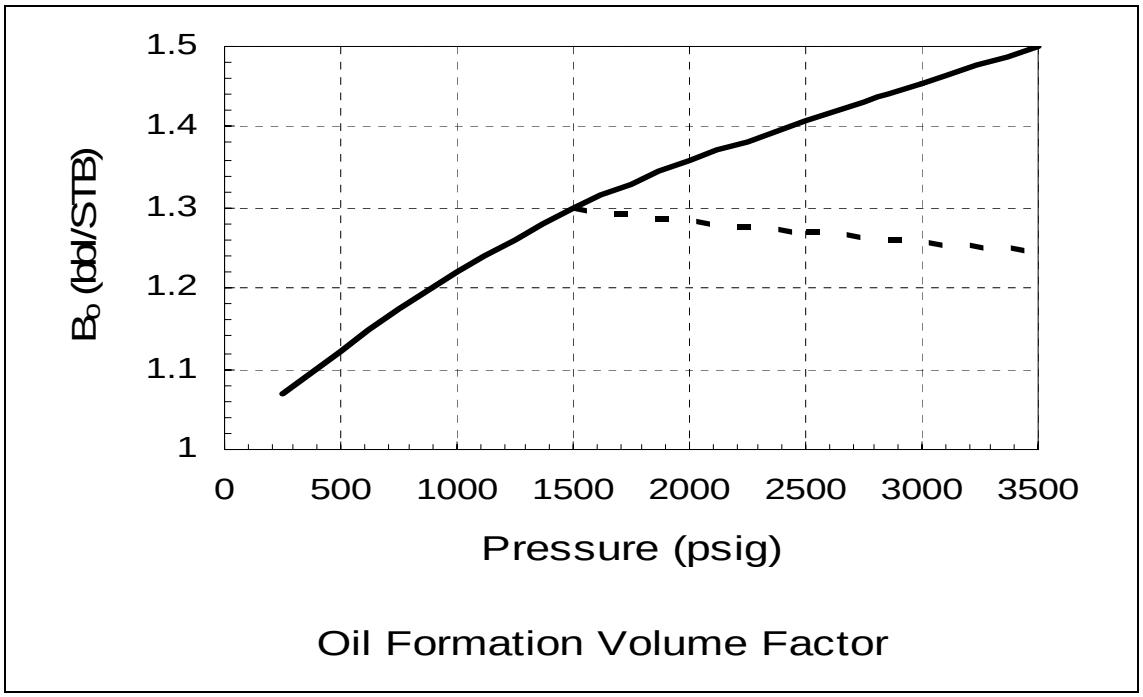

Figure 4.13: Oil formation volume in M2

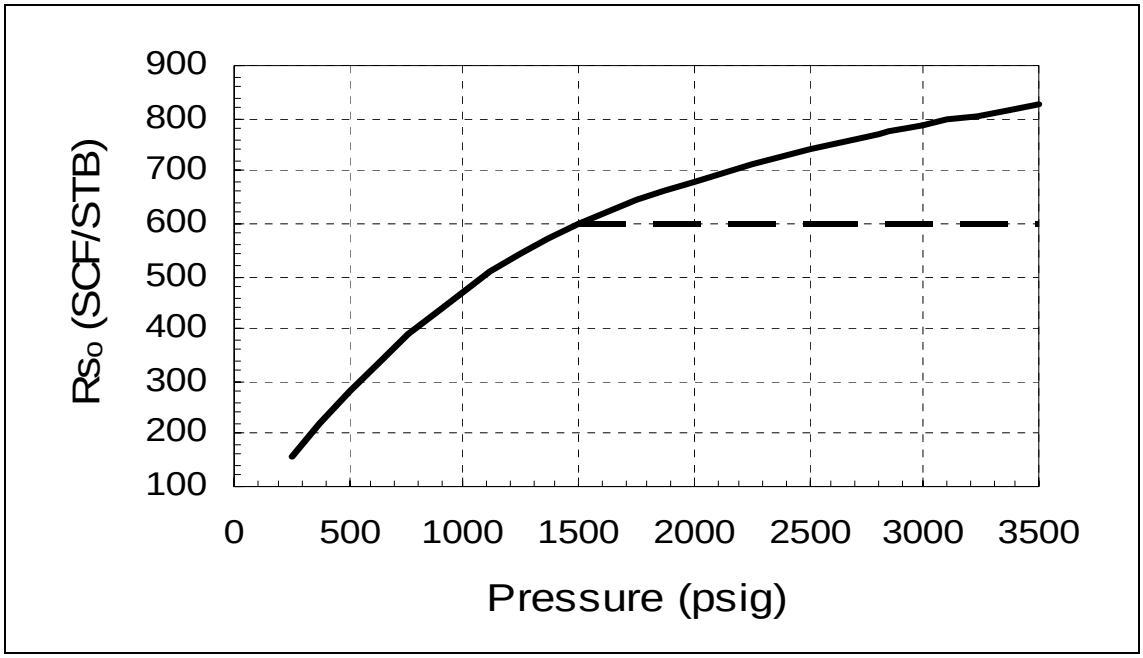

Figure 4.14: Solution gas-oil in M2

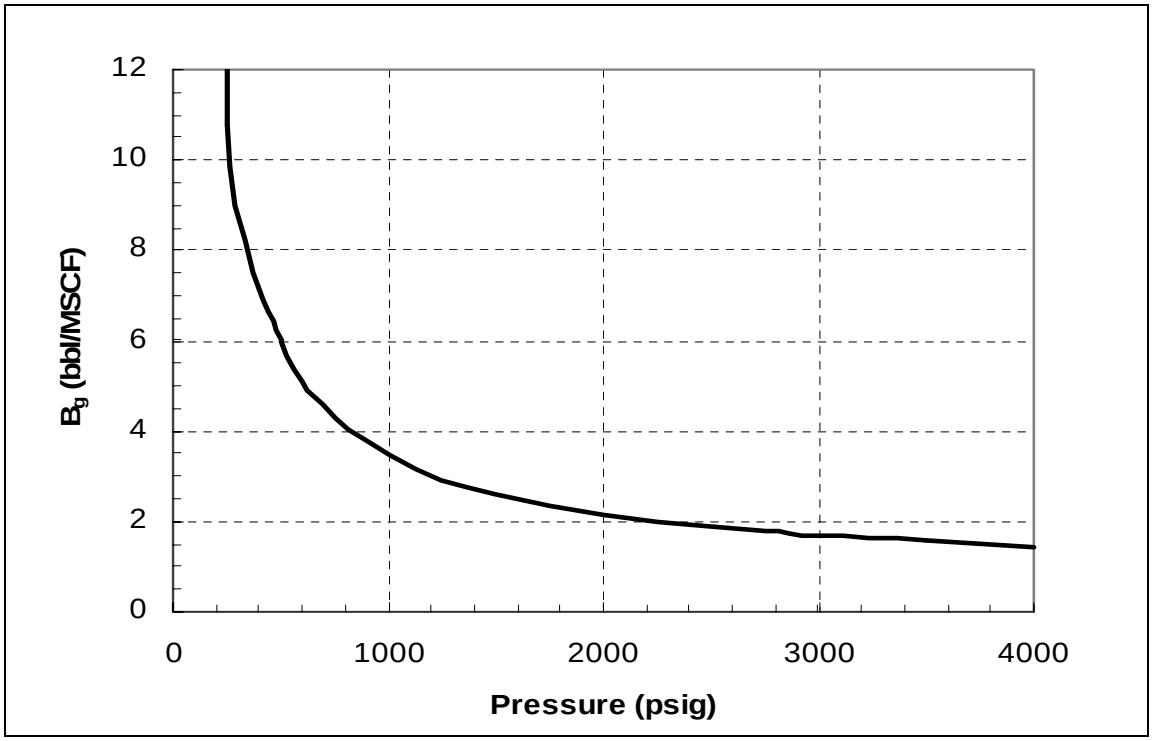

Figure 4.15: Gas formation volume in M2

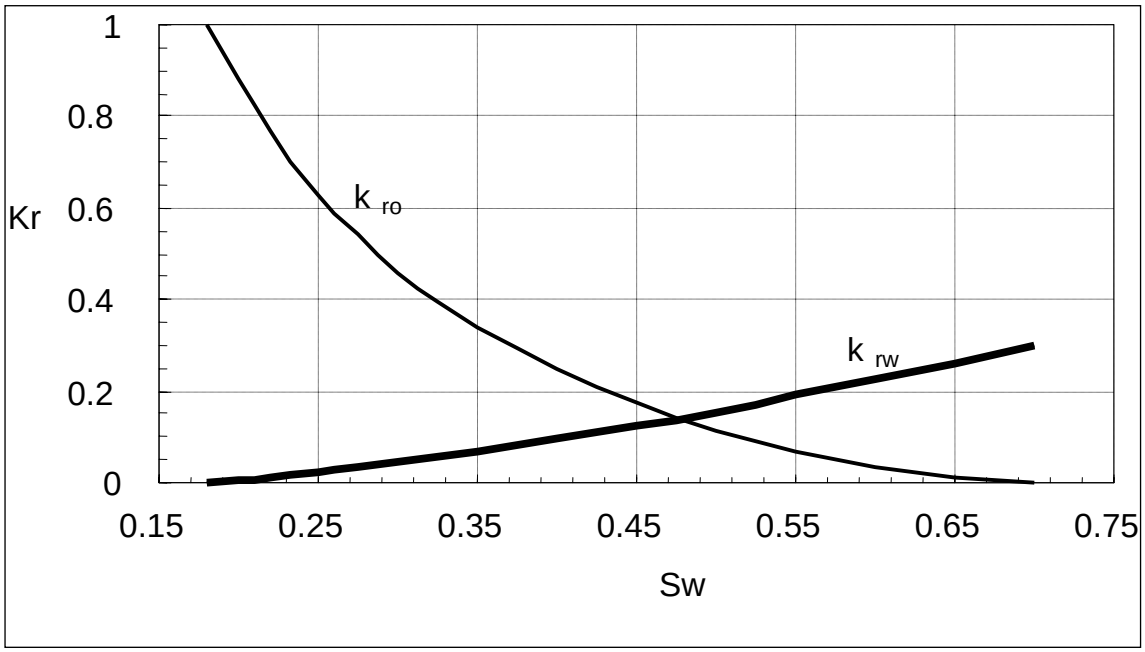

Figure 4.16: Oil/Water relative permeability in M2

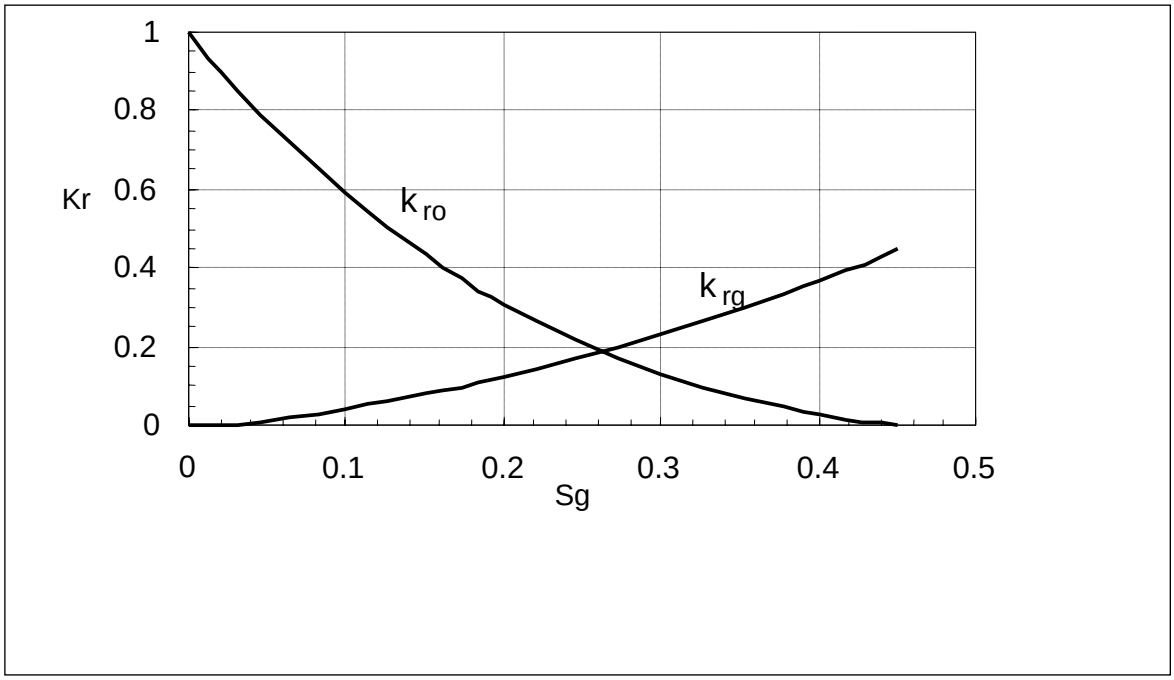

Figure 4.17: Oil/Gas relative permeability in M2

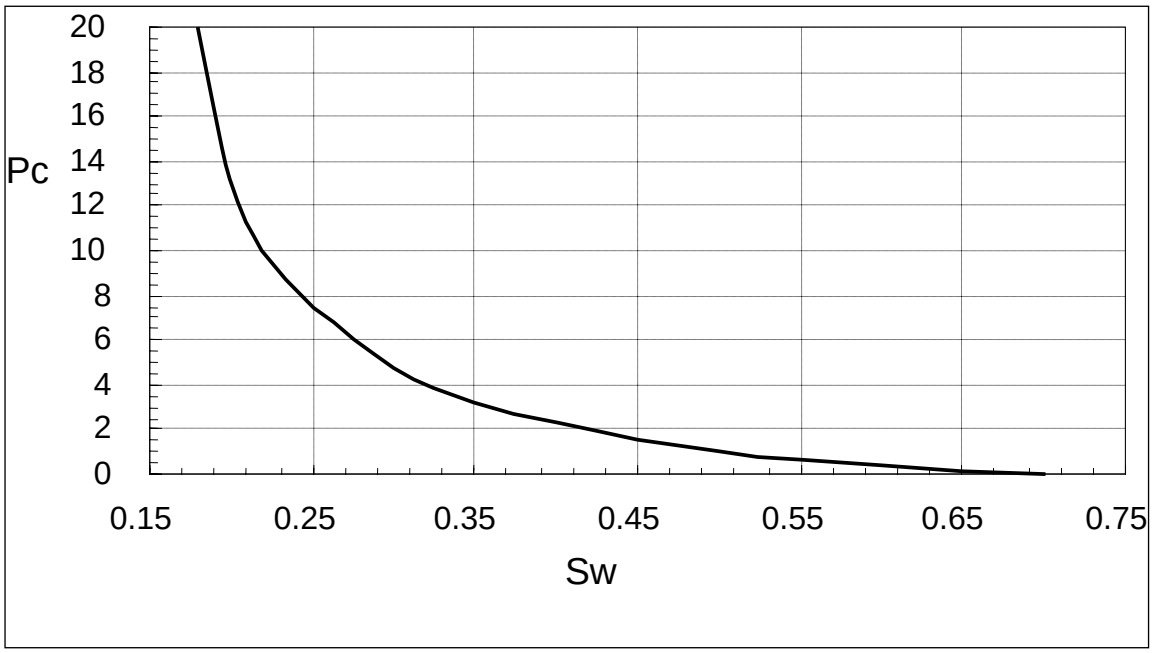

Figure 4.18: Capillary pressure in M2

FrontSim does not incorporate capillary pressure. However, it has the option to use capillary pressure data for the generation of initial saturations distribution. **Figure** 4.18 shows the capillary pressure data used in this study.

The behavior of formation volume factor (Bo: rb/stb) and viscosity (μ_o: cp) are depicted as a function of oil phase pressure in **Figure** 4.12 and **Figure** 4.13. Oil API gravity at standard conditions is 49.91.

Solution gas properties are given in **Figure** 4.14 and **Figure** 4.15 with the gas formation volume factor (B_g) and viscosity (μ_g) are depicted as function of pressure. The gas gravity with respect to air at standard condition is 0.701.

The water gravity with reference to pure water was specified as 1.004 at standard conditions. Water viscosity is 0.47 cp, the water formation volume factor Bw is 1.02 rb/stb. The permeability in Y and X directions is equal while in Z-direction it is multiplied by 0.6.

4.2.2.3 (M3) Field Properties

Permeability distribution in the X-direction and initial oil saturation data for the top layer of M3 field are shown in **Figures** 4.19 and 4.20 respectively.

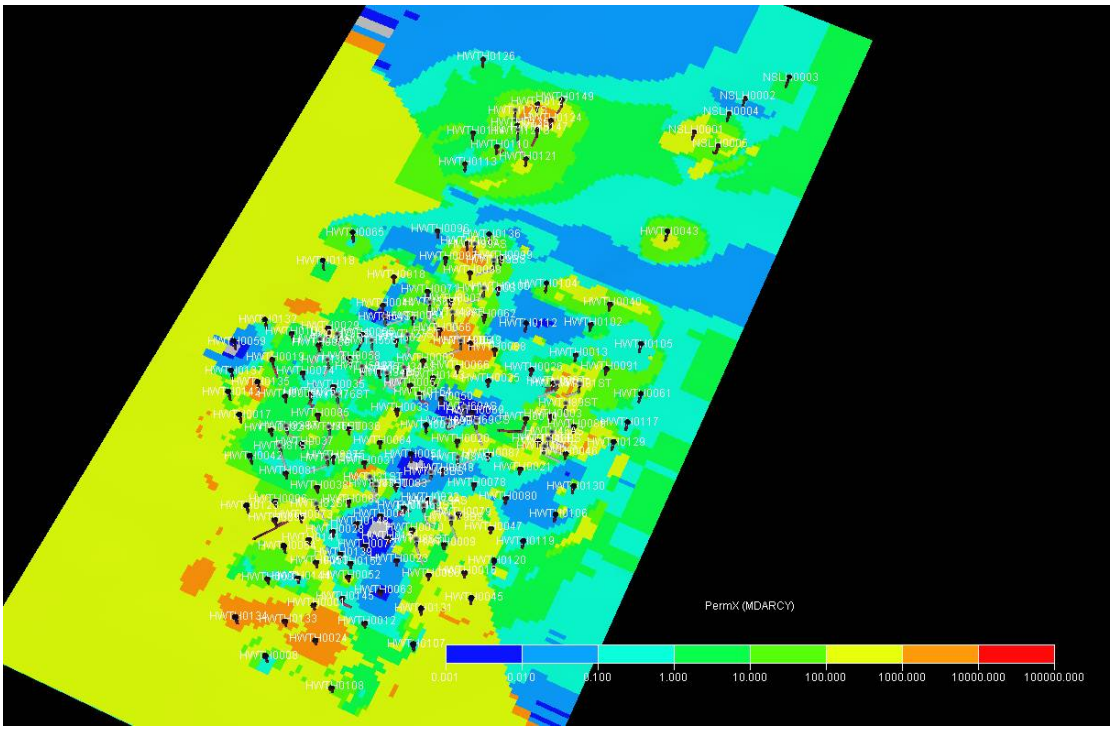

Figure 4.19: Permeability in X-Direction for M3 Field

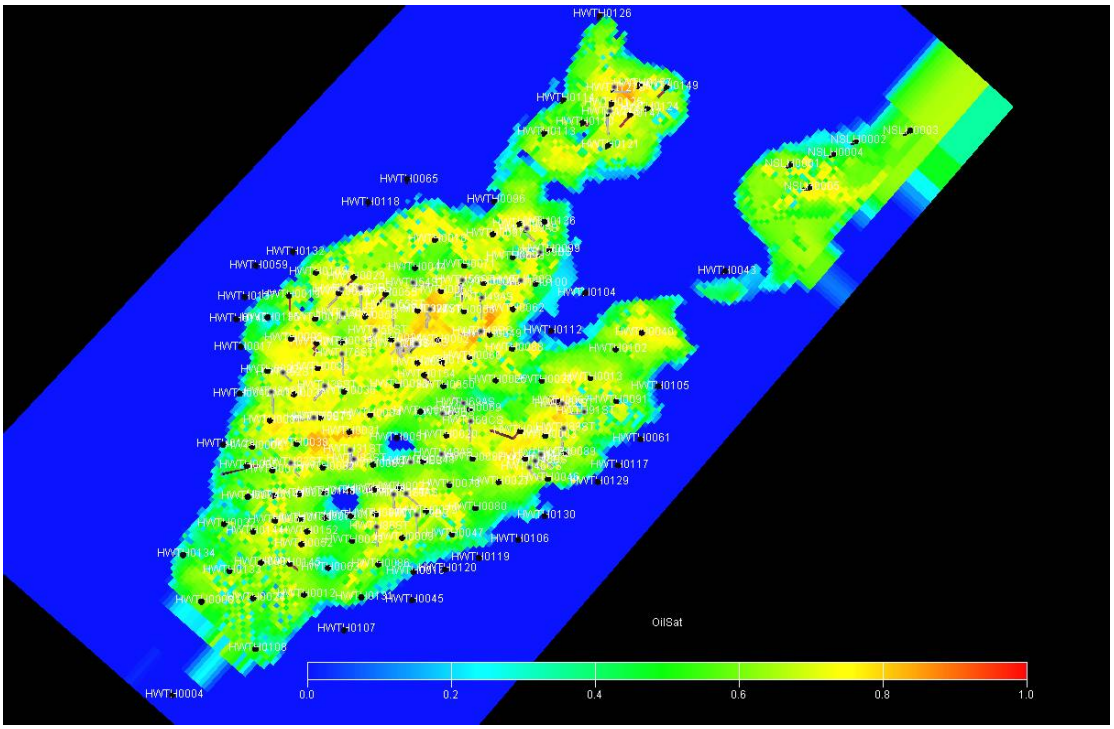

Figure 4.20: Initial oil saturation in X-Direction for M3 Field

The reservoir was divided into two saturation regions based on the initial streamline distribution. Water/oil and Gas/oil relative permeability data are shown in **Figures** 4.21 through 4.25.

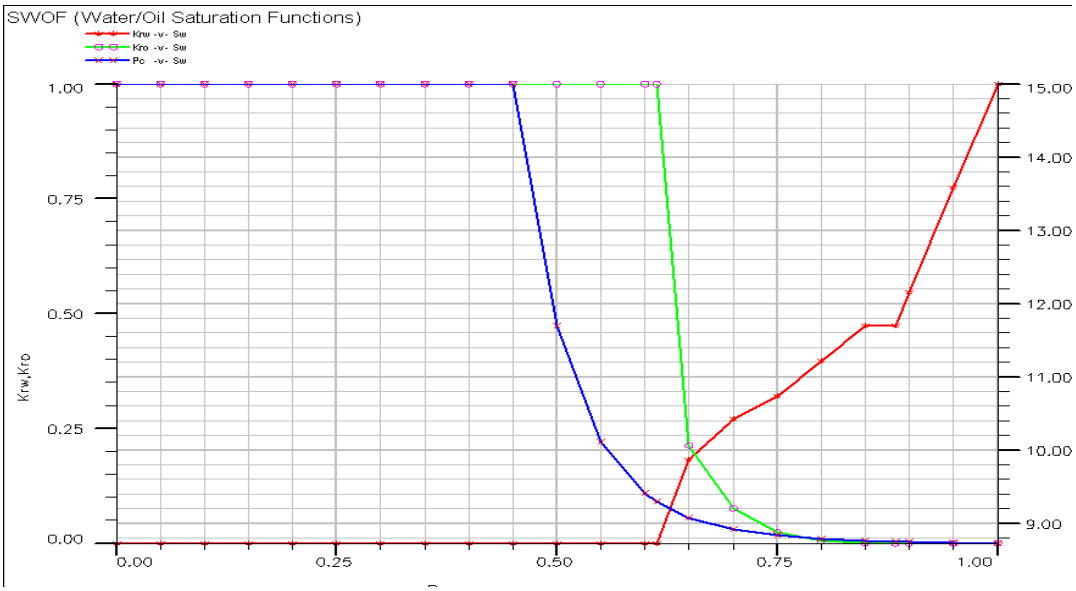

Figure 4.21: Water/Oil relative permeability and capillary pressure for saturation Region 1

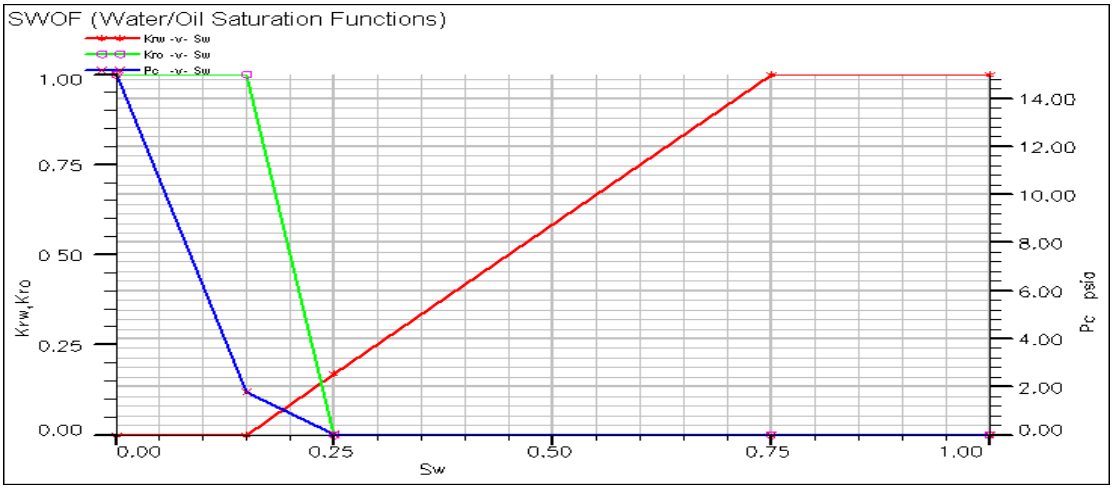

Figure 4.22: Water/Oil relative permeability and capillary pressure for saturation Region 2

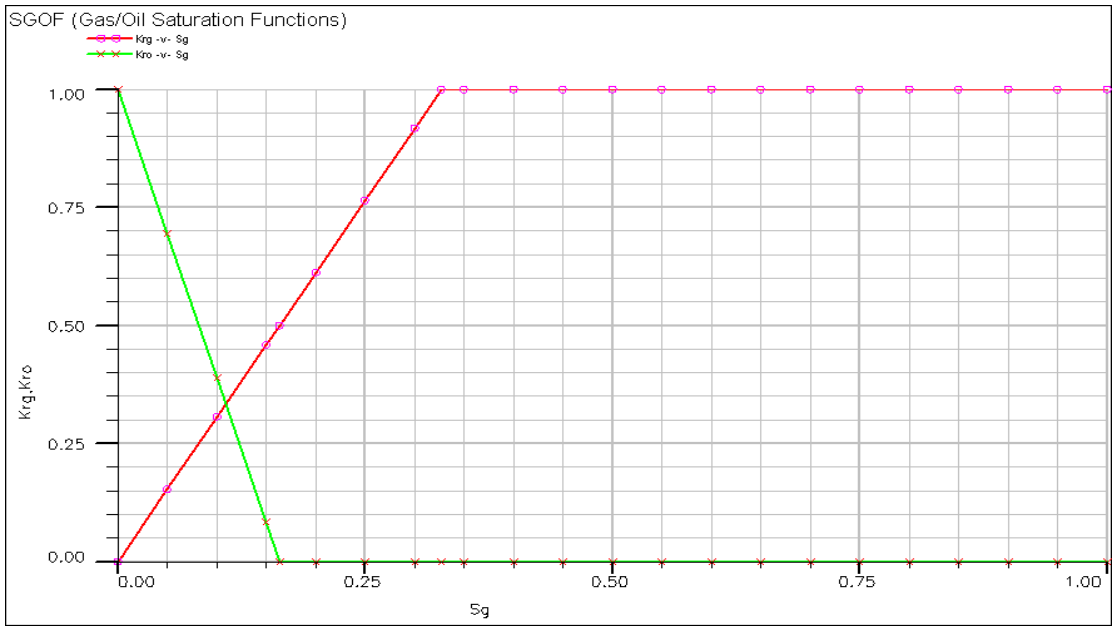

Figure 4.23: Gas/Oil relative permeability for saturation region-1.

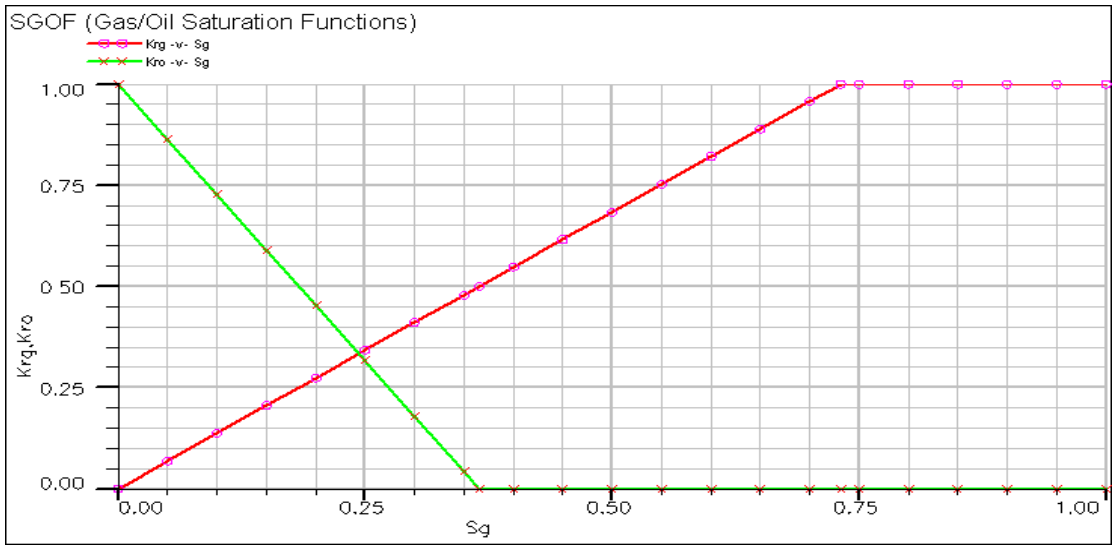

Figure 4.24: Gas/Oil relative permeability for saturation region-2.

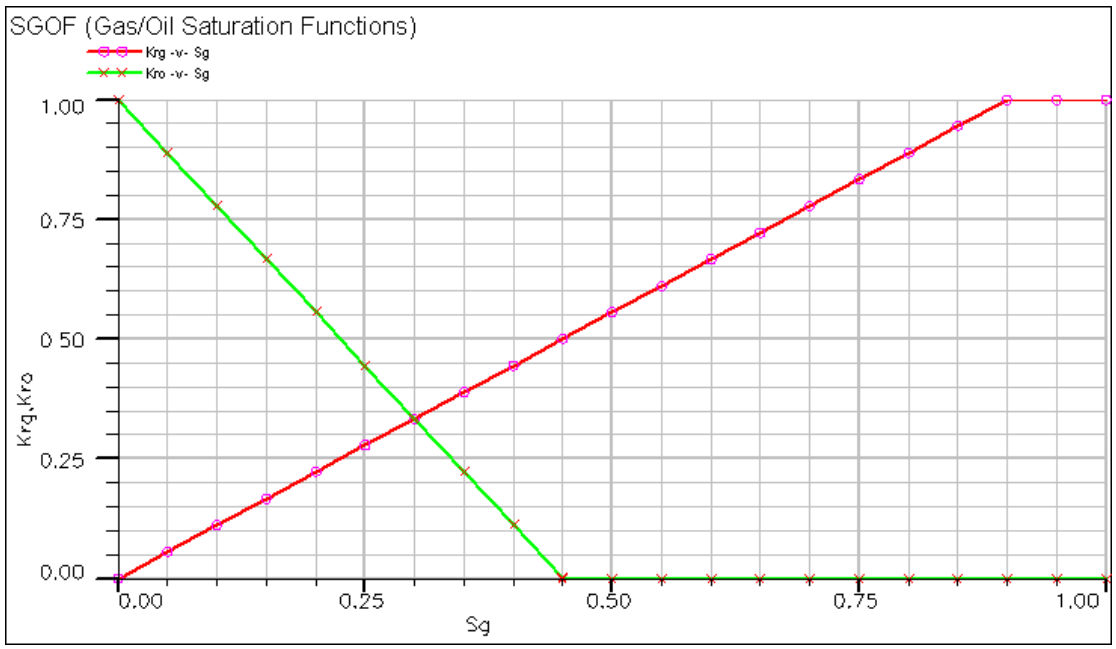

Figure 4.25: Gas/Oil relative permeability for saturation

FrontSim does not incorporate capillary pressure. However, it has the option to use capillary pressure data for the generation of initial saturations distribution. **Figures** 4.21 through 4.22 show the capillary pressure data used in this study.

Dead oil properties are shown in **Figure** 4.26. The behavior of formation volume factor (Bo: rb/stb) and viscosity (μ_o: cp) are depicted as a function of oil phase pressure in figure 4.26. Oil API gravity at standard conditions has been fixed at 49.91.

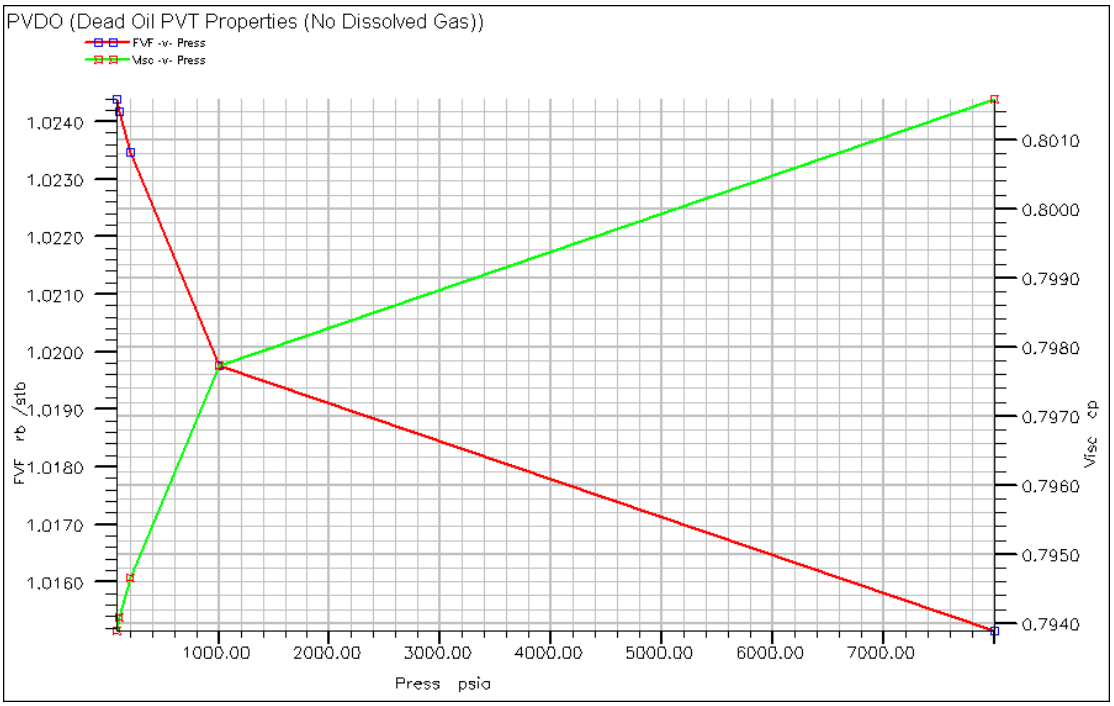

Figure 4.26: Dead oil PVT properties of M3

Dry gas properties are given in **Figure** 4.27 with the gas formation volume factor Bg (Mscf/stb) and viscosity (μ_g:cp) depicted as a function of gas phase pressure. The gas gravity with respect to air at standard condition is 0.701.

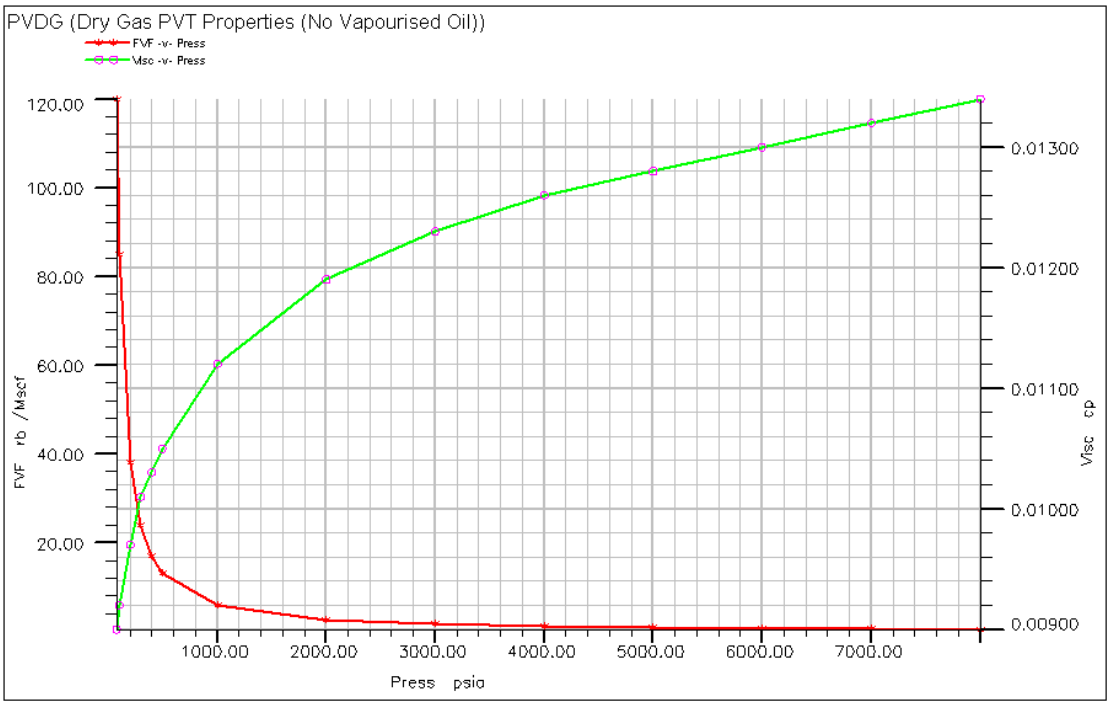

Figure 4.27: Dry gas PVT properties of M3

The water gravity with reference to pure water was specified as 1.0040 at standard conditions. Water viscosity is 0.47 cp, the water formation volume factor Bw is 1.02 rb/stb and water compressibility is 3.0 x 10^{-6} psi^{-1} at a reference pressure of 2675 psia.

4.2.2.4 (M4) Field Properties

Permeability and initial oil saturation data for the top layer of M4 Field are shown in **Figures** 4.28 and 4.29 respectively.

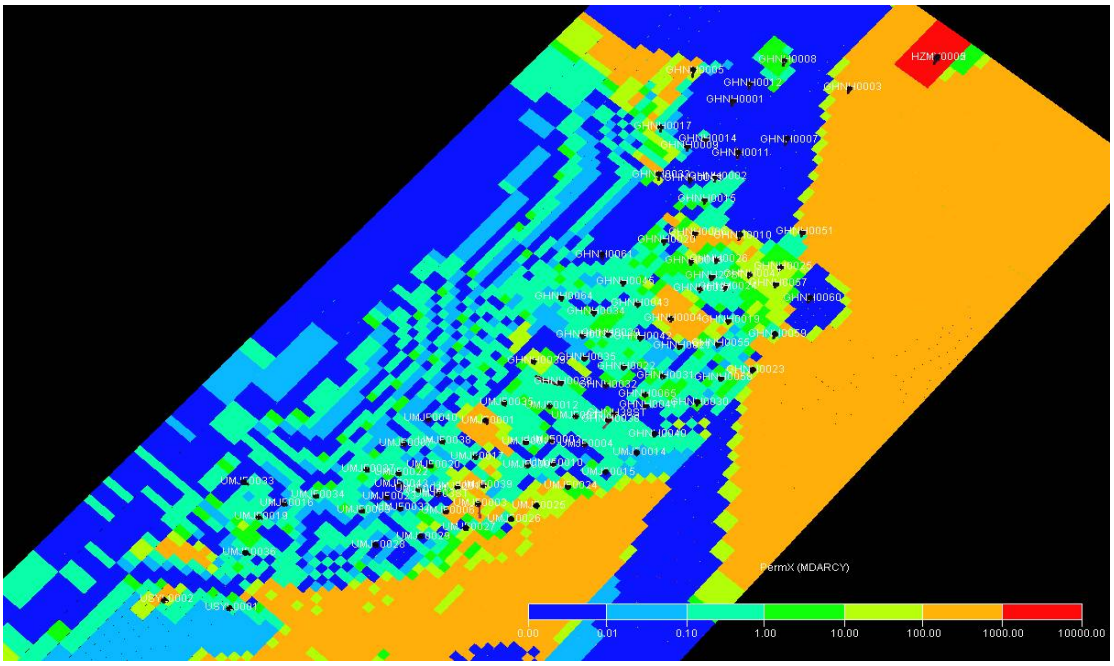

Figure 4.28: Permeability in X-Direction for M4 Field

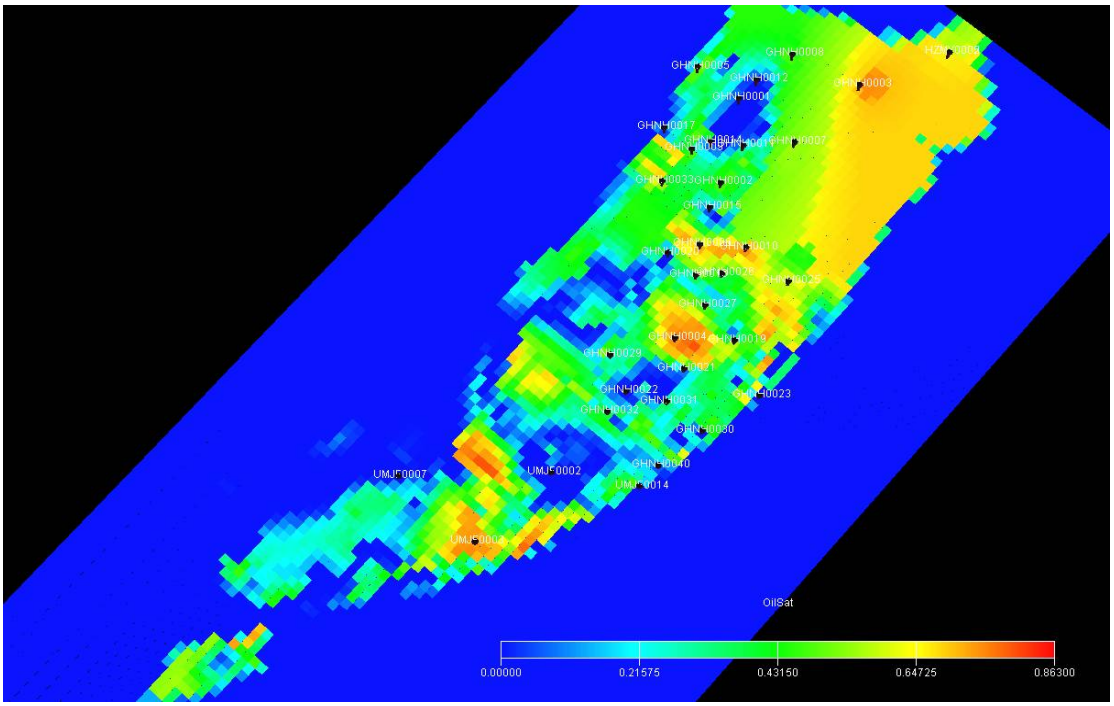

Figure 4.29: Initial oil saturation X-Direction for M4 Field

The reservoir was divided into two saturation regions. Water/oil and Gas/oil relative permeability data are shown in **Figures** 4.30 through 4.33. These curves were used to match the relatively fast moving water-front in a similar approach to the one used for M4 field.

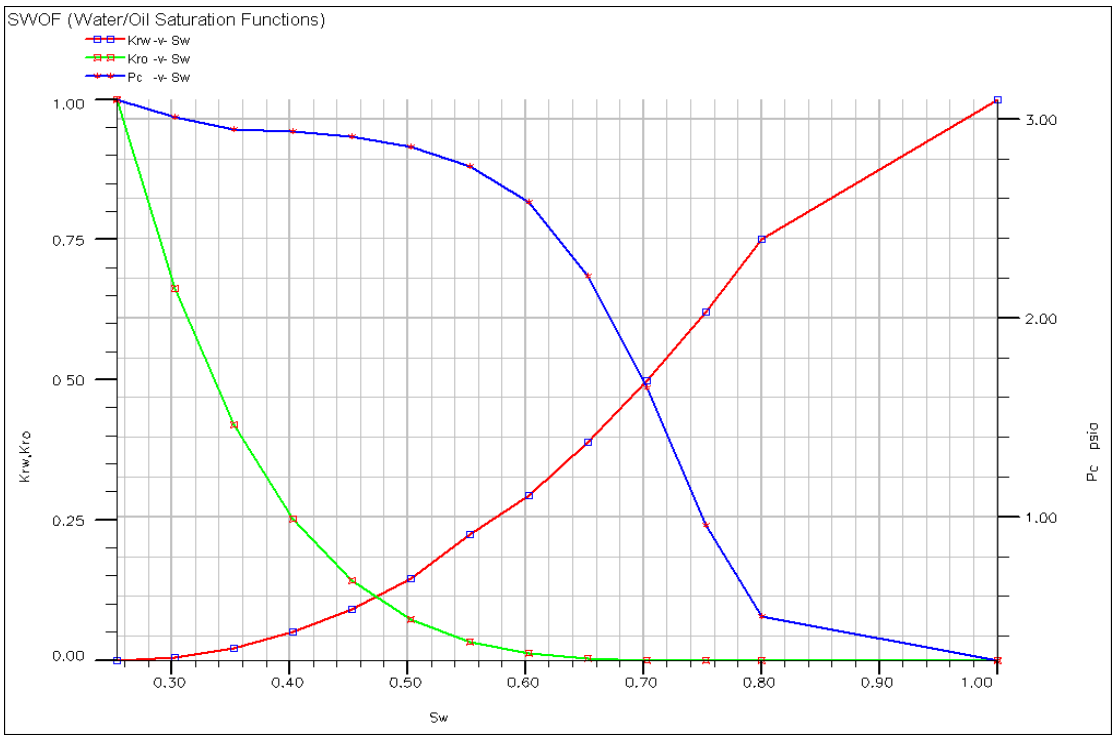

Figure 4.30: Water/Oil relative permeability and capillary pressure for saturation region-1.

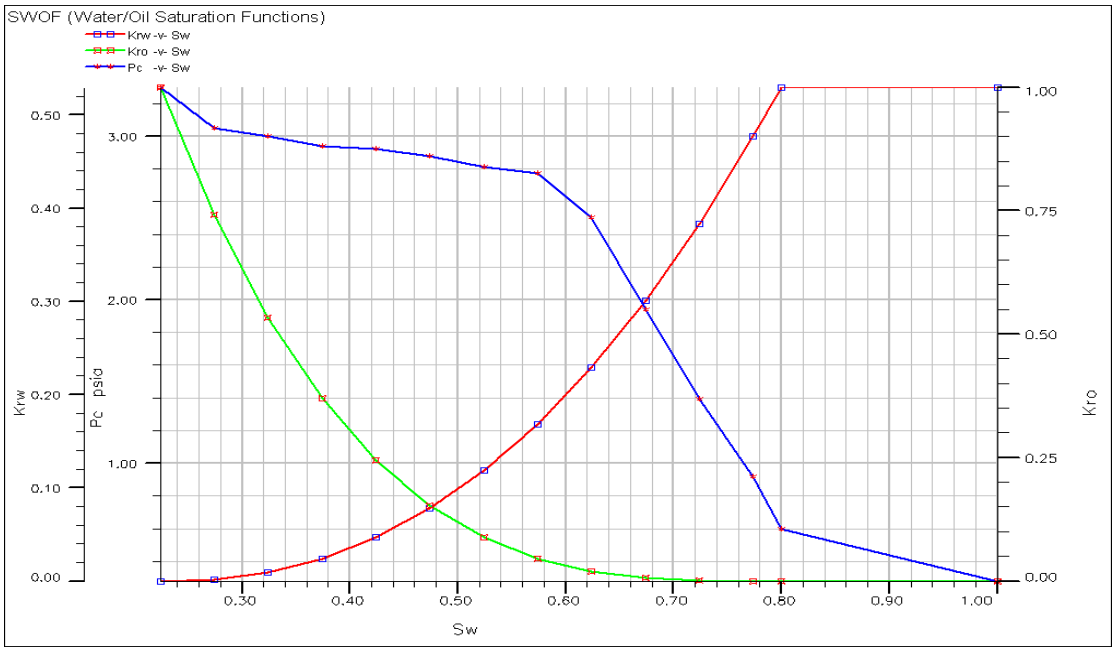

Figure 4.31: Water/Oil relative permeability and capillary pressure for saturation region-2.

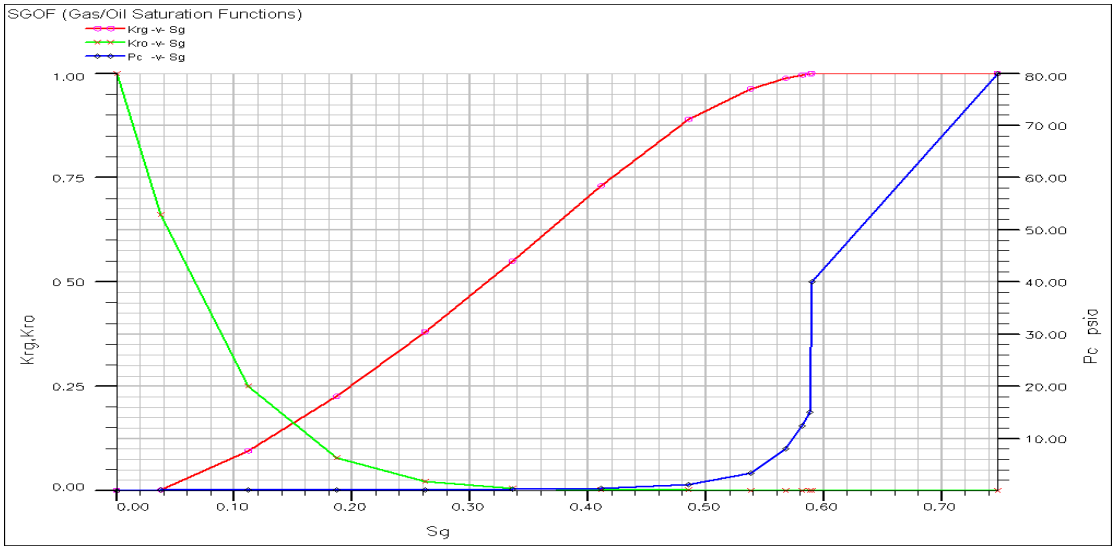

Figure 4.32: Gas/Oil relative permeability for saturation region-1.

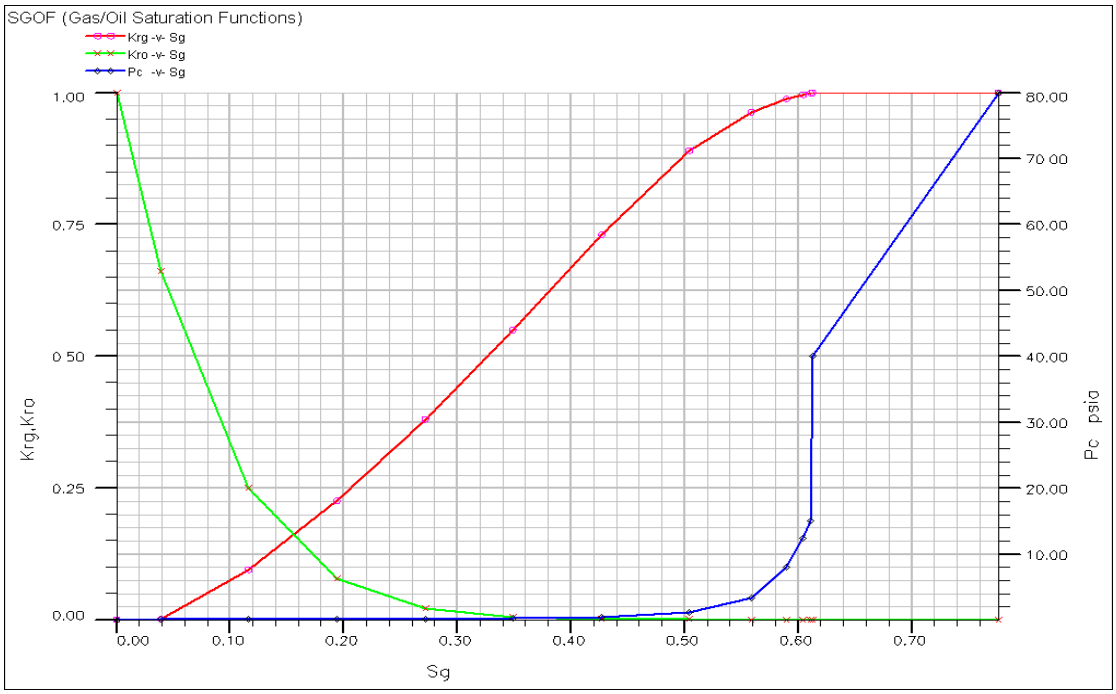

Figure 4.33: Gas/Oil relative permeability for saturation region-2.

Again and as mentioned in the corresponding section related to M4, FrontSim does not incorporate capillary pressure. However, it has the option to use capillary pressure data for the generation of initial saturation distribution. **Figures** 4.30 through 4.33 show the capillary pressure data used in this study.

Oil properties are shown in **Figure** 4.34. The behavior of formation volume factor (Bo: rb/stb) and viscosity (μ_o: cp) are depicted as a function of oil phase pressure in **Figure** 4.34. Oil API gravity at standard conditions is fixed at 49.91.

Dry Gas properties are shown in **Figure** 4.35 with the gas formation volume factor (Bg: Mscf/stb) and viscosity (μ_g: cp) depicted as a function of gas phase pressure. The gas gravity with respect to air at standard condition is 0.701.

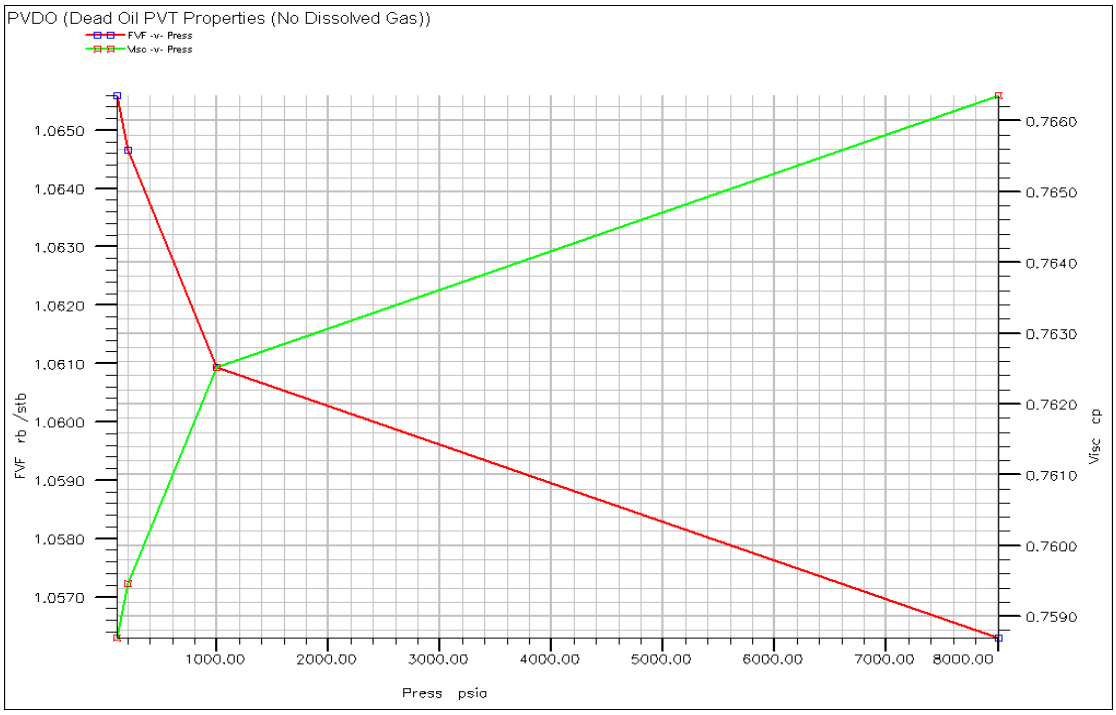

Figure 4.34: Dead oil PVT properties of M4 Field

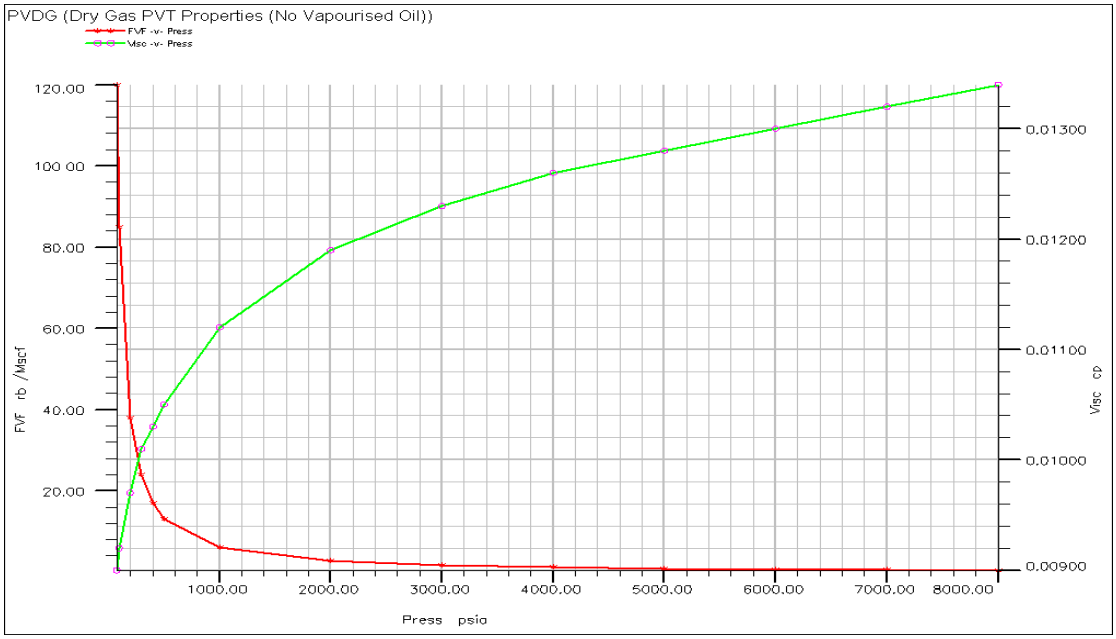

Figure 4.35: Dry gas PVT properties of M4 Field

The water gravity with reference to pure water was specified as 1.0040 at standard conditions. Water viscosity is 0.47 cp, the water formation volume factor Bw is 1.020 rb/stb and water compressibility is 3.0×10^{-6} psi^{-1} at a reference pressure of 2607 psia.

4.2.3 History Matching Data

The recurrent data used in the Eclipse model were translated into FrontSim format (SCHEDULE section). For the first two models (M1 and M2) no history was available for these models. On the other hand, for both real models M3 an M4 monthly production/injection data from August 1994 until December 2004 were available and were also used in the streamline simulation study.

Three phase data sets frequently need tuning to avoid divergence. The most common signs are lack of convergence due to high material balance errors or unphysical solution values. These can often be solved by using the suited solution techniques from Explicit for one of the following solution methods: AIM, IMPES or fully implicit methods. In this case the fully implicit solution technique was used for the FrontSim simulation runs. More details about these methods are explained in Appendix B.

4.2.4 Grid Data

The originally created Eclipse model utilizes block-centered (BC) grid geometry while in FrontSim only corner-point (CP) geometry is to be used. There are several ways to specify corner point geometry (**Figure** 4.36).

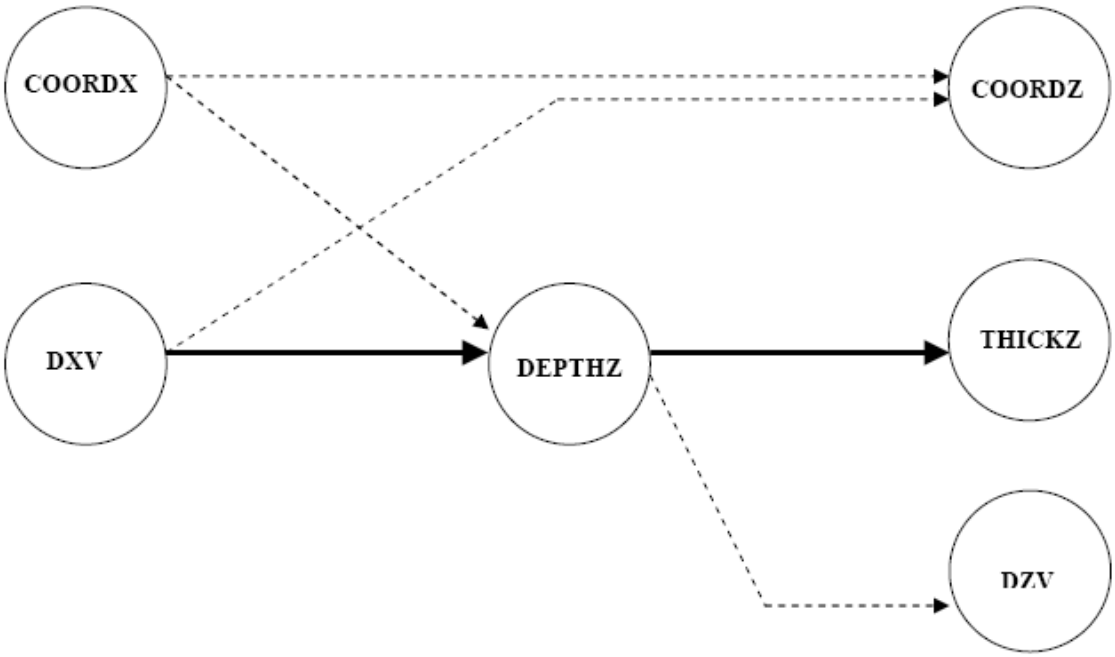

Figure 4.36: Corner point geometry used in FrontSim.

A description of a method used in this study to convert BC grid geometry to CP geometry follows:

XYZ coordinates of each one of the eight nodes in a block must be specified. This is done in FrontSim with the keywords COORD and ZCORN which are compatible with ECLIPSE. GridSim module was used to convert the grid geometry to corner-point.

However, the simulation from both FrontSim and Eclipse showed problems due to grids overlapping [5].

In order to overcome this issue Ghori [5] introduced a mechanism to avoid overlapping and to construct an acceptable Corner Point grid system close enough to the Center Point grid system. Following is the procedure that was employed in the conversion:

1. The base corner-point grid from the original block-centered model was imported into the **GRID** program and the following data were exported: SPECGRID, DXV, DYV, TOPS (within BOX limits for top layer only), DZ (full grid) and ACTNUM as GRDECL file.

2. The resulting GRDECL file was renamed to CPG.FILL and edited to include the appropriate controls for the **FILL** program. The **FILL** program was run to create a new "include file" defining the grid corner-point geometry: CPG.FILLED (Details of Fill file).

3. The new grid geometry was "healed" so that there were no faults and no *NNCs* in the grid. Also, use of a single layer of TOPS values has removed the problems with overlapping cells that occurred in the previous model.

4. The changes to the cell corner points have resulted in some small differences in pore volumes compared to the original model. This has been resolved by importing the original pore volumes (PV_{ijk}^{old}) into the **GRID** program. The new

cell volumes (CV_{ijk}^{new}) were calculated using a dummy porosity value of 1.0 and the corrected porosity obtained by calculating:

$$\phi_{ijk}^{new} = PV_{ijk}^{old} / CV_{ijk}^{new}$$

Where,

ϕ_{ijk}^{new} = new cell porosity,

PV_{ijk}^{old} = old cell pore volume, and

CV_{ijk}^{new} = new cell bulk volume.

5. The corrected porosity was exported into PORO_NEW.GRDECL and was included at the end of the GRID section in the ECLIPSE deck, to overwrite the porosities given in any other included files.

The new grid system has the same connectivity in *I* and *J* directions as the original grid (with possible minor changes to the transmissibility values). However, the grid has been reconstructed to remove the problem of overlaps and this may have some effects on connectivity in the K direction (e.g. some gaps may be removed or some pinch-outs may change).

4.2.5 Validation of Grid geometry

In order to validate the new corner point geometry, the simulation results of both grid systems were compared with the simulation results from block-centered geometry using Eclipse. **Figures** 4.37 through 4.39 show the comparison between the two grid

systems in M3 model. It can be seen from **Figures** 4.37 through 4.39 that the new corner-point geometry reproduces simulation results which are in excellent agreement with the block-centered geometry.

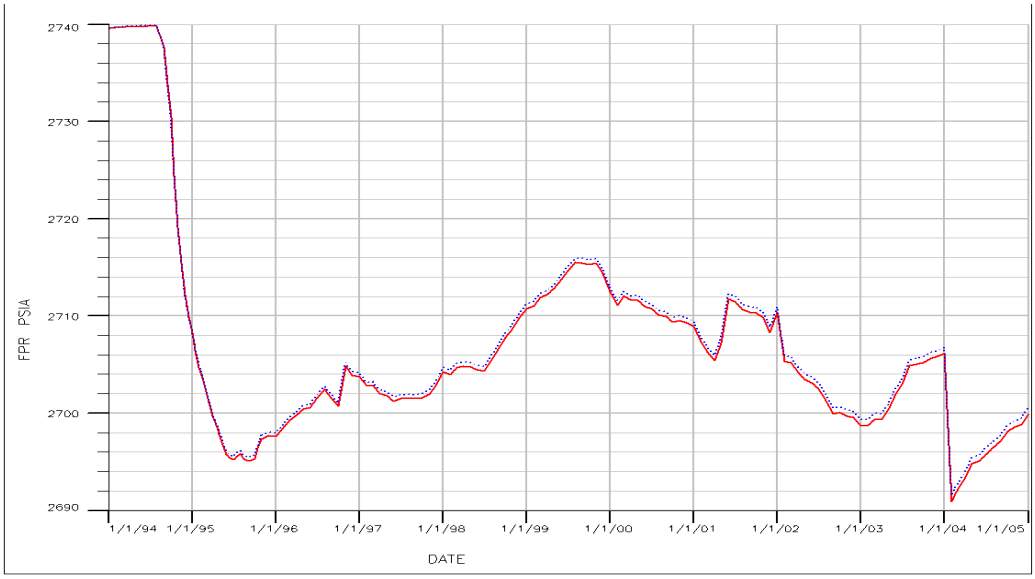

Figure 4.37: Field pressure (block centered versus corner point geometry).

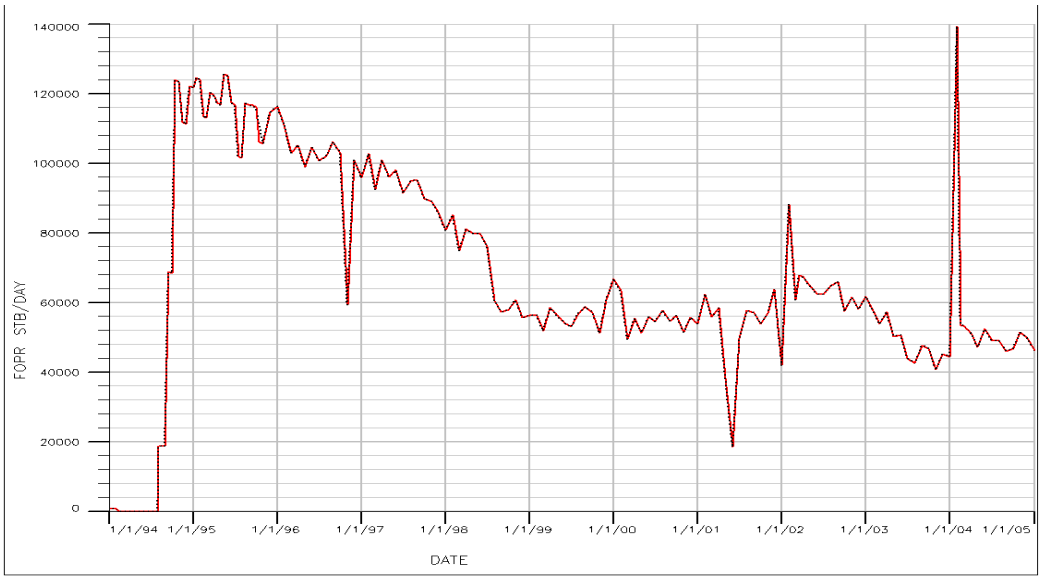

Figure 4.38: Field oil production (block centered versus corner point geometry).

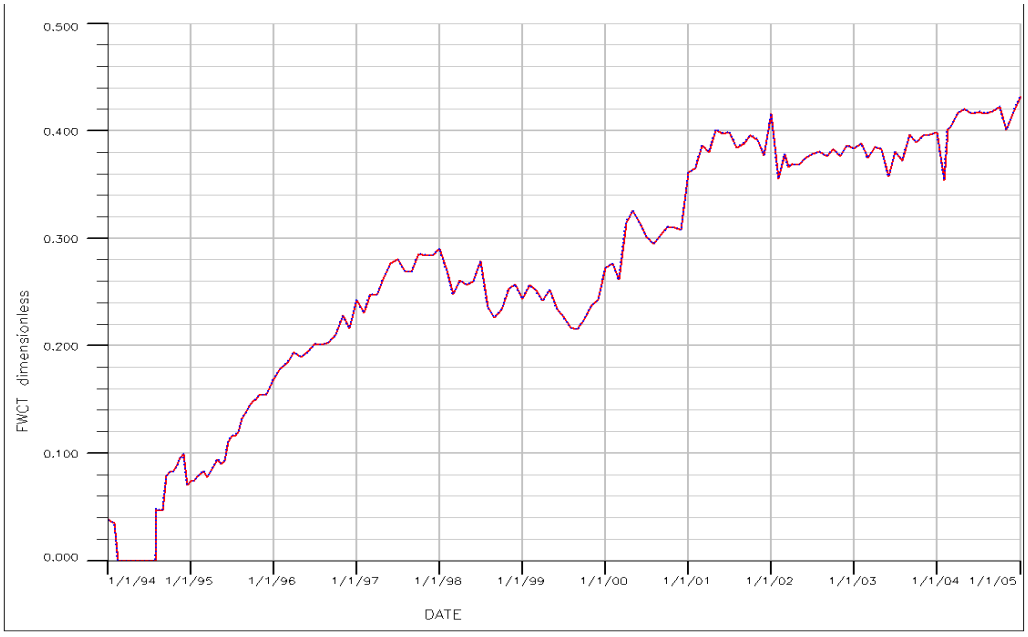

Figure 4.39: Field water cut (block centered versus corner point geometry).

CHAPTER 5

IMPLEMENTATION OF OPTIMIZATION METHODS

In this study, optimization processes are programmed for the specific objective of improving the outcome of the injection efficiency. As a benefit, the hydrocarbon recovery for the treated reservoirs shall increase which is the primary goal from this study. The discussed methods represent direct methodology that can be programmed within the simulator program and be performed without human interfere. In this chapter, we shall be discussing the optimization process emphasizing:

1) Criteria for optimization validations.
2) Highlights of the methods programming.

5.1 Criteria for Optimization Validations

The most important pieces of information provided by the streamlines are: a) well allocation factors and b) well pore volumes. Well allocation factors quantify the amount of flow in a particular well due to other wells in the system. Well pore volumes are the reservoir volumes associated with each individual well.

5.1.1 Well Allocation Factors and Pore Volumes

The determination of the well allocation factor between well pairs is the key in balancing well patterns in water floods. In streamline simulation, for each injector, the amount of injected fluid supporting any producer in the field can be determined exactly.

Therefore, the allocation of fluid between injectors and producers in a pattern is obtained automatically. Any fluid loss to wells outside a pattern can be immediately pointed out. Consequently, reservoir engineers can easily optimize field performance.

An important component in optimizing field performance is to be able to compare and rank the efficiency of injectors. More efficient injectors, for example, should probably receive a higher portion of available injection water than the less efficient injectors.

Failure of a waterline might reduce the amount of water available to a number of injectors forcing some to be closed; knowledge of the efficiency of the injectors is invaluable in such circumstances.

One of the methods of determining the efficiency of an injector is to compute the amount of offset oil produced as a function of volume injected. This is exactly the type of information streamlines provide.

Cross-plotting volume injected with offset oil produced for each injector gives a powerful snapshot of the efficiency of the injectors over the entire field.

The most efficient injectors will be those injectors that produce the most amount of oil for every barrel of water injected. On the other hand, the most inefficient wells would be those that inject high volumes of water but produce little in terms of offset oil.

These wells are prime candidates for shut-in, particularly in cases where the amount of

water is limited or could possibly be used more efficiently elsewhere in the field.

A producer with a high fractional flow is less efficient than one with a low fractional flow. But since streamline simulation allows determination of pore volume associated with any well, a significantly more powerful analysis might be to cross-plot oil production versus average oil saturation (or even movable surface oil volumes) for each producer.

Such a plot would immediately identify efficient producers: those producing at high rates while contacting relatively low oil saturations. Similarly, inefficient producers would be wells producing at low rates while contacting high average oil saturations.

The study provided balanced injection/production rates for the flooding pattern by using the approach mentioned above. Well allocation factors obtained from the streamline simulation results were used to optimize injector efficiency.

Injection rate for each injector versus the offset oil/liquid production rate due to that injector are plotted. Less efficient injectors are identified from this plot and balanced injection rates for the flooding pattern are provided.

Injector contribution can be defined as the ratio between the injector injection rate to the total injection rate. Also, efficiency improving can be calculated using the following equation

5.1.2 Methodology of Adjusting Injection Targets

During the route of water flooding operations, the efficiency of injectors and

producers will change. This may be due to the movement of the waterfront in the reservoir. Also, the water injection capabilities or production requirements might change. Therefore, it would be a good practice to check the injector's efficiencies on a quarterly basis.

The following tasks will be performed to optimize injection/production rates in a flooding pattern and provide a summary of the recommended procedure.

1. Aided by visualization tools, select injection-production well pairs that are communicating.

2. Cross-plot water volumes injected with offset oil produced for each injector. Water injection rate on X-axis and offset oil produced on Y-axis.

3. Apply the proposed methods to get the recommended water injection rates.

4. Make necessary changes in the simulation input data for the well under consideration and re-run simulator.

5. Process the resulting data to compare with original case in terms of change in injection efficiency, oil production, water cut and injection contribution.

For production wells, the following tasks must be performed.

1. Plot oil production versus average oil saturation for each producer.

2. Identify producers having high rates with relatively low oil saturations as efficient producers.

3. Identify producers having low rates with relatively high average oil saturations as inefficient producers.

4. Apply the proposed methods to get the recommended water injection rates.

5. After applying the optimization methods for injectors, necessary changes in the simulation input data for the well under consideration and re-run simulator.

6. Process the resulting data to compare with original case in terms of change in injection efficiency, oil production, water cut and injection contribution.

5.1.3 Flow Visualization

Instead of plotting spatial saturations as a function of time, streamlines offer an immediate snapshot of the flow field. With this it is possible to see how wells, reservoir geometry, and reservoir heterogeneity interact and dictate where flow is coming from (injectors) and where flow is going to (producers). Real fields rarely show streamlines conforming to the expected distribution of fluids even in regular flooding patterns.

Thus, it is not unusual to see wells communicating with other wells far outside the expected patterns. With Streamline Simulation (SL) it is possible to see the entire flow field at once. Flood front movements are visualized and fluid flow trajectories between

injectors and producers are plotted and evaluated through a visualization software package, Floviz.

It is possible to visualize a particular injector that supports a number of producers using Floviz or any other visualization package. However, determining the amount of water injected that is responsible in the production of oil in a production well can only be possible by analyzing the well allocation file generated by FrontSim.

The well allocation file can be generated at any time step or interval of a simulation run. **Figure** 5.1 shows a sample of the well allocation file. The extension of this file is ALLOC.

ALLOC Allocation/bundle report 30.0000 Days report step 1, 31 Jan 2000

Streamline Bundle			Surface Rate					Surface Volumes			Total Reservoir Rate		Pore Volume
Start	End	Flow Direct	Oil	Water	Gas	Oil	Water	Gas					
			SM3/D	Fraction	SM3/D	Fraction	SM3/D	Fraction	SM3	SM3	SM3	RM3/D	Fraction	RM3
P1			1.92e+001		0.00e+000		2.95e+003		2.04e+004	7.12e+002	3.15e+006	2.50e+001	9.87e-001	2.74e+004
P1	I1	Outflow	1.92e+001	1.00e+000	0.00e+000	0.00e+000	2.95e+003	1.00e+000	2.04e+004	7.12e+002	3.15e+006	2.50e+001	1.00e+000	2.74e+004
P2			3.83e+001		0.00e+000		5.93e+003		5.25e+004	1.45e+003	8.12e+006	5.00e+001	1.00e+000	7.00e+004
P2	I2	Outflow	3.25e+001	8.47e-001	0.00e+000	0.00e+000	5.02e+003	8.47e-001	3.13e+004	1.23e+003	4.85e+006	4.24e+001	8.47e-001	4.22e+004
P2	I1	Outflow	5.86e+000	1.53e-001	0.00e+000	0.00e+000	9.06e+002	1.53e-001	2.12e+004	2.21e+002	3.27e+006	7.64e+000	1.53e-001	2.78e+004
P3			1.92e+001		0.00e+000		2.95e+003		3.13e+004	7.22e+002	4.84e+006	2.50e+001	1.00e+000	4.16e+004
P3	I2	Outflow	1.92e+001	1.00e+000	0.00e+000	0.00e+000	2.95e+003	1.00e+000	3.13e+004	7.22e+002	4.84e+006	2.50e+001	1.00e+000	4.16e+004
P4			3.83e+001		0.00e+000		5.93e+003		4.80e+004	1.46e+003	7.42e+006	5.00e+001	1.02e+000	6.42e+004
P4	I1	Outflow	3.65e+000	9.53e-002	0.00e+000	0.00e+000	5.65e+002	9.53e-002	2.22e+004	1.40e+002	3.44e+006	4.77e+000	9.53e-002	2.91e+004
P4	I3	Outflow	3.47e+001	9.05e-001	0.00e+000	0.00e+000	5.36e+003	9.05e-001	2.58e+004	1.33e+003	3.99e+006	4.52e+001	9.05e-001	3.50e+004
P5			7.66e+001		0.00e+000		1.19e+004		1.11e+005	2.86e+003	1.71e+007	1.00e+002	9.92e-001	1.47e+005
P5	I1	Outflow	4.88e+001	6.37e-001	0.00e+000	0.00e+000	7.55e+003	6.37e-001	3.62e+004	1.81e+003	5.60e+006	6.37e+001	6.37e-001	4.92e+004
P5	I2	Outflow	9.78e+000	1.28e-001	0.00e+000	0.00e+000	1.51e+003	1.28e-001	2.63e+004	3.65e+002	4.06e+006	1.28e+001	1.28e-001	3.47e+004
P5	I3	Outflow	1.98e+000	2.59e-002	0.00e+000	0.00e+000	3.07e+002	2.59e-002	1.40e+004	7.40e+001	2.15e+006	2.59e+000	2.59e-002	1.83e+004
P5	I4	Outflow	1.61e+001	2.10e-001	0.00e+000	0.00e+000	2.48e+003	2.10e-001	3.42e+004	6.00e+002	5.30e+006	2.10e+001	2.10e-001	4.53e+004
P6			3.83e+001		0.00e+000		5.93e+003		4.35e+004	1.45e+003	6.72e+006	5.00e+001	1.01e+000	5.82e+004
P6	I2	Outflow	1.45e+001	3.80e-001	0.00e+000	0.00e+000	2.25e+003	3.80e-001	1.82e+004	5.52e+002	2.81e+006	1.90e+001	3.80e-001	2.42e+004
P6	I4	Outflow	2.38e+001	6.20e-001	0.00e+000	0.00e+000	3.68e+003	6.20e-001	2.53e+004	9.02e+002	3.92e+006	3.10e+001	6.20e-001	3.40e+004
P7			1.92e+001		0.00e+000		2.95e+003		2.92e+004	7.11e+002	4.52e+006	2.50e+001	9.87e-001	3.89e+004
P7	I3	Outflow	1.92e+001	1.00e+000	0.00e+000	0.00e+000	2.95e+003	1.00e+000	2.92e+004	7.11e+002	4.52e+006	2.50e+001	1.00e+000	3.89e+004
P8			3.83e+001		0.00e+000		5.93e+003		5.42e+004	1.44e+003	8.40e+006	5.00e+001	9.97e-001	7.23e+004
P8	I3	Outflow	2.02e+001	5.31e-001	0.00e+000	0.00e+000	3.15e+003	5.31e-001	3.02e+004	7.64e+002	4.38e+006	2.66e+001	5.31e-001	3.77e+004
P8	I4	Outflow	1.80e+001	4.69e-001	0.00e+000	0.00e+000	2.78e+003	4.69e-001	2.60e+004	6.75e+002	4.02e+006	2.34e+001	4.69e-001	3.46e+004
P9			1.92e+001		0.00e+000		2.95e+003		2.85e+004	7.23e+002	4.41e+006	2.50e+001	1.01e+000	3.80e+004
P9	I4	Outflow	1.92e+001	1.00e+000	0.00e+000	0.00e+000	2.95e+003	1.00e+000	2.85e+004	7.23e+002	4.41e+006	2.50e+001	1.00e+000	3.80e+004
I1			0.00e+000		9.62e+001		0.00e+000		1.00e+005	2.90e+003	1.55e+007	1.00e+002	1.00e+000	1.34e+005
I1	P1	Inflow	0.00e+000	0.00e+000	2.36e+001	2.46e-001	0.00e+000	0.00e+000	2.04e+004	7.12e+002	3.15e+006	2.46e+001	2.46e-001	2.74e+004
I1	P2	Inflow	0.00e+000	0.00e+000	7.35e+000	7.65e-002	0.00e+000	0.00e+000	2.12e+004	2.21e+002	3.27e+006	7.65e+000	7.65e-002	2.78e+004
I1	P5	Inflow	0.00e+000	0.00e+000	6.05e+001	6.29e-001	0.00e+000	0.00e+000	2.62e+004	1.81e+003	5.60e+006	6.29e+001	6.29e-001	4.92e+004
I1	P4	Inflow	0.00e+000	0.00e+000	4.64e+000	4.82e-002	0.00e+000	0.00e+000	2.22e+004	1.40e+002	3.44e+006	4.82e+000	4.82e-002	2.91e+004

Figure 5.1: Sample of the Well Allocation file

5.1.4 Well Allocation File

The allocation file provides a wealth of information which may be difficult to grasp in tabular form. Graphical representation of the tabular data helps optimize the useful application of the FrontSim simulation results.

The ALLOC file gives the volume associated with each injector/producer pair. For a production well it gives the rates or volume coming from each injector that is in contact with this producer. Similarly, for an injector, it gives the volumes or rates going towards each producer that is in contact with this injector. The format of this file is given below. For each time step:

1. Column 1 shows name of injection or production well of the parent well.
2. Column 2 shows name of injection or production well of the child well.
3. Column 3 shows whether it is an injector (INFLOW) or a producer (OUTFLOW).
4. Column 4 gives surface oil injection/production rate.
5. Column 5 gives fraction of surface oil injection/production rate.
6. Column 6 gives surface water injection/production rate.
7. Column 7 gives fraction of surface water injection/production rate.
8. Column 8 gives surface gas injection/production rate.
9. Column 9 gives fraction of surface gas injection/production rate.
10. Column 10 gives total surface oil volumes for each well.
11. Column 11 gives total surface water volumes for each well.
12. Column 12 gives total surface gas volumes for each well.

13. Column 13 gives total reservoir injection/production rate.
14. Column 14 gives fraction of total reservoir injection/production rate.
15. Column 15 gives total pore volume associated with each well.

5.2 Highlights of methods programming

The unique feature for these methods is that they can be automated within the simulator to give more optimization options in real time. Each method of optimization has different methodology but at the end all of the methods only change injection rate for each injection well to improve flooding efficiency. With the recent advances in the knowledge of programming a reasonably accurate improvements of the production efficiency can be achieved. In this section, all of the three optimization methods methodologies are highlighted.

5.2.1 E-plot software

From the description in the previous section, it is easily apparent how complicated the format is and that the enormous amount of detail provided in the ALLOC file cannot be readily utilized. Therefore, A PC-based software (E-Plot) developed in KFUPM-RI-CPM by Ghori [5] was used to help viewing the injection targets. This software is capable of extracting well allocation factors from the streamline simulation runs and generating efficiency plots. The user can see the less efficient injectors and incorporate

the changes in the input data file for FrontSim, run again and visualize the effect of those changes.

The graphical representation for this software will help in optimizing a given Injectors' efficiency by answering the following questions: For injector X:

1. What are the producers being supported.
2. The amount of water injected for each connected producer.
3. The amount of water lost to the aquifer or elsewhere.

For producer Y:

1. What are the injector(s) supporting that well (Y).
2. Percentage of oil produced and attributed to each supporting injector.
3. Water cut attributed to each supporting injector.
4. Amount of production attributed to the aquifer.

This software (E-Plot) is very beneficial in highlighting the changes of the water flooding scheme by the influence of the proposed optimization methods. The user interface of this software is highlighted in Appendix C.

5.2.2 Huthali Method Program

Huthali Method is programmed with two different programming languages: MATLAB and FORTRAN. The main code is written with Matlab and it has the ability to run the streamline simulator (FrontSim) and the FORTRAN code and make iteration to the optimization process till the conditions are met. It is important to mention that the

Schedule section of simulation data file should be divided into separate files such as, wells specification (WELLSPECS), injectors control data (WCONDNJ) and producer control data (WCONDPROD). These files are then included into data file of the models simulation input. Time of flight is defined is the required time for the water front to travel from the injector to the producer in one streamline.

The following tasks will be performed to optimize injection/production rates and provide a summary of the recommended injection rate:

1- Run the main program in Matlab where it will clear all the previous output files.

2- Matlab will run FrontSim within and extract the output.

3- Fortran code will trace all the streamlines and calculate time of flight for each streamline.

4- Matlab will use sequential quadratic programming algorithm (SQP) procedures which are used to minimize the arrival time residuals. This step generates the required changes in rates to equalize water flood front arrival time at the producing wells.

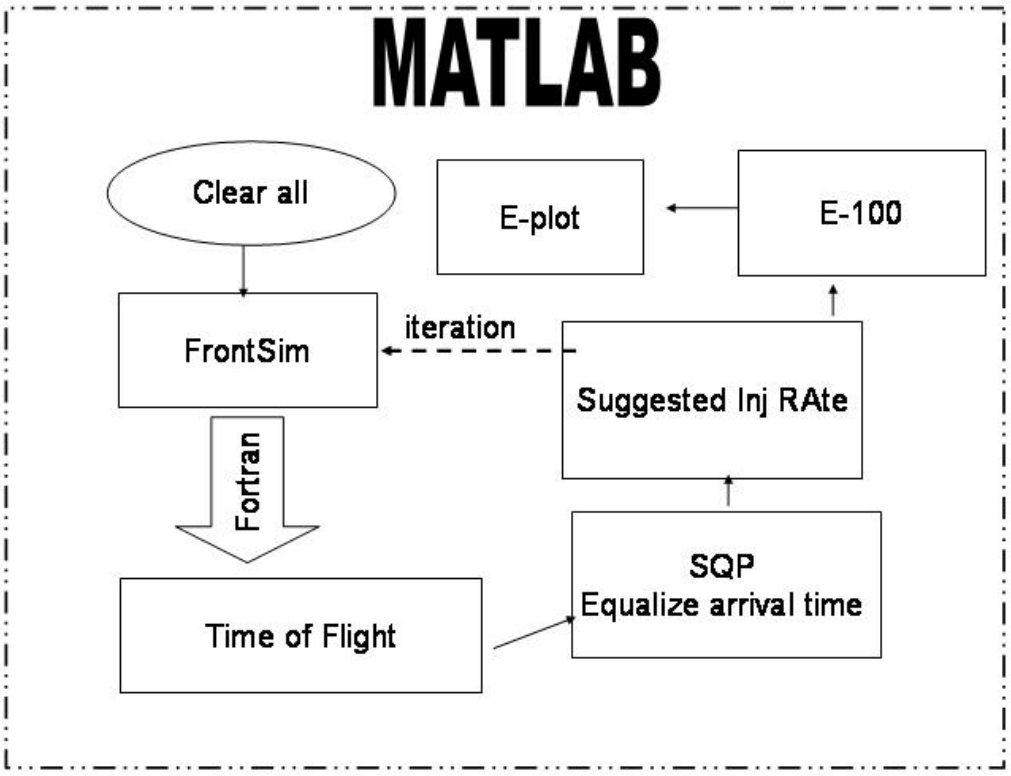

Figure 5.2: Methodology of Huthali Method Program

5.2.3 Pamila and Thiele Methods Programs

For both of Pamila and Thiele methods, they are programmed in Excel. They can be summaries into the following steps:

1- After running the models in FrontSim Allocation file (.alloc) is generated.

2- Using E-plot injectors' efficiency table is generated.

3- Calculate the reservoir average efficiency. $\bar{e} = \frac{total\ \ produced\ oil}{total\ \ injected\ water}$

4- Calculate weighting average of the streams efficiency for each injector as following

$$e_i \geq \bar{e} \Rightarrow \omega_i = MIN\ (\omega_{\max}, \omega_{\max}.(\frac{e_i - \bar{e}}{e_{\max} - \bar{e}})^{\alpha})$$

$$e_i \leq \bar{e} \Rightarrow \omega_i = MAX\ (\omega_{\min}, \omega_{\min}.(\frac{\bar{e} - e_i}{\bar{e} - e_{\min}})^{\alpha})$$

α is equal to 1 as recommended in the method literature.

5- In Thiele et al. method the new injection rate is calculated using the following equation

$$q_i^{new} = (1 + \omega_i).q_i^{old}$$

6- In Pamila method correction factor is calculated as shown

$$C = \frac{\sum qi_{old}}{\sum qi_{new}}\ .$$

Then, each injector injection rate is multiplied with the correction factor

$$q = C\, q_i^{new}$$

7- For Pamila method more than one iteration is required

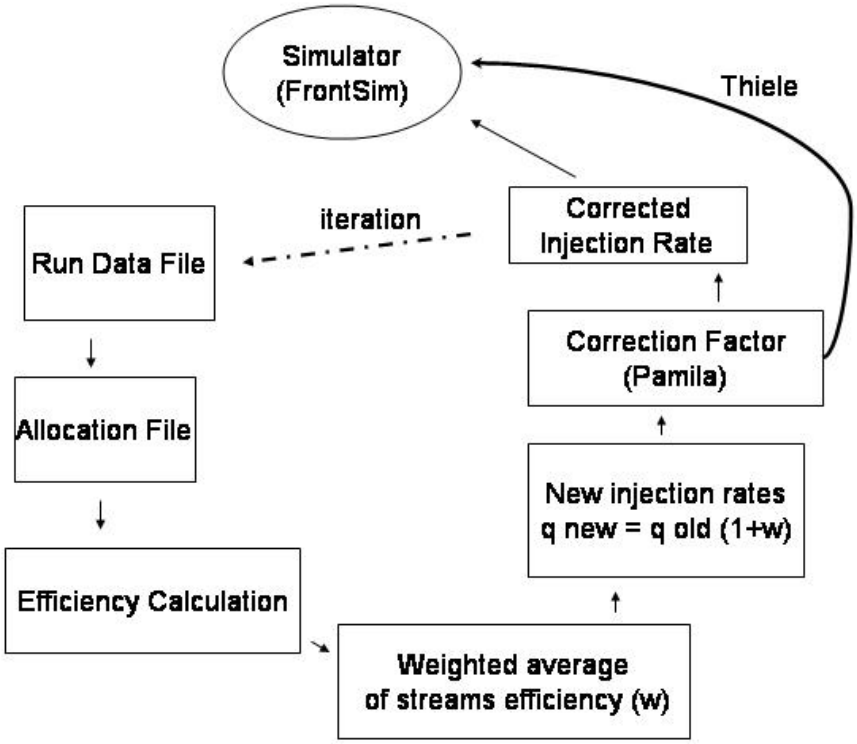

Figure 5.3: Methodology of Pamila and Thiele methods program

CHAPTER 6

RESULTS AND DISCUSSIONS

Simulation runs were made using the streamline simulator for the specific objective of ascertaining the strengths and weaknesses of the tested methods in productivity scale.

In this chapter, we shall be presenting the simulating results emphasizing:

1) The influence of proposed methods on water flooding efficiency.
2) Comparison study between all the methods in terms of productivity enhancement.

6.1 Optimization of Injection-Production Rates

The optimization procedures are applied to all of the four models. The results of the optimization processes are explained in the followings:

6.1.1 M1 model case

M1 model is a very simple one layer model with homogenous properties. It contains four injectors and nine producers distributed in four adjacent five spot patterns. The handiness in that model will be useful for simplifying the optimization methods methodology. The primary injection rates were set to 100 STB/D. The injection efficiency result is explained in Table 6.1

Table 6.1: M1 Injection efficiency

Injectors NAME	Injection Rate STB/D	Injection Contribution	Production Rate STB/D	Time	Injector Efficiency
I1	96.09	0.2499	58.78	6 months	0.612
I3	96.18	0.2501	59.68	6 months	0.621
I2	96.2	0.2501	60.38	6 months	0.628
I4	96.1	0.2499	65.42	6 months	0.681
Total	385		244	Average	0.635

Injection contribution is the ratio between individual injector injection rates to the total injection rate. From the first look to the result, it's clear that injection contribution for each injector is 25%. This means that each injector is contributed in one quarter of the reservoir. After that, the weighting average of streams efficiency for each injector is determined. Then, recommended injection rates is calculated and shown in the Table 6.2.

Table 6.2: Thiele and Pamila suggested injection rates for M1

Injectors NAME	Injection Rate STB/D	Injector Efficiency	1+wi	Thiele	Pamila
				Suggested Injection Rate STB/D	
I1	96.09	0.611718	1.3	99.5	99.3
I3	96.18	0.620503	1.2	98.73	98.17
I2	96.2	0.627651	1.1	97.4	97.5
I4	96.1	0.680749	0.96	95.89	95.65

For Huthali Method, time of flight for each producer is calculated as shown in Table 6.3 and the suggested injection rate is displayed in Table 6.4. Time of flight is defined as the required time for the water front to travel from the injector to the producer in one streamline.

Table 6.3: TOF for streamlines in M1

Well Name	Number of Injectors	Num. Of Streamlines	Num. of Fast Streamlines	Average TOF (days)
P1	1	147	13	549.73
P2	1	120	18	550.55
P3	1	172	34	550.36
P4	1	126	25	550.76
P5	1	173	34	549.57
P6	1	160	45	549.74
P7	1	149	29	550.72
P8	1	165	51	550.75
P9	1	189	44	551.5

Using time of flight, SQP is applied to delay the water breakthrough hence increasing the efficiency of the injection. Table 6.4 is showing the suggested injection rate using Huthali Method.

Table 6.4: Huthali suggested injection rates for M1

Injectors NAME	Injection Rate STB/D	Huthali Injection Rate STB/D
I1	96.09	97.4
I3	96.18	96.6
I2	96.2	96.5
I4	96.1	95.1

From the previous tables, it's clear that the suggested injection rate is very close for the three methods and there is not big difference from the original injection rate. As a result, the homogenous model M1 is not showing clear variations in the suggested injection rates for all the three methods. This model is skipped to the second model which is more heterogonous than the first one.

6.1.2 M2 model case

This model (M2) is a 6 layers heterogeneous reservoir with anticline dome shape. The full field model dimension of M2 is 100 X 80 X 6 with 6561 active cells. This model is simulated for two years. Table 6.5 shows the primary injectors' rates and efficiencies without any optimization interfere.

Table 6.5: Original Injection Rates for M2

Injectors NAME	Injection Rate STB/D	Injection Contribution	Production Rate STB/D	Time	Injector Efficiency
I1	1477	0.2738	537	2 years	0.363
I3	1585	0.2938	772	2 years	0.487
I2	906	0.1679	307	2 years	0.339
I4	1363	0.2526	627	2 years	0.460
Total	5331		2243		**0.421**

Thiele optimization process is applied to calculate the recommended injection rates. Table 6.6 shows the injectors' rates and efficiencies in the specified time period.

Table 6.6: Thiele Suggested Injection Rates for M2

Injectors NAME	Injection Rate STB/D	Injection Contribution	Production Rate STB/D	Time	Injector Efficiency
I1	1486	0.2754	651	2 years	0.438
I3	1585	0.2938	679	2 years	0.428
I2	943	0.1748	707	2 years	0.750
I4	1381	0.2560	650	2 years	0.471
Total	5395		2687		**0.498**

After applying Pamila optimization process, the suggested injection rates are shown in Table 6.7.

Table 6.7: Pamila Suggested Injection Rates for M2

Injectors NAME	Injection Rate STB/D	Injection Contribution	Production Rate STB/D	Time	Injector Efficiency
I1	1491	0.2761	633	2 years	0.424
I3	1585	0.2935	728	2 years	0.459
I2	943	0.1746	714	2 years	0.758
I4	1381	0.2558	692	2 years	0.501
Total	5400		2767		**0.513**

After that, Huthali optimization process is run and the suggested injection rate is displayed in table 6.8.

Table 6.8: Huthali Suggested Injection Rates for M2

Injectors NAME	Injection Rate STB/D	Injection Contribution	Production Rate STB/D	Time	Injector Efficiency
I1	800	0.2500	524	2 years	0.655
I3	800	0.2501	599	2 years	0.749
I2	800	0.2499	585	2 years	0.732
I4	800	0.2500	608	2 years	0.760
Total	3200		2316		**0.724**

6.1.3 M3 model case

M3 is a real model in the Middle East. The full field model dimension of M3 is 100 x 190 x 24, with 411,237 active cells. This model has 130 wells that can be classified into 19 injectors and 111 producers. M3 is divided into two segments according the streamlines distribution where each segment is optimized separately. The results for each segment are presented for 6 months, one year and three years.

6.1.3.1 Segment A

At the beginning, the model is simulated for 6 months. Table 6.9 shows the primary injectors' rates and efficiencies without any optimization interfere.

Table 6.9: Original Injection Rates for M3.A (6 months)

	Injectors	Injection Rate STB/D	Injector Contribution	Production Rate STB/D	Time	Injector Efficiency
Segment A	W0045	7332	0.1401	1137	6 months	0.155
	W0061	3047	0.0582	664	6 months	0.218
	W0104	9711	0.1855	3036	6 months	0.313
	W0106	4464	0.0853	1177	6 months	0.264
	W0112	17664	0.3374	6527	6 months	0.370
	W0117	579	0.0111	144	6 months	0.248
	W0120	3226	0.0616	673	6 months	0.209
	W0129	1313	0.0251	341	6 months	0.260
	W0130	5009	0.0957	1620	6 months	0.323
		52345		15319		**0.293**

Thiele optimization process is applied to calculate the recommended injection rates. Table 6.10 shows the injectors' rates and efficiencies in the specified time period.

Table 6.10: Thiele Suggested Injection Rates for M3.A (6 months)

	Injectors	Injection Rate STB/D	Injector Contribution	Production Rate STB/D	Time	Injector Efficiency
Segment A	W0045	7339	0.1401	2583	6 months	0.352
	W0061	3047	0.0582	1129	6 months	0.370
	W0104	9718	0.1855	3492	6 months	0.359
	W0106	4463	0.0852	1399	6 months	0.313
	W0112	17690	0.3377	4945	6 months	0.280
	W0117	578	0.0110	405	6 months	0.700
	W0120	3229	0.0617	1174	6 months	0.363
	W0129	1314	0.0251	379	6 months	0.289
	W0130	4999	0.0954	1882	6 months	0.377
		52377		17387		**0.332**

After applying Pamila optimization process, the suggested injection rates are shown in Table 6.11.

Table 6.11: Pamila Suggested Injection Rates for M3.A (6 months)

	Injectors	Injection Rate STB/D	Injector Contribution	Production Rate STB/D	Time	Injector Efficiency
Segment A	W0045	9334	0.1717	2383	6 months	0.255
	W0061	3048	0.0561	1579	6 months	0.518
	W0104	9712	0.1786	3464	6 months	0.357
	W0106	4459	0.0820	1356	6 months	0.304
	W0112	12194	0.2243	4817	6 months	0.395
	W0117	2078	0.0382	473	6 months	0.228
	W0120	4228	0.0778	1730	6 months	0.409
	W0129	1314	0.0242	346	6 months	0.263
	W0130	6003	0.1104	1462	6 months	0.244
		52370		17612		**0.336**

After that, Huthali optimization process is run and the suggested injection rate is displayed in table 6.12.

Table 6.12: Huthali Suggested Injection Rates for M3.A (6 months)

	Injectors	Injection Rate STB/D	Injector Contribution	Production Rate STB/D	Time	Injector Efficiency
Segment A	W0045	7334	0.1400	2347	6 months	0.320
	W0061	3049	0.0582	929	6 months	0.305
	W0104	9717	0.1855	2917	6 months	0.300
	W0106	4468	0.0853	1578	6 months	0.353
	W0112	17682	0.3376	6570	6 months	0.372
	W0117	579	0.0111	251	6 months	0.434
	W0120	3224	0.0616	1039	6 months	0.322
	W0129	1314	0.0251	405	6 months	0.308
	W0130	5009	0.0956	1659	6 months	0.331
		52376		17695		**0.338**

Then, model is simulated for 1 year .Table 6.13 shows the primary injectors' rates and efficiencies without any optimization interfere.

Table 6.13: Original Injection Rates for M3.A (1 year)

	Injectors	Injection Rate STB/D	Injector Contribution	Production Rate STB/D	Time	Injector Efficiency
Segment A	W0045	5327	0.1058	985	1 year	0.185
	W0061	3044	0.0605	706	1 year	0.232
	W0104	9710	0.1929	3195	1 year	0.329
	W0106	4464	0.0887	1176	1 year	0.263
	W0112	17670	0.3510	6499	1 year	0.368
	W0117	580	0.0115	153	1 year	0.264
	W0120	3226	0.0641	642	1 year	0.199
	W0129	1311	0.0260	335	1 year	0.256
	W0130	5010	0.0995	1578	1 year	0.315
		50342		15270		**0.303**

Thiele optimization process is applied to calculate the recommended injection rates. Table 6.14 shows the injectors' rates and efficiencies in the specified time period.

Table 6.14: Thiele Suggested Injection Rates for M3.A (1 year)

	Injectors	Injection Rate STB/D	Injector Contribution	Production Rate STB/D	Time	Injector Efficiency
Segment A	W0045	5332	0.1059	1137	1 year	0.213
	W0061	3047	0.0605	664	1 year	0.218
	W0104	9711	0.1929	3036	1 year	0.313
	W0106	4464	0.0887	1177	1 year	0.264
	W0112	17664	0.3509	6527	1 year	0.370
	W0117	579	0.0115	144	1 year	0.248
	W0120	3226	0.0641	673	1 year	0.209
	W0129	1313	0.0261	341	1 year	0.260
	W0130	5009	0.0995	1620	1 year	0.323
		50345		15319		**0.304**

After applying Pamila optimization process, the suggested injection rates are shown in Table 6.15.

Table 6.15: Pamila Suggested Injection Rates for M3.A (1 year)

	Injectors	Injection Rate STB/D	Injector Contribution	Production Rate STB/D	Time	Injector Efficiency
Segment A	W0045	5350	0.0859	985	1 year	0.184
	W0061	2758	0.0406	706	1 year	0.256
	W0104	9710	0.1929	3195	1 year	0.329
	W0106	4464	0.0887	1176	1 year	0.263
	W0112	17670	0.3510	6499	1 year	0.368
	W0117	570	0.0115	153	1 year	0.268
	W0120	2726	0.0442	642	1 year	0.236
	W0129	1325	0.0260	335	1 year	0.253
	W0130	5025	0.0995	1578	1 year	0.314
		49598		15270		**0.308**

After that, Huthali optimization process is run and the suggested injection rate is displayed in Table 6.16.

Table 6.16: Huthali Suggested Injection Rates for M3.A (1 year)

	Injectors	Injection Rate STB/D	Injector Contribution	Production Rate STB/D	Time	Injector Efficiency
Segment A	W0045	4327	0.0955	860	1 year	0.199
	W0061	2043	0.0451	457	1 year	0.224
	W0104	9702	0.2142	3276	1 year	0.338
	W0106	4464	0.0985	1325	1 year	0.297
	W0112	17652	0.3897	6813	1 year	0.386
	W0117	579	0.0128	208	1 year	0.359
	W0120	2227	0.0491	529	1 year	0.238
	W0129	2301	0.0508	499	1 year	0.217
	W0130	2006	0.0443	990	1 year	0.494
		45301		14956		**0.330**

Then, the model is simulated for three years. Table 6.17 shows the primary injectors' rates and efficiencies without any optimization interfere.

Table 6.17: Original Injection Rates for M3.A (3 years)

	Injectors	Injection Rate STB/D	Injector Contribution	Production Rate STB/D	Time	Injector Efficiency
Segment A	W0045	7334	0.1349	2383	3 year	0.325
	W0061	6048	0.1112	1579	3 year	0.261
	W0104	9712	0.1786	3464	3 year	0.357
	W0106	4459	0.0820	1356	3 year	0.304
	W0112	12194	0.2243	4817	3 year	0.395
	W0117	2078	0.0382	473	3 year	0.228
	W0120	7228	0.1329	1730	3 year	0.239
	W0129	1314	0.0242	346	3 year	0.263
	W0130	4003	0.0736	1462	3 year	0.365
		54370		17612		**0.324**

Thiele optimization process is applied to calculate the recommended injection rates. Table 6.18 shows the injectors' rates and efficiencies in the specified time period.

Table 6.18: Thiele Suggested Injection Rates for M3.A (3 years)

	Injectors	Injection Rate STB/D	Injector Contribution	Production Rate STB/D	Time	Injector Efficiency
Segment A	W0045	7336	0.1349	2012	3 year	0.274
	W0061	6044	0.1111	2402	3 year	0.397
	W0104	9721	0.1787	3274	3 year	0.337
	W0106	4463	0.0821	1504	3 year	0.337
	W0112	12195	0.2242	4591	3 year	0.376
	W0117	2078	0.0382	625	3 year	0.301
	W0120	7236	0.1330	2448	3 year	0.338
	W0129	1314	0.0242	889	3 year	0.677
	W0130	4001	0.0736	1387	3 year	0.347
		54388		19132		**0.352**

After applying Pamila optimization process, the suggested injection rates are shown in Table 6.19.

Table 6.19: Pamila Suggested Injection Rates for M3.A (3 years)

	Injectors	Injection Rate STB/D	Injector Contribution	Production Rate STB/D	Time	Injector Efficiency
Segment A	W0045	7338	0.1349	2581	3 year	0.352
	W0061	6041	0.1112	2129	3 year	0.352
	W0104	9713	0.1786	3280	3 year	0.338
	W0106	4464	0.0820	1606	3 year	0.360
	W0112	12175	0.2243	4921	3 year	0.404
	W0117	2078	0.0382	609	3 year	0.293
	W0120	7235	0.1329	2260	3 year	0.312
	W0129	1314	0.0242	655	3 year	0.499
	W0130	4002	0.0736	1436	3 year	0.359
		54358		19477		**0.358**

After that, Huthali optimization process is run and the suggested injection rate is displayed in table 6.20.

Table 6.20: Huthali Suggested Injection Rates for M3.A (3 years)

	Injectors	Injection Rate STB/D	Injector Contribution	Production Rate STB/D	Time	Injector Efficiency
Segment A	W0045	7339	0.1350	3149	3 year	0.429
	W0061	6037	0.1110	1857	3 year	0.308
	W0104	9705	0.1785	3286	3 year	0.339
	W0106	4464	0.0821	1707	3 year	0.382
	W0112	12198	0.2243	5252	3 year	0.431
	W0117	2077	0.0382	593	3 year	0.285
	W0120	7234	0.1330	2072	3 year	0.286
	W0129	1314	0.0242	422	3 year	0.321
	W0130	4003	0.0736	1486	3 year	0.371
		54372		19822		**0.365**

6.1.3.2 Segment B

For segment B, the model is simulated for 6 months .Table 6.21 shows the primary injectors' rates and efficiencies without any optimization interfere.

Table 6.21: Original Injection Rates for M3.B (6 months)

	Injectors	Injection Rate STB/D	Injector Contribution	Production Rate STB/D	Time	Injector Efficiency
Segment B	W0008	1396	0.0489	1095	6 months	0.784
	W0059	5941	0.2083	1131	6 months	0.190
	W0064	990	0.0347	1017	6 months	1.027
	W0107	1981	0.0694	1164	6 months	0.588
	W0123	262	0.0092	658	6 months	2.510
	W0131	2977	0.1044	1085	6 months	0.364
	W0132	992	0.0348	389	6 months	0.393
	W0134	117	0.0041	65	6 months	0.554
	W0135	5948	0.2085	2792	6 months	0.469
	W0137	7922	0.2777	1920	6 months	0.242
		28526		11316		**0.397**

Thiele optimization process is applied to calculate the recommended injection rates. Table 6.22 shows the injectors' rates and efficiencies in the specified time period.

Table 6.22: Thiele Suggested Injection Rates for M3.B (6 months)

	Injectors	Injection Rate STB/D	Injector Contribution	Production Rate STB/D	Time	Injector Efficiency
Segment B	W0008	2397	0.0812	1062	6 months	0.443
	W0059	3945	0.1336	926	6 months	0.235
	W0064	1990	0.0674	1875	6 months	0.942
	W0107	2973	0.1007	1535	6 months	0.516
	W0123	2262	0.0766	830	6 months	0.367
	W0131	2977	0.1008	1157	6 months	0.389
	W0132	992	0.0336	436	6 months	0.439
	W0134	117	0.0040	57	6 months	0.492
	W0135	5946	0.2014	2901	6 months	0.488
	W0137	5921	0.2006	1848	6 months	0.312
		29520		12628		**0.428**

After applying Pamila optimization process, the suggested injection rates are shown in Table 6.23.

Table 6.23: Pamila Suggested Injection Rates for M3.B (6 months)

	Injectors	Injection Rate STB/D	Injector Contribution	Production Rate STB/D	Time	Injector Efficiency
Segment B	W0008	2397	0.0812	1039	6 months	0.433
	W0059	2941	0.0996	522	6 months	0.178
	W0064	3991	0.1351	3403	6 months	0.853
	W0107	2973	0.1007	1347	6 months	0.453
	W0123	2262	0.0766	889	6 months	0.393
	W0131	2985	0.1011	1093	6 months	0.366
	W0132	993	0.0336	409	6 months	0.411
	W0134	117	0.0040	49	6 months	0.416
	W0135	5952	0.2015	2959	6 months	0.497
	W0137	4921	0.1666	1426	6 months	0.290
		29532		13135		**0.445**

After that, Huthali optimization process is run and the suggested injection rate is displayed in table 6.24.

Table 6.24: Huthali Suggested Injection Rates for M3.B (6 months)

	Injectors	Injection Rate STB/D	Injector Contribution	Production Rate STB/D	Time	Injector Efficiency
Segment B	W0008	2397	0.0812	866	6 months	0.361
	W0059	2942	0.0996	662	6 months	0.225
	W0064	3991	0.1352	3321	6 months	0.832
	W0107	2973	0.1007	1474	6 months	0.496
	W0123	2262	0.0766	613	6 months	0.271
	W0131	2982	0.1010	1097	6 months	0.368
	W0132	993	0.0336	538	6 months	0.542
	W0134	117	0.0040	55	6 months	0.470
	W0135	5949	0.2015	3046	6 months	0.512
	W0137	4923	0.1667	1755	6 months	0.357
		29528		13426		**0.455**

After that, the model is simulated for one year. Table 6.25 shows the primary injectors' rates and efficiencies without any optimization interfere.

Table 6.25: Original Injection Rates for M3.B (1 year)

	Injectors	Injection Rate STB/D	Injector Contribution	Production Rate STB/D	Time	Injector Efficiency
Segment B	W0008	2402	0.0813	695	1 year	0.290
	W0059	941	0.0318	353	1 year	0.375
	W0064	5996	0.2030	4651	1 year	0.776
	W0107	4973	0.1684	1939	1 year	0.390
	W0123	2261	0.0765	659	1 year	0.292
	W0131	2988	0.1012	1258	1 year	0.421
	W0132	993	0.0336	461	1 year	0.464
	W0134	117	0.0039	42	1 year	0.361
	W0135	5947	0.2013	3210	1 year	0.540
	W0137	2923	0.0989	924	1 year	0.316
		29540		14192		**0.480**

Thiele optimization process is applied to calculate the recommended injection rates.

Table 6.26 shows the injectors' rates and efficiencies in the specified time period.

Table 6.26: Thiele Suggested Injection Rates M3.B (1 year)

	Injectors	Injection Rate STB/D	Injector Contribution	Production Rate STB/D	Time	Injector Efficiency
Segment B	W0008	1402	0.0475	541	1 year	0.386
	W0059	941	0.0318	292	1 year	0.310
	W0064	7999	0.2707	5825	1 year	0.728
	W0107	3976	0.1346	1496	1 year	0.376
	W0123	1261	0.0427	453	1 year	0.359
	W0131	2985	0.1010	1110	1 year	0.372
	W0132	993	0.0336	509	1 year	0.513
	W0134	117	0.0040	40	1 year	0.344
	W0135	7449	0.2521	3653	1 year	0.490
	W0137	2425	0.0821	566	1 year	0.234
		29548		14486		**0.490**

After applying Pamila optimization process, the suggested injection rates are shown in Table 6.27.

Table 6.27: Pamila Suggested Injection Rates M3.B (1 year)

	Injectors	Injection Rate STB/D	Injector Contribution	Production Rate STB/D	Time	Injector Efficiency
Segment B	W0008	1395	0.0305	430	1 year	0.308
	W0059	851	0.0149	202	1 year	0.237
	W0064	8028	0.3217	6563	1 year	0.818
	W0107	4025	0.1683	1663	1 year	0.413
	W0123	1261	0.0427	329	1 year	0.261
	W0131	2951	0.1010	1092	1 year	0.370
	W0132	993	0.0336	504	1 year	0.507
	W0134	119	0.0040	27	1 year	0.226
	W0135	7440	0.2519	3813	1 year	0.512
	W0137	2030	0.0313	513	1 year	0.253
		29093		15135		**0.520**

After that, Huthali optimization process is run and the suggested injection rate is displayed in Table 6.28.

Table 6.28: Huthali Suggested Injection Rates M3.B (1 year)

	Injectors	Injection Rate STB/D	Injector Contribution	Production Rate STB/D	Time	Injector Efficiency
Segment B	W0008	902	0.0305	471	1 year	0.522
	W0059	441	0.0149	169	1 year	0.383
	W0064	9497	0.3216	7666	1 year	0.807
	W0107	4967	0.1682	1749	1 year	0.352
	W0123	761	0.0258	336	1 year	0.442
	W0131	2988	0.1012	1110	1 year	0.372
	W0132	994	0.0337	562	1 year	0.565
	W0134	117	0.0040	36	1 year	0.305
	W0135	6439	0.2181	3250	1 year	0.505
	W0137	425	0.0144	98	1 year	0.230
		27531		15447		**0.561**

After that, the model is simulated for three years. Table 6.29 shows the primary injectors' rates and efficiencies without any optimization interfere.

Table 6.29: Original Suggested Injection Rates M3.B (3 years)

	Injectors	Injection Rate STB/D	Injector Contribution	Production Rate STB/D	Time	Injector Efficiency
Segment B	W0008	902	0.0354	567	3 years	0.629
	W0059	441	0.0173	147	3 years	0.334
	W0064	9497	0.3722	7234	3 years	0.762
	W0107	4964	0.1945	1835	3 years	0.370
	W0123	760	0.0298	391	3 years	0.515
	W0131	2983	0.1169	1144	3 years	0.383
	W0132	995	0.0390	757	3 years	0.761
	W0134	117	0.0046	26	3 years	0.224
	W0135	4434	0.1737	2566	3 years	0.579
	W0137	426	0.0167	239	3 years	0.561
		25520		14507		**0.584**

Thiele optimization process is applied to calculate the recommended injection rates.

Table 6.30 shows the injectors' rates and efficiencies in the specified time period.

Table 6.30: Thiele Suggested Injection Rates M3.B (3 years)

	Injectors	Injection Rate STB/D	Injector Contribution	Production Rate STB/D	Time	Injector Efficiency
Segment B	W0008	902	0.0384	654	3 years	0.725
	W0059	441	0.0188	198	3 years	0.448
	W0064	9504	0.4040	7312	3 years	0.769
	W0107	2961	0.1258	1199	3 years	0.405
	W0123	760	0.0323	569	3 years	0.748
	W0131	2983	0.1268	1149	3 years	0.385
	W0132	996	0.0423	698	3 years	0.700
	W0134	116	0.0049	45	3 years	0.392
	W0135	4435	0.1885	2363	3 years	0.533
	W0137	427	0.0182	258	3 years	0.605
		23526		14365		**0.614**

After applying Pamila optimization process, the suggested injection rates are shown in Table 6.31.

Table 6.31: Pamila Suggested Injection Rates M3.B (3 years)

	Injectors	Injection Rate STB/D	Injector Contribution	Production Rate STB/D	Time	Injector Efficiency
Segment B	W0008	903	0.0384	694	3 years	0.769
	W0059	441	0.0187	206	3 years	0.467
	W0064	9506	0.4041	7173	3 years	0.755
	W0107	2461	0.1046	969	3 years	0.394
	W0123	760	0.0323	579	3 years	0.762
	W0131	2480	0.1054	1012	3 years	0.408
	W0132	996	0.0423	769	3 years	0.772
	W0134	116	0.0049	50	3 years	0.433
	W0135	4432	0.1884	2311	3 years	0.522
	W0137	426	0.0181	299	3 years	0.702
		22520		14445		**0.624**

After that, Huthali optimization process is run and the suggested injection rate is displayed in Table 6.32.

Table 6.32: Huthali Suggested Injection Rates M3.B (3 years)

	Injectors	Injection Rate STB/D	Injector Contribution	Production Rate STB/D	Time	Injector Efficiency
Segment B	**W0008**	902	0.0384	654	3 years	0.725
	W0059	441	0.0188	198	3 years	0.448
	W0064	9504	0.4040	7312	3 years	0.769
	W0107	2461	0.1046	1199	3 years	0.487
	W0123	760	0.0323	569	3 years	0.748
	W0131	2483	0.1055	1149	3 years	0.463
	W0132	996	0.0423	698	3 years	0.700
	W0134	116	0.0049	45	3 years	0.392
	W0135	4435	0.1885	2363	3 years	0.533
	W0137	427	0.0182	258	3 years	0.605
		22526		14063		**0.641**

6.1.4 M4 model case

M4 is a real model in the Middle East. The full field model dimension of M4 is 48 x 118 x 36, with 154699 active cells. This model has 97 wells that can be classified into 5 injectors and 92 producers. M4 is simulated and optimized for three years. Table 6.33 shows the primary injectors' rates and efficiencies without any optimization interfere.

Table 6.33: Original Suggested Injection Rates for M4 (3 years)

Injectors	Injection Rate STB/D	Injector Contribution	Production Rate STB/D	Time	Injector Efficiency
N0005	3177	0.3848	984	3 years	0.310
N0011	2430	0.2943	2077	3 years	0.855
N0023	792	0.0959	627	3 years	0.791
N0060	1349	0.1634	898	3 years	0.665
N0061	509	0.0616	216	3 years	0.424
	8258		4801		**0.581**

Thiele optimization process is applied to calculate the recommended injection rates. Table 6.34 shows the injectors' rates and efficiencies in the specified time period.

Table 6.34: Thiele Suggested Injection Rates for M4 (3 years)

Injectors	Injection Rate STB/D	Injector Contribution	Production Rate STB/D	Time	Injector Efficiency
N0005	3383	0.4094	1173	3 years	0.347
N0011	2180	0.2638	1936	3 years	0.888
N0023	792	0.0958	623	3 years	0.787
N0060	1350	0.1633	947	3 years	0.701
N0061	559	0.0676	230	3 years	0.411
	8264		4909		**0.594**

After applying Pamila optimization process, the suggested injection rates are shown in Table 6.35.

Table 6.35: Pamila Suggested Injection Rates for M4 (3 years)

Injectors	Injection Rate STB/D	Injector Contribution	Production Rate STB/D	Time	Injector Efficiency
N0005	3379	0.4093	1253	3 years	0.371
N0011	2177	0.2637	1908	3 years	0.876
N0023	791	0.0958	641	3 years	0.811
N0060	1349	0.1634	974	3 years	0.722
N0061	559	0.0677	224	3 years	0.401
	8256		5000		**0.606**

After that, Huthali optimization process is run and the suggested injection rate is displayed in Table 3.36

Table 6.36: Huthali Suggested Injection Rates for M4 (3 years)

Injectors	Injection Rate STB/D	Injector Contribution	Production Rate STB/D	Time	Injector Efficiency
N0005	3378	0.4070	1532	3 years	0.454
N0011	2177	0.2623	1842	3 years	0.846
N0023	836	0.1007	460	3 years	0.550
N0060	1349	0.1626	1033	3 years	0.766
N0061	559	0.0674	261	3 years	0.467
	8036		4760		**0.618**

6.2 The Three Methods Comparison Study

After all the three methods optimizations are performed for all models, comparison study is initiated to clearly evaluate the improvement in flooding efficiency by each method. For all the models optimization methods, the resulting injection rates, production rates and average flooding efficiencies will be listed in tables. Efficiencies for all three are compared to the original model without any optimization applied and the improvement is presented in percentages.

As previously mentioned, M1 model analysis is skipped because it is not showing clear contrast between the three methods efficiency results. For M2 model flooding optimizations, Table 6.37 is showing optimization results with three methods. It is clear that Huthali method shows the highest impact for flooding efficiency. On the other hand, Pamila and Thiele methods increased the production rate for M2 model.

Table 6.37: Comparison between three methods for M2

	M2			
	Injection Rate STB/D	Production Rate STB/D	average Efficiency	Efficiency Improvement %
Original	5331	2243	**0.421**	-
Thiele	5395	2687	**0.498**	18.3
Pamila	5400	2767	**0.513**	21.9
Huthali	3200	2316	**0.724**	72.0

For M3 model Segment A flooding optimizations, Table 6.38 is showing optimization results with three methods after 6 months. It shows that all three methods helps in

increasing the flooding efficiency but there is not big gap in efficiency between all methods. Because of the size and complexity of that model the contrast between methods is not clear within 6 months.

Table 6.38: Comparison between three methods for M3.A (6 months)

6 months	Injection Rate STB/D	Production Rate STB/D	Injector Efficiency	Efficiency Improvement %
original	52345	15319	0.293	-
Thiele	52377	17387	0.332	13.3
Pamila	52370	17612	0.336	14.7
Huthali	52376	17695	0.338	15.4

After running the optimization methods for 1 year in M3 model segment A, the top improvement in efficiency is achieved with Huthali method as shown in Table 6.39. On the other hand, Thiele optimization procedure provided the highest oil produced but not far from Pamila method and Huthali method gave the least oil produced.

Table 6.39: Comparison between three methods for M3.A (1 year)

1 year	Injection Rate STB/D	Production Rate STB/D	Injector Efficiency	Efficiency Improvement %
original	50342	15270	0.303	-
Thiele	50345	15319	0.304	3.8
Pamila	49598	15270	0.308	5.1
Huthali	45301	14956	0.33	12.6

Afterwards, the model is simulated for 3 years and the results of optimization methods are listed in Table 6.40. It is obvious that Huthali optimization method gave the greatest injection efficiency and production rate. We can see that Pamila method increases the flooding efficiency more than Thiele method optimization process and produced more

oil. This is because Huthali et al. method is dependant on delaying the breakthrough in the streamlines with redistributing injection rates. Retribution will lower the efficiency and productivity of the fast streamline but it will increase the efficiency of other streamlines. Because of that it can be seen that optimization with Huthali method will give you more efficiency but less productivity in short time scale.

Table 6.40: Comparison between three methods for M3.A (3 year)

3 year	Injection Rate STB/D	Production Rate STB/D	Injector Efficiency	Efficiency Improvement %
original	54370	17612	0.324	-
Thiele	54388	19132	0.352	20.1
Pamila	54358	19477	0.358	22.2
Huthali	54372	19822	0.365	24.6

Then, the optimization methods were applied for 6 months in M3 model segment B, the top improvements in efficiency and oil production rate are achieved with Huthali method as shown in Table 6.41.

Table 6.41: Comparison between three methods for M3.b (6 months)

6 months	Injection Rate STB/D	Production Rate STB/D	Injector Efficiency	Efficiency Improvement %
original	28526	11316	0.397	-
Thiele	29520	12628	0.428	7.8
Pamila	29532	13135	0.445	12.1
Huthali	29528	13426	0.455	14.6

Afterwards, the model is simulated for 1 year and the results of optimization methods are listed in Table 6.42. It is obvious that Huthali optimization method gave the greatest injection efficiency and production rate.

Table 6.42: Comparison between three methods for M3.b (1 year)

1 year	Injection Rate STB/D	Production Rate STB/D	Injector Efficiency	Efficiency Improvement %
original	29540	14192	0.48	-
Thiele	29548	14486	0.49	23.4
Pamila	29093	15135	0.52	31.0
Huthali	27531	15447	0.561	41.3

Then, the optimization methods was applied for 3 years in M3 model segment B, the top improvements in efficiency and oil production rate are achieved with Huthali method as shown in Table 6.43.

Table 6.43: Comparison between three methods for M3.b (1 year)

3 year	Injection Rate STB/D	Production Rate STB/D	Injector Efficiency	Efficiency Improvement %
original	25520	14507	0.584	-
Thiele	23526	14365	0.614	54.7
Pamila	22520	14445	0.624	57.2
Huthali	22526	14663	0.641	61.5

Finally, M4 model was simulated and optimized with the three methods for 3 years. The results are illustrated in Table 6.44. It is clear that Huthali method improves the efficiency more the other two methods but the production rate with Huthali optimization is the lowest. This is because Huthali et al. method is dependent on delaying the breakthrough in the streamlines with redistributing injection rates. Retribution will lower the efficiency and productivity of the fast streamline but it will increase the efficiency of other streamlines. Because of that it can be seen that optimization with Huthali method will give more efficiency but less productivity in short time scale.

Table 6.44: Comparison between three methods for M3.b (1 year)

3 year	Injection Rate STB/D	Production Rate STB/D	Injector Efficiency	Efficiency Improvement %
original	8258	4801	**0.581**	-
Thiele	8264	4909	**0.594**	2.2
Pamila	8256	5000	**0.606**	4.3
Huthali	8036	4760	**0.618**	6.4

CHAPTER 7

CONCLUSIONS AND RECOMMENDATIONS

7.1 Conclusions

Two synthetic and two real models were simulated to study the impact of the proposed optimization methods in the flooding efficiency and find the strengths and weaknesses for each method. The results obtained from the streamline simulator showed consequences to improve water flooding performance. All of the three methods can be automated and programmed to perform directly within the simulator. Based on the results of this study, the following conclusions can be deduced:

1) Huthali method is the finest method between all of the three methods from the aspects of getting the best water flooding performance.
2) From the production point of view, Thiele and Pamila methods give better result in increasing the oil production rates in the short terms.
3) However, Huthali method is superb in very long term because it will setback water breakthrough by equalizing water flood front arrival time at the producing wells. This will affect the production in short term but it will give more oil recovery in long term because it will enhance the water flooding efficiency.

4) All of the three methods did not solve the problem of the missed water injected to the aquifer or reservoir borders because it was neglected.

7.2 Recommendations

Given the right degree of knowledge and resources, this work can be extended in the following areas:

1. The economic impact should be analyzed with the optimization methods.
2. Controlling the water loss to the aquifer and boundaries should be considered.
3. New optimization method can be developed using excellent new optimization algorithms such as genetic algorithm.

Nomenclature

$\hat{i}$	Unit vector along x-axis
$\hat{j}$	Unit vector along y-axis
$\hat{k}$	Unit vector along z-axis
k	Isotropic permeability, Darcy
P	Pressure, Atm.
P^n	Pressure at present time level, atm.
P^{n+1}	Pressure at next time level, atm.
P^v	Iterative pressure for next time level, atm.
P_i	Pressure at cell center of current node along x-axis, atm.
P_{i-1}	Pressure at cell center of previous node along x-axis, atm.
P_{i+1}	Pressure at cell center of next node along x-axis, atm.
P_j	Pressure at cell center of current node along y-axis, atm.
P_{j-1}	Pressure at cell center of previous node along y-axis, atm.
P_{j+1}	Pressure at cell center of next node along y-axis, atm.
P_k	Pressure at cell center of current node along z-axis, atm.
P_{k-1}	Pressure at cell center of previous node along z-axis, atm.
P_{k+1}	Pressure at cell center of next node along z-axis, atm.

P_{cell}	Applied chamber pressure, atm.
P_{ini}	Initial pressure, atm.
P_{node}	Pressure at cell center of current node, atm.
∂P	Pressure change, atm.
r_e	Radius of the cutting, cm
r_j	Radial distance to center of current differential volume element, cm
$r_{j-\frac{1}{2}}$	Radial distance to near boundary of differential volume element, cm
$r_{j+\frac{1}{2}}$	Radial distance to far boundary of differential volume element, cm
r_{j-1}	Radial distance to center of previous differential volume element, cm
r_{j+1}	Radial distance to center of next differential volume element, cm
∂r	Differential radius, cm
S_{fluid}	Fluid Saturation
S_g	Gas saturation
$S_{g_{ini}}$	Initial gas saturation
S_o	Oil saturation
∂S_o	Change in oil saturation
t	Time, sec
Δt	Time Step size, sec
∂t	Time differential, sec

V	Volume, cm^3
V_j	Volume of current volume element, cm^3
V_{ini}	Initial Volume, cm^3
V_{fluid}	Fluid Volume, cm^3
V_p	Pore Volume, cm^3
$\vec{v}_o$	Oil flow velocity vector, cm/sec
$\vec{v}_x$	Fluid flow velocity along x-axis, cm/sec
x_i	x-axis distance to center of current differential length element, cm
$x_{i-\frac{1}{2}}$	x-axis distance to near boundary of differential length element, cm
$x_{i+\frac{1}{2}}$	x-axis distance to far boundary of differential length element, cm
x_{i-1}	x-axis distance to center of previous differential length element, cm
x_{i+1}	x-axis distance to center of next differential length element, cm
Δx_i	Current differential length element along x-axis, cm
Δx_{i-1}	Differential length element along x-axis of previous element, cm
Δx_{i+1}	Differential length element along x-axis of next element, cm
∂x	Differential length element along x-axis, cm
$x \quad length$	Length of cutting along x-axis, mm
y_j	y-axis distance to center of current differential length element, cm

y_{j-1}	y-axis distance to center of previous differential length element, cm
y_{j+1}	y-axis distance to center of next differential length element, cm
Δy_j	Current differential length element along y-axis, cm
Δy_{j-1}	Differential length element along y-axis of previous element, cm
Δy_{j+1}	Differential length element along y-axis of next element, cm
∂y	Differential length element along y-axis, cm
$y \quad length$	Length of cutting along y-axis, mm
z_k	z-axis distance to center of current differential length element, cm
z_{k-1}	z-axis distance to center of previous differential length element, cm
z_{k+1}	z-axis distance to center of next differential length element, cm
Δz_k	Current differential length element along z-axis, cm
Δz_{k-1}	Differential length element along z-axis of previous element, cm
Δz_{k+1}	Differential length element along z-axis of next element, cm
∂z	Differential length element along z-axis, cm
$z \quad length$	Length of cutting along z-axis, mm
∇	Divergence
ϕ	Cutting porosity
μ	Fluid viscosity, cp
μ_o	Oil Viscosity, cp

References

1. Akhil Datta-Gupta and M J. King : " Streamline Simulation : Theory and Practice " SPE Textbook Vol.11, 2007.
2. Forrest Craig :" the Reservoir Engineering Aspects of Water Flooding " SPE monograph Vol.3 , 1971.
3. Whillhite GP. "Waterflooding". Textbook Series, vol. 3. Society of Petroleum Engineers, 1986
4. Thiele M.R and Batycky RP : "Water Injection Optimization Using a Streamline-based Workflow" , SPE 84080, 2003.
5. Ghori S.G., Jilani S.Z. , I.R. Vohra and C. Lin : "Improving Injector Efficiency Using Streamline Simulation: A Case Study of Waterflooding in Saudi Arabia" SPE 93031, 2006.
6. Pamela A.Marescalco : "Improving oil fields recovery through real-time water flooding" Wiley InterScience (www.interscience.wiley.com) International Journal for Numerical Methods in Fluids , 2008.
7. Grinestaff, G.H. and Caffrey, D.J.: "Waterflood Management: A Case Study of the Northwest Fault Block Area of Prudhoe Bay,Alaska, Using Streamline Simulation and Traditional Waterflood Analysis," SPE 63152 , 2000.

8. Schlumberger Eclipse. E 100 Reference Manual. Schlumberger, 2006.

9. Schlumberger Eclipse. FrontSim Reference Manual. Schlumberger, 2006.

10. James W. Amyx, and Daniel M. Bass, JR., and Robert L. Whiting : "Petroleum Reservoir Engineering Physical Properties" , McGraw-Hill Book Company. Inc., New Yourk, 1960.

11. Morris Muskat : " Physical Principles of oil Production" , McGraw-Hill Book Company. Inc., New Yourk, 1981.

12. Terrado M., Yudono S. , Thakur G. : "Waterflooding Surveillance and Monitoring : Putting Principles Into Practice". SPE 102200, 2006.

13. Batycky R.P , Theile M.R , Baker R.O and Chugh S.H : "Revisiting Reservoir Flood-Surveillance Methods Using Streamlines" SPE 95402, 2008.

14. Baker, R.O : "Reservoir Management for Waterfloods" J.Cnd Pet. Tech 3, 1998.

15. Fawzy T, Mackay C : "The Application of Streamline Calculation to The Management of Oilfield Scale" SPE 119605. 2009.

17. A Alhuthli, A Datta-Gupta , B Yuen and J Fontanilla : "Field Application of Waterflood Optimization via Optimal Rate Control With Smart Wells" SPE 118948. 2009.

Appendix A

Streamline Simulation Background

In this Appendix, the idea of streamline simulation is discussed mathematically to clarify the basics of streamline simulation. All of the data explained here is abstracted from the book: "Streamline Simulation: Theory and Practice " [1] .

The underlying idea of the streamline method is to decouple the full 3D problem into multiple 1D problems along streamlines. Fluids are moved along the natural streamline grid, rather than between discrete grid blocks as in conventional methods. Permeability effects and well conditions dictate the paths that the streamlines take in 3D, while the physics of the displacement is captured by the 1D solutions mapped along streamlines.

A.1 MATHEMATICAL BACKGROUND

The streamline simulator involves two components; (i) tracing the streamline paths, and (ii) mapping 1D solution along the streamlines. The streamline simulator is based on first solving for the pressure field and then for the saturation distribution. This is an Implicit in Pressure, Explicit in Saturation method (IMPES). For conventional finite difference methods, one advantage of an IMPES formulation over the fully implicit formulation is that numerical diffusion due to discretization error is reduced. The trade off is that smaller time step sizes must be taken due to stability considerations. The

governing equation for flow of a component i with n_p phases flowing in a porous medium is defined as,

$$\sum_{j=1}^{n_p}\left\{\frac{\partial}{\partial t}\left(\phi w_{ij}\rho_j S_j\right)+\nabla\bullet\left(w_{ij}\rho_j\vec{u}_j-\phi\rho_j S_j\vec{\vec{D}}_{ij}\bullet\nabla w_{ij}\right)=q_s w_{ij}\rho_j\right\} \quad (1)$$

Where**,**

ϕ = Porosity,

w_{ij} = Mass fraction of component i in phase j,

ρ_j = Density of phase j,

S_j = Saturation of phase j,

$\vec{u}_j$ = Darcy's velocity vector of phase j

$\vec{\vec{D}}_{ij}$ = Dispersion coefficient tensor,

q_s = Source or sink volume flow rate.

The Darcy's velocity is given as

$$\vec{u}_j = -\frac{\vec{\vec{K}}k_{rj}}{\mu_j} \bullet \left(\nabla P_j + \rho_j g \nabla D\right) \tag{2}$$

where,

g = gravity,

P_j = Phase pressure,

D = Depth.

If fluids are incompressible (ρ_j = constant) and there is no dispersion ($\vec{\vec{D}}_{ij}$ = 0), Eq. 1 becomes

$$\sum_{j=1}^{n_p} \left\{ \frac{\partial}{\partial t}\left(\phi w_{ij} \rho_j S_j\right) + \nabla \bullet w_{ij} \vec{u}_j = q_s w_{ij} \right\} \tag{3}$$

This equation is called the saturation equation. Summing Eq. 3 and using the constraint

$\sum_i^{nc} w_{ij} = 1$ gives

$$\nabla \bullet u_t = q_s \tag{4}$$

where, u_t is the total velocity of all the phases. By neglecting capillary pressure, the total velocity can be obtained from Eq. 2 as

$$\vec{u}_j = -\vec{\vec{K}} \bullet \left(\lambda_t \nabla P + \lambda_g \nabla D\right) \tag{5}$$

where λ_t is the total mobility and λ_g is the total mobility due to gravity and are given as

$$\lambda_t = \sum_{j=1}^{n_p} \frac{k_{rj}}{\mu_j}, \qquad \lambda_g = \sum_{j=1}^{n_p} \frac{k_{rj}\rho_j g}{\mu_j}.$$

Combining Eq. 4 and Eq. 5

$$\nabla \bullet \vec{\vec{K}} \bullet \left(\lambda_t \nabla P + \lambda_g \nabla D\right) = -q_s \tag{6}$$

Eq. 6 is an elliptic partial differential equation with *P* as the dependent variable. It is generally refers as the "pressure equation". Eq. 6 is solved for pressure and substituted in Eq. 5 to get Darcy's velocity.

For immiscible case the mass fraction $w_{ij} = 1$ for $i = j$ and $w_{ij} = 0$ for $i \neq j$; this reduces Eq. 3 to

$$\phi \frac{\partial S_j}{\partial t} + \nabla \bullet \vec{u}_j = q_s f_j^s \tag{7}$$

Substitute Darcy's velocity from Eq. 5 in the above equation yields,

$$\phi \frac{\partial S_j}{\partial t} + \nabla \bullet f_j \vec{u}_t + \nabla \bullet \vec{G}_j = q_s f_j^s \tag{8}$$

where, f_j is the fractional flow

$$f_j = \frac{k_{rj} / \mu_j}{\sum_i^{n_p} k_{ij} / \mu_i} \tag{9}$$

and $\vec{G}_j$ is the gravitational term given as

$$\vec{G}_j = \vec{\vec{K}} \bullet g \nabla D \frac{k_{rj} / \mu_j}{\sum_{i=1}^{n_p} \frac{k_{ri}}{\mu_i}} \sum_{i=1}^{n_p} \frac{k_{ri}}{\mu_i} \left(\rho_i - \rho_j \right) \tag{10}$$

For incompressible flow, $\nabla \bullet \vec{u}_t = 0$, which reduces Eq. (8) to

$$\phi\frac{\partial S_j}{\partial t}+\vec{u}_t\bullet\nabla f_j+\nabla\bullet\vec{G}_j=q_s f_j^s \tag{11}$$

This equation is referred as "saturation equation". Eq. 6 and Eq. 11 outline the governing set of nonlinear equations for the IMPES method to be used in the streamline simulator. These equations are nonlinear since coefficients are functions of unknown variables (P or S_j). Before a solution to saturation equation is sought, a coordinate transformation is required. Streamlines are launched from grid block faces containing injectors or grid blocks with expansion of fluids. As the streamlines are traced from sources to sinks, a time-of-flight (TOF) along the streamlines can be defined.

$$\tau(s)=\int_0^s\frac{\phi(\varsigma)}{|u_t(\varsigma)|}d\varsigma \tag{12}$$

TOF gives the time required to reach a point *s* on a streamline based on the total velocity.

The understanding is that using a TOF-variable along streamlines rather than a volume-variable along streamtubes came through the reformulation of the 3D mass conservation equations in terms of TOF. The time of flight concept was first shown by King et al. [1993].

The streamlines with small TOFs are equivalent to streamtubes with small volumes, i.e. fast flow regions. Conversely, streamlines with large TOF are equivalent to

streamtubes with large volumes, i.e. slower flow regions. Reformulating the transport problem along a streamline using TOF rather than along a streamtube using volume is the one key development that has allowed SL flow simulation to succeed for use in complex, 3D problems.

The saturation equation (Eq. 11) needs to be transformed into the new coordinate system. To perform coordinate transformation, we can rewrite Eq. 12 as

$$\frac{\partial \tau}{\partial s} = \frac{\phi}{|u_t|},$$

which can be written as

$$|u_t|\frac{\partial}{\partial s} \equiv \vec{u}_t \bullet \nabla = \phi \frac{\partial}{\partial \tau}. \tag{13}$$

Substituting Eq. 13 into Eq. 11 gives

$$\frac{\partial S_j}{\partial t} + \frac{\partial f_j}{\partial \tau} + \frac{1}{\phi}\nabla \bullet \vec{G}_j = \frac{q_s f_j^s}{\phi} \tag{14}$$

Eq. 14 is the governing pseudo-1D material balance equation for phase *j* transformed along a streamline coordinate. It is pseudo-1D since the gravity term is typically not aligned along the direction of a streamline. To solve Eq. 14 we simply split the equation into two parts. First a convective step along streamlines governed by

$$\frac{\partial S_{c,j}}{\partial t}+\frac{\partial f_j}{\partial \tau}=0 \tag{15}$$

which includes boundary conditions at the wells, is solved to construct an intermediate saturation distribution, $S_{c,j}$. Then, a gravity step is taken along gravity lines and saturations are moved using

$$\frac{\partial S_j}{\partial t}+\frac{g}{\phi}\frac{\partial G_j}{\partial z}=0 \tag{16}$$

With $S_{c,j}$ as the initial condition to construct S_j at the next time step. It is generally assumed that the gravity lines are aligned in the z coordinate direction. Eq. 15 is solved numerically using single point upstream weighting scheme explicit in time. Eq. 16 is solved using an explicit upstream weighting method. An additional advantage of decoupling Eq. 14 in this way is that Eq. 16 is only solved in flow regions where gravity effects are important. For example, in locations where fluids are completely segregated, Eq. 14 will not be solved, since $\frac{\partial G}{\partial z}=0$.

A.2 NUMERICAL SOLUTION

The pressure equation (Eq. 6) is solved for the pressure and saturation equation (Eq. 14) is solved for saturation. These two equations are strongly coupled for compressible system whereas for incompressible system they can be easily decoupled. In the streamline simulation method an IMPES type formulation is used. The pressure equation is solved with an implicit formulation whereas saturation equation is solved explicitly.

A.2.1 Construction of Streamlines

A streamline is defined as the instantaneous curve in space along which every point is tangent to the local velocity vector. The algorithm used to trace the streamline through a single cell is often referred to as the Pollock [1988] method. The starting point for the method is a single cell with flow rate calculated for each of the cell faces. The flow rate is assumed to be uniform on each of the faces. As a result of the pressure equation the total flow rate in/out of each of the faces can be calculated based on the total Darcy velocity.

Pollock's algorithm is based on three assumptions within one grid cell:

1. Uniform flow rate on each cell face

2. Linear variation of velocity field in each coordinate direction

3. Orthogonal grid

The flow rate calculated from the pressure equation complies with assumption (1). FrontSim supports general corner point grids, which definitely is not orthogonal. To comply with (3) an iso-parametric transformation onto a unit cube is needed for each of the grid cells. The streamline tracing in FrontSim is done entirely on a unit cube. The coordinates in the following equations are assumed to be in the unit cube coordinate system. Details on this transformation can be found in several papers (see references in section 7).

For the bi-/tri-linear velocity field, the interstitial velocity (v=u/φ) in the x-direction is defined as:

$$v_x = v_{xo} + g_x(x - x_o) \tag{17}$$

where

$$g_x = \frac{v_{x\Delta x} - v_{xo}}{\Delta x}$$

where, v_{xo} is the x-velocity at $x - x_o$ and g_x is the velocity gradient in the x-direction. Since $v_x = dx/dt$, we can integrate the expression of the x-velocity (and

similarly in the y- and z-direction) to get the exit times out of each face given an arbitrary entry point (x_i, y_i, z_i) (Figure A.1).

$$\Delta t_x = \frac{1}{g_x} \ln\left[\frac{v_{xo} + g_x(x_e - x_o)}{v_{xo} + g_x(x_i - x_o)}\right],$$

$$\Delta t_y = \frac{1}{g_y} \ln\left[\frac{v_{yo} + g_y(y_e - y_o)}{v_{yo} + g_y(y_i - y_o)}\right],$$

$$\Delta t_z = \frac{1}{g_z} \ln\left[\frac{v_{zo} + g_z(z_e - z_o)}{v_{zo} + g_z(z_i - z_o)}\right] \tag{18}$$

Eq. 18 determines the time at which the particle exit at the *x*, *y*, and *z* faces, respectively. Since the streamline must exit from the face having the smallest travel time,

$$\Delta t_m = \min(\Delta t_x, \Delta t_y, \Delta t_z)\ , \tag{19}$$

the exit locations are easily calculated by re-solving for x_e, y_e, and z_e using the minimum time:

$$x_e = \frac{1}{g_x} \ln\left[v_{xi} \exp(g_x \Delta t_m) - v_{xo}\right] + x_o\ ,$$

$$y_e = \frac{1}{g_y}\ln\left[v_{yi}\exp(g_y \Delta t_m) - v_{yo}\right] + y_o ,$$

$$z_e = \frac{1}{g_z}\ln\left[v_{zi}\exp(g_z \Delta t_m) - v_{zo}\right] + z_o . \quad (20)$$

In Figure A.2a the streamline enters the Y_0 face of a single cell and exits the X_1 face through the exit point. Given the entry point, (x_A, y_A, z_A), the exit point, (x_B, y_B, z_B), $v_x = \Delta x / \Delta t$, and integrating Eq. 17, the Δt (or *d*TOF) can be expressed by Eq. 18.

As mentioned previously, the points on the streamline are represented as points in the unit cube coordinate system for each of the cells through which the streamline traces. If the point needs to be output for visualization, it is transformed back into the real coordinate system for the corner point grid.

A.2.2 Summary of Streamline Procedure

FrontSim is based on a sequential approach where the governing equations for pressure and saturations are solved sequentially. The IMPES (Implicit Pressure Explicit Saturations) method is based on a sequential approach as well, but suffers severely from the time step length-limiting CFL (Courant-Friedrich-Levy) condition that occurs, as fluid cannot move more than one cell during one time step. One of the advantages of the sequential approach over the fully implicit approach is the opportunity it gives to use a

fit for purpose numerical method for each of the equations to be solved. FrontSim solves the near elliptic pressure equation implicitly (as IMPES) and the near hyperbolic saturation equations are solved with a streamline method where a variety of fit-for-purpose numerical methods can be chosen on each streamline and gravity line. The computations required within one single time step with user-defined boundary conditions including well flow targets are:

1. Solve the pressure equation for the time step.
2. Compute the total Darcy velocities based on the pressure potentials.
3. Compute a set of streamlines to represent the computational domain for the saturation solver.
4. Map saturations or concentrations onto the streamlines.
5. Solve the saturation equation individually on each of the streamlines.
6. Solve for the gravity segregation.
7. Accumulate all the solution variables on each individual streamline or gravity line to form the solution on the global grid at the end of the time step.

Update the time dependant information and repeat these steps for each time step in the simulation. Each of the steps is described in more detail below.

A.2.2.1 Solve the pressure equation

The pressure Eq. 6 is solved for the time step based on rock properties, current fluid distribution and boundary conditions. The rock properties are the static user-defined data in the model such as permeabilities, porosities net-to-gross etc. These are defined on a discretized domain, the grid, which is the same as the numerical grid used to discretize the pressure equation. The pressure nodes are assumed to be in the center of each grid cell. From the static data and the grid geometry the transmissibilities between the grid cells are computed. The transmissibilities are constant throughout the simulation. Since FrontSim is based on a sequential approach, the pressure solution is calculated for the end of the time step based on the saturations at the beginning of the time step.

The boundary conditions can be open wells with given targets and limits, aquifer models, pressure boundaries and flux boundaries defined by the user. These conditions can change for any user-defined time step. Due to the sequential approach the rate targets for the wells are always translated into total (sum of phase/components) rate at reservoir condition in FrontSim. If the split between the phase rates are changing considerably during the time step, FrontSim might have difficulties to honor exactly a target set for one single phase-rate. This is a common feature of any IMPES type simulator, but since the time steps are a lot larger for streamline-based simulators, this artifact becomes more visible. It is recommended to use total reservoir rates as target if possible.

A.2.2.2 Compute the Total Darcy Velocity

The total Darcy velocity, equation Eq. 5, is needed for the streamline calculations. In FrontSim the flow rates at every grid cell face or non-neighbor connection (NNC) represent the velocity field. The flow rate is computed as the total flow rate at reservoir conditions normal to the connection.

A.2.2.3 Generate Streamlines

For practical purposes a streamline can be seen as a trajectory in the Darcy velocity field. It is defined as a set of points in 3-dimensional space. A streamline start point is a point on the streamline to where the flow rate represented by the streamline is assigned. This point can be anywhere in the grid depending on the algorithm to select the streamlines. Usually it is a point in a source or sinks or in a cell that was not visited by any of the originally computed streamlines. The tracing operation will trace both backward and forward from this point to create the streamline. For incompressible flow the flow rate assigned to a streamline will be equal at both endpoints. Therefore, FrontSim will by default distribute start points at each active source (injectors, aquifers etc.) in the model.

For compressible flow the algorithm is more complex. For example, for primary depletion with no injection the streamlines can start from any grid cell in the model, often at a boundary, and the flow rate will increase along the streamline consistent with

the compressibility in each of the grid cells it traces through. In this case, FrontSim will by default distribute streamlines at both sources and sinks in the model.

The number of streamlines necessary to represent the computational domain depends on the number of grid cells in the model, the number of wells and magnitude of flow. The number of streamlines in FrontSim will by default be approximately 10% of the number of active cells plus a number associated with the number of active wells; it can be scaled by a user-defined multiplier.

The set of streamlines are always updated whenever a new pressure solution is calculated, which normally is for each time step in the simulation. The shape of the streamlines can change considerably between time steps. The main reason is change in boundary conditions like flow rates in wells or wells that are turned on and off. Change of mobility due to the change of saturation and pressure distribution in the previous time step can also have a large impact on the shape of the streamlines.

A.2.2.4 Solve the saturation equation individually on each of the streamlines

The set of streamlines with its properties forms the discretization of the computational domain on which the saturation is solved. The underlying resolution of the saturations is the pressure grid and an updated saturation distribution on this grid is needed for the pressure solver for each time step. The points, in terms of TOF, where the streamline crosses the global grid cell faces are the basic discretization for the 1D numerical grid. This is referred to as the streamline discretization.

The 1D numerical discretization along the streamlines depends on the method used to solve the saturation equation. If the Front-Tracking method is chosen the streamline discretization is used directly. The speeds of the fronts are calculated as a function of the slope of the fractional flow curve. The method is very fast and accurate for models with low compressibility such as water-oil cases. For three-phase simulation a finite difference method is used to solve the saturations on the streamlines. Due to difficulties in convergence a uniform grid is applied along the streamline.

For three-phase cases there are two different finite difference methods available. The different options can be selected by using the first parameter of keyword TUNEFS1D.

The default option is the FULLIMP method on the streamline. This method is a fully implicit standard finite difference method to solve for both pressure and saturations along the streamlines.

An explicit volumetric Finite Difference Method is also available (TUNEFS1D with parameter 1 set to EXPL). The method is based on a volumetric approach and an upstream scheme. This is usually faster than the FULLIMP method, but does not account for the pressure change due to change of saturation distribution during the time step.

A.2.2.5 Numerical methods for the gravity lines

The numerical methods used to solve along the gravity lines are usually the same as is used to solve along the streamlines. If the front-tracking method is used on the streamlines it will also be used on the gravity lines. The sources and sinks (wells and boundary conditions) are only relevant for the streamlines, not the gravity lines.

When the saturation solver finishes each individual streamline/gravity line, the solution is mapped down to the global grid. In this procedure all the volumes on the streamlines going through the same cell is accumulated. Most parameters will be pore volume weighted for the cell. As an example, the water saturation SW_j in a grid cell number *j* is:

$$SW_j = \sum \left(PV_{str} \times SW_{str} \right) / PV_j$$

Where, PV_{str} is the pore volume along a streamline in a grid cell, SW_{str} is the water saturation on the streamline, and PV_j is the pore volume of cell number *j*. The sum is taken over all segments in all streamlines going through cell number *j*.

A.2.3 Streamline parameters

From the perspective of the saturation solver there are three properties needed to define the streamline. They are time of flight (TOF), flow rate and a pointer to a unique grid cell in the underlying numerical grid. The flow rate and TOF are defined in points

along the streamline, and the grid cell pointer is defined for each linear segment between the points defining the streamline. For the grid cell pointer to be unique, there have to be points defined for every grid cell face that the streamline passes through. The grid cell pointer is used for picking up relevant information defined on the grid and to map solution variables between the streamline and global numerical grid. Figure A.2 shows how points and segments are defined with respect to the grid. The streamline method does not require the boundaries of a streamtube to be calculated. The streamline can be thought of as the center of a streamtube and the combination of the TOF and flow rate is used to calculate the pore volume in any of the streamline segments. For a segment *i* on the streamline the pore volume *PV* is calculated as:

$$PV_i = dTOF \times Q_i$$

where *dTOF* is the increment of TOF and Q_i is the total flow rate into segment *i* at reservoir conditions. The 3D space coordinates are not used for the simulation itself, but necessary for any visualization of the streamlines. They are calculated for output purposes only.

A.2.3.1 Stop criteria

The tracing continues until one of the following stop criteria is reached:

- An active well is positioned in the current cell. The streamline is traced to the center of the cell and terminated.

- The streamline exits through a boundary. This may be either an open boundary defined by pressure/flux (PSIDE, FLUXSIDE) or an aquifer connected to this cell face.

For compressible flow two more criteria are available:

- Sink/source in grid cells not containing wells

  In this case either all the faces in a grid cell have flow rates into the cell (sink) or they have only flow rates out from the cell (source). Any cell in the grid can act as a sink/source in compressible cases, but they are most likely to be close to the closed boundaries of the grid. If the difference between the total inflow and outflow in the model is large, many streamlines are likely to have one endpoint in this type of cell.

- Low flow

  This is very similar to the situation for the sink/source cells. The flow rate calculated along the streamline reaches a predefined minimum close to zero, and the streamline tracing is terminated.

A.2.3.2 Flow rate and compressibility

The start point for the streamline tracing is allocated a total flow rate at reservoir conditions. The flow rate needs to be defined at all points in the streamline. If the model has incompressible data, the flow rates are constant for the streamline. If the model has

compressible data, the flow rate will most likely change along the streamline. FrontSim calculates the change of this flow rate consistent with the change of flow rate in the underlying grid.

A.2.4 Injector's efficiency

Streamline simulation provides a more robust and quantitative way to determine injector's efficiency. With the help of streamlines it is known where the flow is going and where it is coming from. The streamlines connecting injectors with producers can exactly determine how much fluid is being transported from an injector to a particular producer. The amount of fluid between an injector and a producer is called the well allocation factor.

If the ALLOC mnemonic in the RPTSCHED keyword is set, FrontSim will generate allocation reports in a separate (.ALLOC) file. This ASCII-formatted file contains allocation factors and pore volumes (drainage area) for wells and for injector-producer pairs. A Well Allocation Factor (WAF) is a number that indicates the percentage of flow at a given well due to supporting wells. For a producer supported by multiple injectors, the WAF's indicate the percentage of flow at the producer due to each supporting injector. Similarly, for an injector supporting multiple producers, the WAF's indicate the percentage of injection to each producer. Well allocation factors are calculated based on the fluxes carried along the streamlines connecting producers and injectors. As a result the WAF's will change when ever there is a change in streamline

paths – due to changing well conditions, mobility effects, or even modifying grid properties. For example, within 3DSL a well allocation factor at well i due to support from well l is defined as follows,

$$WAF_{il} = \left[\sum_{j=1}^{n_p} \sum_{k=1}^{n_{sl}} \frac{q_{jil}^{k}}{q_i^{w}} \right] \times 100$$

Where q_{jil}^{k} is the phase j flux of streamline k between wells i and l at well i and q_i^w is the total flow rate of well i. All rates in the above calculations are based on reservoir volumes, not surface volumes. For incompressible systems, the flux along each streamline is a constant such that total flux into a well pair is the same as total flux out of a well pair. For compressible systems, some streamlines may be arriving/leaving a well from/to the far field. The total flux of these far field streamlines is accounted for in the "other" category in the WAF file. Also for compressible systems, the flux is not a constant along the streamline.

The injector efficiency are calculated as

$$Injector \cdot Efficiency = \frac{Offset\ Liquid\ \mathrm{Pr}oduced}{Total\ WaterInjected\ by\ the\ Injector}$$

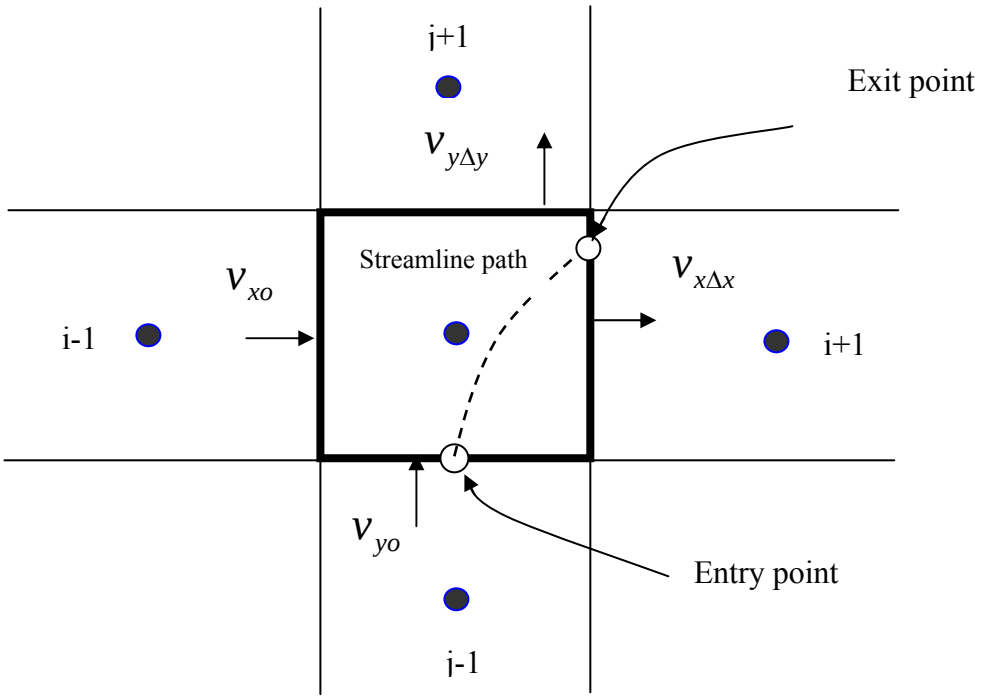

Figure A.1. Construction of streamlines.

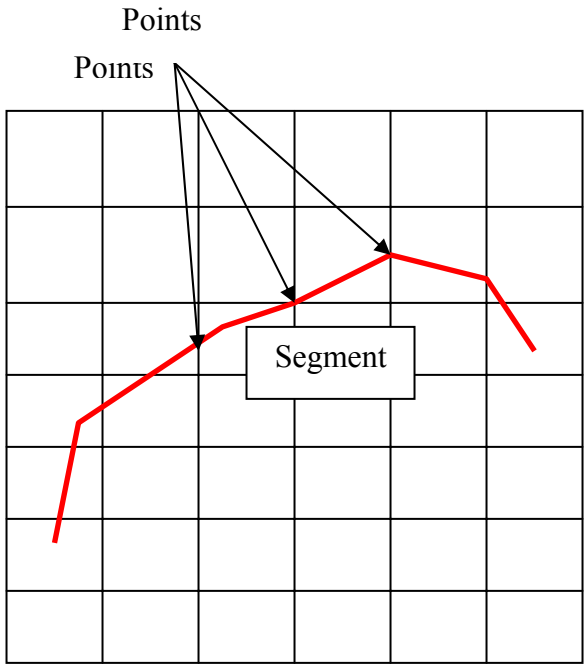

Figure A.2a. Streamline tracing through grid, showing points and segments between the points.

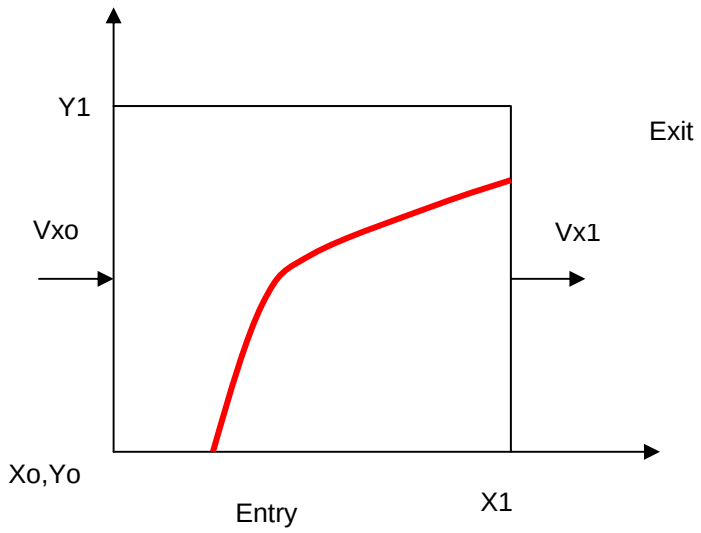

Figure A.2b. Streamline (red) through a single cell

Appendix B

Streamline Solution

- After having constructed 1-dimensional models we then solve them using standard finite volume techniques. There are four choices available to the user; these are controlled using the TUNEFS1D keyword. The four options are
  - IMPLICIT
  - AIM
  - IMPES
  - EXPLICIT.
- The first three of these use, essentially, a cut-down version of ECLIPSE 300 to solve the streamlines. In each of these cases streamlines are bundled together in groups containing approximately 1000 cells (although this can be controlled by the user), with each streamline separated from the next by a zero transmissibility, "no flow" barrier.
- They are then solved using a standard finite volume technique. The solutions are solved using mini-timestepping, that is to say intermediate timesteps are used to solve the streamlines, and the solution is marched forward to the end of the timestep used in FrontSim. During each mini-timestep, pressure is recalculated along the streamline as well as the saturations or molar densities. This means that at the end of the timestep we may end up with a pressure along the streamline

which is different from that used to calculate the original streamline. At the end of the timestep, the solution is mapped back to the original user grid.

The parameters IMPLICIT, IMPES and AIM indicate the method of solving these 1-dimensional streamlines. They respectively represent a fully implicit solution, an IMPES (IMplicit Pressure, Explicit Saturation), and an adaptive implicit solution of each mini-timestep. The limits on the length of the mini-timestep and the number of Newton iterations per mini-timestep are controlled using the TUNEFS1D keyword.

AIM

The Adaptive Implicit method (AIM) is a compromise between the fully implicit and IMPES procedures. Cells with a high throughput ratio are chosen to b e implicit for stability and to obtain large time steps , while the majority of cells can still be treated as IMPES where the solution may be changing little. All completions are treated implicitly.

Explicit

The fourth option is simply to do a single-step explicit saturation update along the streamline. This is much faster than the other 3 solution techniques, but will require that the full field pressure equation be solved more frequently.

The Fully Implicit Method

The fully implicit method if the default solution method. For black oil models this is likely to be the best solution method.

The fully implicit method solves the residual equation using the saturations at the end of the timestep t + dt .

$$R = \frac{M_{t+dt} - M_t}{dt} + F(P_{t+dt}, S_{t+dt}) + Q(P_{t+dt,}, S_{t+dt})$$

This means that we need to solve N cell * M comp simultaneous equations where N-cell is the number of cells and M-comp is the number of components (compositional) or phases (blackoil) in the model. The number of calculations required to do this varies linearly with Ncell and with the 3rd power of Ncomp. Using the fully implicit method for large numbers of components can therefore be quite slow.

IMPES

The IMPES (IMplicit Pressures Explicit Saturations) residual is similar to the fully-implicit residual, except that all flow and well terms are computed using saturations (or R_s. R_v) in a black oil run; or molar densities in a compositional run at the beginning of each time step.

$$R = \frac{M_{t+dt} - M_t}{dt} + F(P_{t+dt}, S_t) + Q(P_{t+dt,}, S_{tt})$$

The mass terms M_{t+dt} are evaluated using both pressures and saturations at the end of the timestep. This makes the non-linear residual equation, $R = 0$, much easier to solve because there are now no nonlinearities arising from relative permeabilities that remain fixed throughout the timestep. However, to solve the IMPES equations correctly it is still necessary to iterate until all residuals have been reduced to a sufficiently small value.

Appendix C

E-Plot User Interface

C.1 User Interface

The user interface is called *ePlot*. This interface was developed using Java programming language on NetBeans platform. The interface can be downloaded with the *jar* file. *ePlot* can be run by double clicking the *jar* file.

The very first step in the generation of efficiency plots is to convert the ALLOC file into a useful format. This can be achieved by clicking on the "Extract" menu item convert from new format.

A file-open dialog box will be displayed. Select the desired ALLOC file and click ok. A save-as dialog box will open. Type the name of the output file and click ok. If you do not want to change the name it will give the root name suffix by 'out'.

Three types of files will be generated, namely: 1) **.plt* file for the injectors' efficiency plot, 2) *.pie file for the construction of pie chart and data for rates supported by injectors to connected producers, and 3) **.wct* for the construction of pie chart and data for a producer showing contribution of water cut due to each supporting injector.

C.2 Efficiency Plot

The efficiency plot window can be opened by clicking on the "Efficiency Plot" button. An open file dialog box will be opened. Select the desired *.plt file and click ok. A select step window will be opened along with an empty chart window .

Select the desired time step; the chart window will plot offset oil produced Vs injection rate. Each symbol on this chart represents an injection well. The chart also shows 4 diagonal lines representing 100%, 75%, 50%, and 25% efficiency for the injectors. It is much easier to identify low efficiency injectors from this chart than from other presentations.

A well with high injection rate and low offset oil production would be considered a low efficiency injector. Several time steps can be plotted on this chart. The color of symbols can be changed for each injector to differentiate injectors' efficiency at different time steps. A data window for the efficiency plot can be opened by clicking on the "View Data" button.

C.3 Injectors' Allocation

The injectors' allocation can be quantified by analyzing pie charts and tables. By clicking on the "Injector Allocation" button in the *ePlot* main window, an open dialog window will open. Select the desired file with the extension *.pie*; a time step window will be opened.

This window shows tabs with time steps and names of injectors in each time step. Select a time step by clicking on the tab; select the desired well. Two windows will be opened; one is a pie chart for the injectors representing percentage contribution towards each connected producer.

The second window shows a table of the information about the injector. The first column provides the list of all the producers supported by this injector and their fractions in parentheses. The second column gives the corresponding oil production rate for each producer.

The third column is the water injection rate from the injector towards each producer. The fourth column provides the corresponding water production rate for each producer. Analysis of these will help identify injector-producer pair efficiency.

C.4 Watercut Charts

At a production well, the supporting injectors' water contribution can be quantified by analyzing pie charts and tables. By clicking on the "Water-cut Chart" button in the *ePlot* main window, an open dialog window will se displayed.

Select the desired file with the extension *.wct*; a time step window will be opened. This window shows tabs with time steps and name of producer in each time step. Select a time step by clicking on the tab; select the desired production well. Two windows will appear.

One is a pie chart for the producer representing percentage contribution of water from each connected injector. The second window shows a table of the information

about the producer. The first column provides the list of all the injectors supporting this producer. The second column gives the oil production rate due to each supporting injector.

The third column provides the water production rate in the producer due to each injector. The third column is the water injection rate from each injector towards this producer. The fourth column is the water cut in this producer.

The most important piece of information from this table is the identification of the most offending injector in the production of water in a producer.

C.5 Excel Applications

The user interface *ePlot* can be used for any field To work on the Injectors' efficiency in each segment, and to incorporate the methodology of monthly injection targets, an Excel application was developed.

Given the data file from e-plot (above: plt file) one should follow the steps outlined below:

1. Copy & paste in Excel the plt file.
2. One time step at a time (usually the last time step).
3. Sort according to injectors well names.
4. Copy & paste in customized Excel sheet.
5. Embedded macros will compute the efficiency for each well.

6. Bo & Bw can be input for each segment in order to have the results expressed in reservoir barrels instead of standard conditions.
7. Tables as outlined below are produced:

Segments	Wtr Inj.	Oil Prod.	Efficiency
#	#	#	#
. …	….	….	…..
Total			
Average			

The generic name of this Excel application is “Efficiency-XXXX.xls” and must be copied and renamed after each run. There are essentially two sheets in the Excel file which are described below:

INPUT-SORTED: The data from the *.plt file (an output of ePlot) is edited and the data are copied for the desired time step, sorted in order of increasing well name, and pasted in this input sheet . Copy the Injectors' data for Segment A in top area of the input data sheet.

C.5.1 ANALYSIS:

Once the data are copied in the INPUT-SORTED sheet, the ANALYSIS sheet computes the efficiency, injection rate contributions, etc. for all the injectors in each segment. A detailed analysis from this sheet would identify injectors which require rate alterations

Vita

Name:	**Hesham Mohammed**
Nationality	Yemeni
Email:	hsmkfupm@hotmail.com
Address:	Prince Homoud Road, Akrabia , Beside Qadisiah Club
	Khobar , Saudi Arabia.
Telephone	+966-503129865
Education:	**MS (Petroleum Engineering), June 2010**
	King Fahd University of Petroleum and Minerals,
	Dhahran (31261), Saudi Arabia
	B.E. (Petroleum Engineering), May 2006
	King Fahd University of Petroleum and Minerals,
	Dhahran (31261), Saudi Arabia
Areas of Interest:	Reservoir Simulation and Management, Enhanced Oil Recovery